

# **OPTIMAL AUTOMOTIVE DOOR-BODY FITTING FOR BODY-IN-WHITE ASSEMBLY**

by

Essam Shalash

A Thesis

Submitted to the Faculty of Graduate Studies and Research  
through the Department of Industrial and Manufacturing Systems Engineering  
in Partial Fulfillment of the Requirements for  
the Degree of Master of Applied Science at the  
University of Windsor

Windsor, Ontario, Canada

1996

© 1996 Essam Shalash



National Library  
of Canada

Acquisitions and  
Bibliographic Services

395 Wellington Street  
Ottawa ON K1A 0N4  
Canada

Bibliothèque nationale  
du Canada

Acquisitions et  
services bibliographiques

395, rue Wellington  
Ottawa ON K1A 0N4  
Canada

*Your file Votre référence*

*Our file Notre référence*

The author has granted a non-exclusive licence allowing the National Library of Canada to reproduce, loan, distribute or sell copies of this thesis in microform, paper or electronic formats.

The author retains ownership of the copyright in this thesis. Neither the thesis nor substantial extracts from it may be printed or otherwise reproduced without the author's permission.

L'auteur a accordé une licence non exclusive permettant à la Bibliothèque nationale du Canada de reproduire, prêter, distribuer ou vendre des copies de cette thèse sous la forme de microfiche/film, de reproduction sur papier ou sur format électronique.

L'auteur conserve la propriété du droit d'auteur qui protège cette thèse. Ni la thèse ni des extraits substantiels de celle-ci ne doivent être imprimés ou autrement reproduits sans son autorisation.

0-612-31001-9

# ABSTRACT

Flexible manufacturing is a multi-faceted term that has been used in the automotive industry to imply a multitude of manufacturing criteria. These criteria include the ability of designing manufacturing cells to handle variable designs over time. A prominent area of application for such criteria in the automotive industry is the body assembly process. The assembly process is, in turn, divided into a number of sub-processes which include fitting car doors to body openings. As these operations take place before the painting of the car body, they are commonly known as Body in White processes. The door fitting problem is ranked within the top issues of car-quality, since an inadequate door fit causes water leakage, wind noise, difficulties in closing and adversely affects the aesthetic value of the car. This thesis presents a novel computer aided method for fitting manufactured car doors to manufactured car body openings using measured points, by laser sensors, on the door and opening peripheries. The fitting process is modeled as an optimization problem where the door location and orientation parameters are the independent variables and the deviation from the nominal gap is the objective function to be minimized. The presented work in this thesis shows that the fitting function is a multi-modal function that cannot be solved for its absolute minimum using gradient descent or direct search methods. A global optimization method, genetic algorithms, is used for the fitting problem and obtained results show less gap deviations than those obtained by direct search. However, since genetic algorithms arrive to a near-optimal value of the objective function, their performance is enhanced by using their resulting optimum independent variables as the starting point for direct search, which yields lower gap deviations than those achieved by genetic algorithms. Another issue that is tackled in this thesis that pertains to the door fitting process is the direct calibration of the robotic door handling workcell. This step is

needed to estimate the location of a grasped door from the laser sensors readings, taking into account the various deviations present in the workcell. These deviations include sensor errors, parts manufacturing deviations and robotic grasping errors. The formulation of the direct calibration method is extended from the two dimensional space problems, which is developed in previous literature, to three dimensional space problems to suit the calibration of the door fitting workcell.

*To my family members with love*

# ACKNOWLEDGMENT

I would like to thank my supervisor Dr. Waguih H. ElMaraghy, for his guidance and support throughout the course of this research.

I am very grateful to Dr. Waguih H. ElMaraghy, the Department of Industrial and Manufacturing Systems Engineering, and the University of Windsor for the Research Scholarships, Graduate Assistantships and the Scholarships I have received for financial support. I would like to thank the secretary of the Industrial and Manufacturing Systems Engineering Department, Jacquie Mummery and Jerry Schuryk, the system manager at the IMS labs.

I would like to extend my thanks to Dr. Hoda ElMaraghy and Dr. Abdel-Fattah Asfour for their encouragement and support.

I am very thankful to my friend Dr. Ashraf Nassef for the fruitful assistance, guidance and support. He and wife Sherine made me feel at home, Mega thanks.

El Houssaine Waled, Yasser ElDeeb, Dr. Hassen Zghal Anis Limaiem were very helpful, thanks.

My greatest thanks go to my family. Their love and devotion were always my driving force.

# TABLE OF CONTENTS

ABSTRACT .....	III
ACKNOWLEDGMENTS .....	V
TABLE OF CONTENTS .....	VII
TABLE OF FIGURES .....	IX
<b>1. CHAPTER ONE .....</b>	<b>1</b>
1.1 General Overview .....	1
1.2 Research Statement And Motivation .....	2
1.3 Research Objectives .....	4
1.4 Thesis Outline .....	4
<b>2. CHAPTER TWO .....</b>	<b>6</b>
2.1 Automobile Body Manufacturing Processes .....	6
2.1.1 BIW Manufacturing Processes .....	8
2.1.2 Door Manufacturing Processes .....	9
2.1.3 Door Hanging and Fitting Process .....	10
2.1.4 Discussion .....	14
2.2 Automobile Body Fit and Dimensional Variation .....	15
2.2.1 The 2 mm program .....	16
2.3 Flexible and Fixtureless Assembly .....	17
2.3.1 Flexible Tooling and Assembly Systems .....	18
2.3.2 Fixtureless Assembly .....	19
2.4 DIRECT CALIBRATION .....	21
2.5 Optimal Door Fitting .....	23
2.5.1 Choice of Fitting Objective Function .....	25
2.5.2 Global vs Local Optimization .....	26
2.6 ISSUES RELATED TO RESEARCH MOTIVATIONS .....	26
2.6.1 Direct Calibration .....	27
2.6.2 Optimal Door-Body Fitting .....	27
<b>3. CHAPTER THREE .....</b>	<b>28</b>
3.1 Automating the Door Fitting Process .....	28
3.2 Proposed Strategy and System layout .....	30
3.2.1 System Layout and Components .....	30
3.2.2 Assembly Sequence .....	35
3.3 Direct Calibration .....	36
3.4 Working Example .....	37
3.4.1 Problem Statement .....	37
3.4.2 Acquisition of Calibration Data .....	39
3.4.3 Determination of Process Mapping .....	40

3.4.4 Production Usage .....	42
3.4.5 Simulation Results .....	42
<b>4. OPTIMAL DOOR FITTING.....</b>	<b>51</b>
4.1 Problem Statement.....	51
4.1.1 Definition of Quality Indexes .....	52
4.2 Formulation of the Optimal Fitting Problem.....	54
4.2.1 Homogeneous transformation .....	54
4.2.2 Objective Function .....	55
4.2.3 Multimodality of the Objective Function.....	57
4.3 Solving the Door Fitting Problem using Genetic Algorithms.....	65
4.3.1 Computer Simulation .....	66
4.4 Hybridizing Genetic Algorithms with Direct Search.....	75
4.4.1 Discretization of the Search Space.....	75
4.4.2 Genetic Drift .....	76
4.4.3 Hybrid Algorithm for solving the door fitting problem .....	77
4.4.4 Comparison of the Results.....	77
4.5 Choice of the Objective Function.....	78
4.5.1 Susceptibility to Bias.....	79
4.5.2 Susceptibility to Measurement Errors .....	80
4.5.3 Susceptibility to Sampling Error.....	83
<b>5. CHAPTER FIVE .....</b>	<b>85</b>
5.1 Introduction .....	85
5.2 Summary and Discussions.....	85
5.3 Contributions.....	87
5.4 Future Research .....	88
<b>APPENDIX A .....</b>	<b>98</b>
<b>APPENDIX B .....</b>	<b>110</b>
<b>APPENDIX C.....</b>	<b>114</b>
<b>VITA AUCTORIS.....</b>	<b>120</b>



# TABLE OF FIGURES

Figure 2.1 Schematic diagram of BIW [source: (Roan, 1993)] .....	6
Figure.2.2 A flow chart for BIW and door manufacturing processes.....	7
Figure .2.3 Press line flow chart of (a) inner panel and (b) outer panel stamping process .....	10
Figure 2.4 Coordinate system convention in the auto-industry .....	11
Figure 2.5 The 6 degree of freedom constrains for positioning a door on body side opening.....	12
Figure 2.6 Hinge assembler [source: (Wu, 1991)] .....	13
Figure 3.1 System layout.....	30
Figure 3.2 Sensing using Laser Triangulation.....	33
Figure 3.3 Part Fixturing according to the 3-2-1 principle .....	35
Figure 3.4 Schematic of the planar door.....	38
Figure 3.5 Schematic diagram of sensor's arrangement (door at nominal location).....	39
Figure 3.6 Residual errors using the forward mapping method (nominal door without noise).....	45
Figure 3.7 Residual errors using forward mapping (nominal doors with noise) .....	46
Figure 3.8 Residual errors using forward mapping (deformed doors without noise).....	47
Figure 3.9 Residual error using the forward mapping methods (deformed doors with noise) .....	48
Figure 3.10 Residual errors for the "deviated doors with noise" case after subtracting the mean error .....	50
Figure 4.1 A schematic diagram showing the concept of a fitable door.....	52
Figure 4.2 Gap and flush between door and body opening.....	52
Figure 4.3 The least squares objective function (function of $x$ and $z$ ).....	58
Figure 4.4 The least squares function (function of $z$ and $\alpha$ ) .....	58
Figure 4.5 Population of chromosomes .....	60
Figure 4.6 An initial random population of the variable $x$ .....	61
Figure 4.7 Distribution of a variable's instances after applying genetic operators: (a) without using the sharing scheme, (b) using the sharing scheme.....	62
Figure 4.8 Using the sharing scheme with: (a) a unimodal and (b) a multimodal function.....	64
Figure 4.9 Histograms of variable $x$ for (a) a unimodal and (b) a multimodal function .....	65
Figure 4.10 Triangular sharing function .....	65
Figure 4.11 Histograms of the independent variables in the door fitting objective function by using the sharing scheme .....	66
Figure 4.12 Nominal door, body opening and gap.....	67

Figure 4.13 Effect of deviating direction .....	68
Figure 4.14 Effect of fitting point locations.....	69
Figure 4.15 Door and body opening before fit .....	69
Figure 4.16 Gap width deviation for the parallel deviation case .....	71
Figure 4.17 Gap parallelism for the parallel deviation case .....	72
Figure 4.18 Maximum deviation for the parallel deviation case .....	73
Figure 4.19 Average GWD, GP and MAXD for the parallel deviation case.....	74
Figure 4.20 Average GWD, GP and MAXD for the perpendicular deviation case .....	75
Figure 4.21 Discretization of the search space in genetic algorithms.....	76
Figure 4.22 A multimodal function with minima values close to each other .....	77
Figure 4.23 Although using the sharing scheme enables the finding of all minima regions, the convergence to the global minimum would not be accurate enough .....	77
Figure 4.24 Simulation results: (a) Door without fit, (b) simplex search fit, (c) genetic algorithm fit, (d) hybrid approach fit.....	79
Figure 4.25 Schematic diagram of the fitting algorithm .....	80
Figure 4.26 The effect of $p$ on the bias of the fit .....	81
Figure 4.27 MAXD vs $p$ for different SDs.....	82
Figure 4.28 $L_p$ - norm uncertainties.....	83
Figure 4.29 Effect of measurement errors on door fit .....	83
Figure 4.30 The maximum gap error vs. $p$ .....	84

# **1. CHAPTER ONE**

## **INTRODUCTION**

### **1.1 General Overview**

Much of today's manufacturing literature declares flexibility as the corporate battleground of the 21st Century. To automotive manufacturers, flexibility has a multifaceted definition, implying, if not including, infinite product variety, profitable lot sizes of one, building different products on the same line, converting from building one product to another quickly at low cost or more simply, as Nissan defines flexibility, "any product, any time, any place, any volume, by anybody."

The key item in current automotive manufacturing is the car body or Body-In-White (BIW), an item that has two important characteristics which reflect its crucial importance: it is the most expensive part in the whole automotive plant, and its changeover in response to market trends occurs most often. Those same characteristics are also the reasons behind the tremendous concern of the North American automotive industry about their future in a very highly competitive marketplace, especially with the presence of the Japanese "monster" in such market. Consequently, solutions have been proposed, cooperation has been achieved, and even political decisions have been made.

BIW is the assembly of an automobile structure before the panels are fitted. As the BIW is assembled, a number of body openings are geometrically formed, e.g., motor compartment, windshield, and deckled openings. In association with these "body

characteristics” are the subassemblies (panels) that have to be fitted in their corresponding openings. Those are the hood, the doors, the fender, etc.

The dimensional quality of the above subassemblies, as well as the openings, will influence the assembly or fitting processes associated with them, which in turn will influence the overall quality of the car as well as the total time to market - the time it takes to get products from design into full production.

The ultimate goal of automotive manufacturers is to shorten the time to market, keeping in mind the quality of their products. For this global goal to be reached, emphasis should be put on all the manufacturing and assembly sub-processes starting from the very beginning until the very end. The key to achieve all that is flexible manufacturing and flexible assembly.

## **1.2 Research Statement And Motivation**

In the current work, the research is focused on one of the sub-assembly processes mentioned above which is concerned with the panels fitting in the BIW. One of those is the car door fitting or assembly. The research problem can thus be stated as solving and automating the problem of car door assembly to minimize flush and gap variation, and consequently minimize the production cost. All this has to be done in a flexible environment.

Most of today's automatic assembly are implemented using a deterministic task approach, which depends on the quality of the parts and the tooling. The behavior of an assembly system is never completely predictable and can be hardly anticipated, due to the numerous sources of uncertainty (Pasek, 1993):

- material and parts variation
- fixturing errors
- positioning errors
- auxiliary manufacturing process equipment error

To improve the quality of the automobile body, with the presence of the above sources of variation, two different - yet coupled - approaches can be pursued. The first approach is to control the dimensional integrity of the BIW and of the subassembly-panels by reducing the variations associated with them in the design stage and the manufacturing stage. This is the process control methodology (Ceglarek, 1993, 1995; Roan, 1993, 1995). The second approach attempts to consider the variations as inputs that would be fed to a flexible and/or adaptive system that would adjust or correct the deterministic tasks in the assembly stage so that a higher level of quality standards are achieved. An example is the door fitting problem where quality at the end is judged or measured by the functionality associated with the door and the door opening and how the door is fit in the opening. Such functionality could be wind noise, water leakage, door closing effort, and maybe some others.

With today's advanced computer, sensing, and actuation techniques, it is possible to keep up with the process changes almost instantaneously and to collect 100% data from the process. Process data collection and its processing are essential for the purpose of identification, calibration, and then automation of the assembly processes.

The main motivation of this research was to study the feasibility of these advanced techniques for on-line quality improvement.

## 1.3 Research Objectives

The research objectives can be itemized as the following:

- Study and critique the existing solutions to the car door fitting/assembly problem in the literature.
- Proper mathematical formulation of the door positioning problem.
- Development of a good and robust solution technique.
- Testing the solution technique.
- Study of the measuring techniques in literature for accurate calibration of positioning tools, robots, and workcell .
- Design of the steps and sequences for automating the process of door assembly.

## 1.4 Thesis Outline

This thesis is divided into 5 chapters and 3 appendices. This chapter provides a general overview of the current work, motivations, research objectives and the thesis outline.

Chapter 2 introduces a brief description of the automobile body manufacturing. This includes the BIW and the Door manufacturing processes, and the door fitting process. Next, some general research directions are described and the importance of car body quality and flexibility is emphasized. Finally, the literature relevant to workcell calibration and optimal fitting is reviewed.

Chapter 3 describes a strategy for automating the door fitting process. Visual on-line sensing, as an important component in the proposed system, is discussed. This is followed by introducing a method for whole workcell calibration. The method is extended from working in 2-D for simple parts to working in 3-D as it is applied to the door fitting

process. The chapter concludes with an example where the different components, parameters and techniques are simulated, and preliminary results are given.

Chapter 4 concentrates on the door fitting problem and how it can be solved to improve the quality of gaps and flushes between the door and body opening. First the optimality issue is discussed and the previous used method is criticized. Next, the door fitting problem is formulated as an optimization problem. Genetic algorithms are introduced as global optimizers and hybridizing it with direct search methods is accomplished. Simulations are conducted for different cases and comparisons are made.

Chapter 5 summarizes the work along with conclusions and recommendations for future work.

## 2. CHAPTER TWO

# BACKGROUND AND LITERATURE SURVEY

### 2.1 Automobile Body Manufacturing Processes

Car body assembly is a process in which stamped sheet metal parts are brought together and then permanently joined by welding, gluing, hemming, tabbing, etc. The automobile at this stage is usually called Body-In-White (BIW). As the BIW is assembled, a number of body openings are geometrically formed, e.g., motor compartment, windshield, decklid, and doors opening (Figure 2.1). The panels (e.g., hood, decklid, doors, etc.) to be fitted in such openings undergo, to a large degree, the same

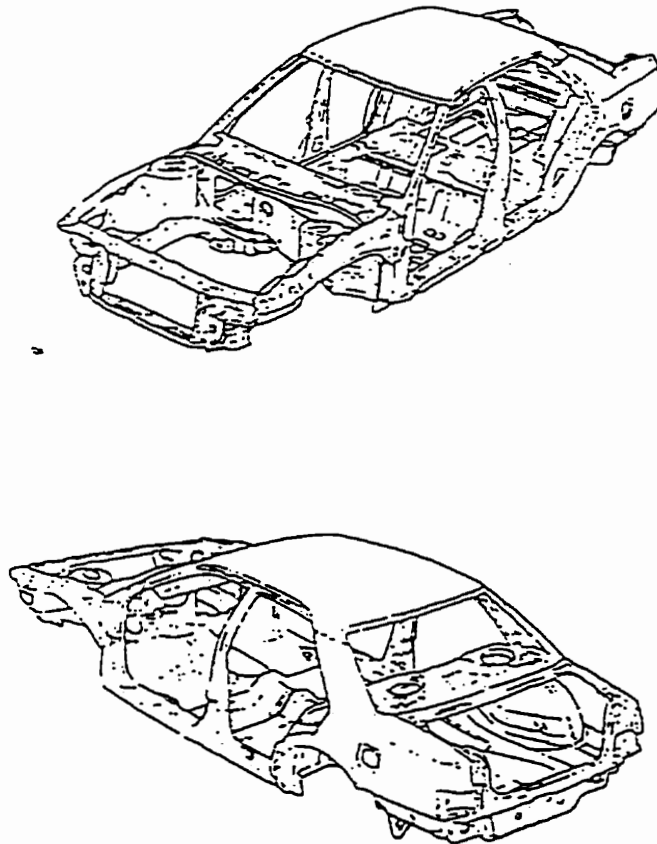


*Figure 2.1 Schematic diagram of BIW [source: (Roan, 1993)]*



manufacturing processes as the body.

Figure. 2.2 shows a flow chart, starting from sheet metal coils until the completion of a BIW and a door. Blanking, stamping, subassembly, and body framing (or final assembly) are the manufacturing processes which produce components for the subsequent operations. For example, parts are produced from blanks through a stamping process. In the body framing process, subassemblies (components) of the BIW, side frames,

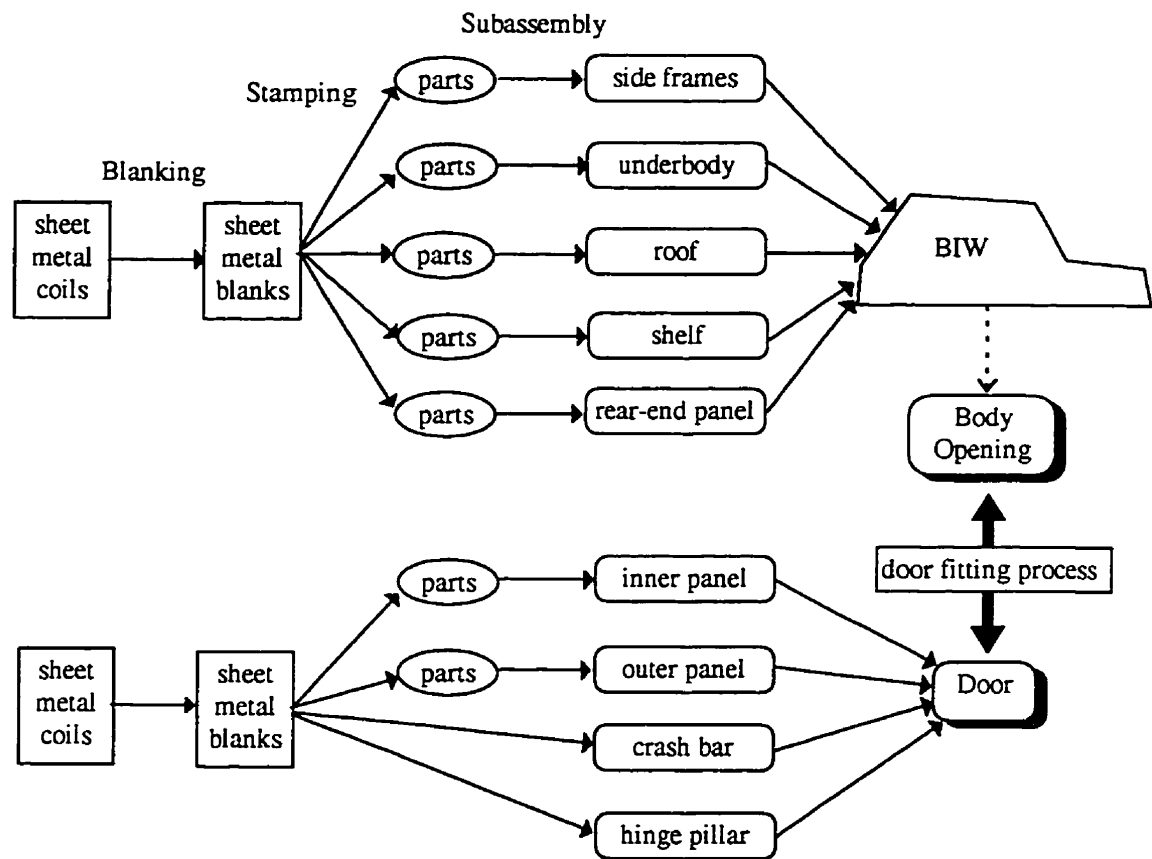


Figure.2.2 A flow chart for BIW and door manufacturing processes

underbody, roof, shelf, and rear-end panel, are welded together to set the geometry of a BIW. It is obvious that each station in the stamping, subassembly, and body framing processes could contribute to the dimensional variation in the BIW and the hang-on panels.

## **2.1.1 BIW Manufacturing Processes**

### **2.1.1.1 Blanking and Stamping Processes**

A blanking process cuts sheet metal coils into blanks by shearing metal using punches and dies. Blanks are flat pieces of metal which will be packed and transferred to the stamping area.

Similar to the blanking operation, the stamping process employs punches and dies as the tools to perform the task. In some stamping plants, blanking is included in the stamping process. The final products of stamping processes, called parts, are sent to the assembly area to be assembled. Because most parts have complicated shapes, a number of stamping stations are necessary for each different part. These stations could include: drawing, trimming, piercing, and flanging operations. Drawing operations will form the shape of a specific part by closing the upper and lower dies. The unwanted material around the perimeter will be cut off by the trimming operations. Piercing operations punch holes, such as the tooling holes in the parts. Bending the rim of a panel to form a strip of surface for the purpose of welding is the function of flanging operations (Roan, 1993).

### **2.1.1.2 Subassembly Processes and Major subassemblies of a BIW.**

A BIW is assembled by welding the underbody, the left and right side frames, the roof, the shelf, and the rear-end panel together. The welding operations are done by robot arms and welding tips while fixtures hold the subassemblies in predetermined positions. The underbody, the left and right side frames and the roof are produced in different subassembly lines. There are about 5 to 10 stations in each subassembly line. The shelf and the rear-end panel are large pieces of metal which are manufactured in the stamping process.

### **2.1.1.3 Body Framing Process**

The body framing process is used to produce the BIW by welding the underbody, the left and right side frames, the roof, the shelf, and the rear end panel together. During

body assembly operations, there are about 60 pallets which carry the auto bodies from station to station in the assembly line

### **2.1.2 Door Manufacturing Processes**

As in the BIW, an automobile door is manufactured through processes, such as blanking, rolling, stamping, and assembly. Generally, an automobile door is made by assembling together the inner panel, the outer panel, the inner and outer belt reinforcements, the crash bar, and the hinge pillar. A schematic diagram of the elements of a typical door is shown in Figure. The inner panel and the outer panel are manufactured by the stamping process. The belt reinforcements and the hinge pillar are made by small presses, and the crash bar is manufactured by a cold rolling process (Wu, 1991).

#### **2.1.2.1 Rolling and Blanking Processes**

Rolling process is applied for the production of crash bar for the door. Due to the hardness of crash bar, multiple rollers are used sequentially to cold roll the material to its final shape. A blanker is used to cut the crash bar to its desired length for door assembly.

Blanking process cuts the sheet metal coils into blanks. The blanks will then be packed and transferred to the drawing operation are of the stamping process.

#### **2.1.2.2 Stamping Process**

The stamping process forms the door panels. A typical stamping process involves five to seven operations, which include, drawing, trimming, piercing, and flanging operations. An inner panel stamping process and an outer panel stamping process are different and are shown in Figure 2.3.

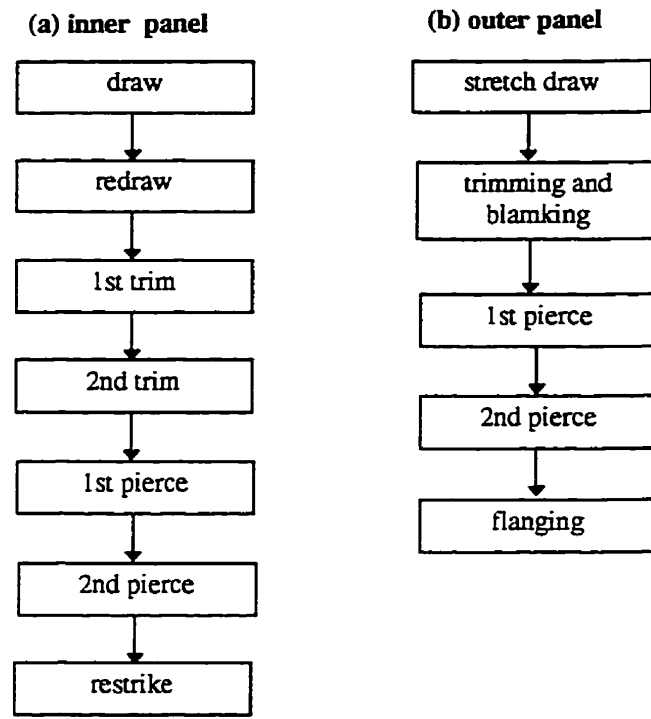


*Figure 2.3 Press line flow chart of (a) inner panel and (b) outer panel stamping process*

### 2.1.3 Door Hanging and Fitting Process

A door is fit to the body opening by first hanging it on the side opening with a hanging fixture. When the gap and flush do not meet the dimensional quality requirement, the door is further fit manually by door-fitting operators (Wu, 1991).

The coordinate system commonly used in automobile manufacturing and assembly processes is described using: Fore/Aft (F/A), High/Low (H/L), and Inboard/Outboard (I/O). Such a coordinate system is shown in Figure 2.4.

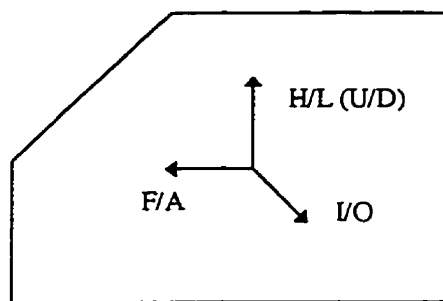


*Figure 2.4 Coordinate system convention in the auto-industry*

The sequence of hanging and fitting of doors from rear to front is:

1. Hang the rear door to the side opening,
2. Fit the rear door to the side opening,
3. Hang the front door to the rear door in F/A, and side opening,
4. Fit the front door to the rear door, and the side opening.

#### **2.1.3.1 Door Hanging Process**

To hang a door on the body side opening, the position of the door to the side opening needs to be determined and its six degrees of freedom need to be constrained. The constraining of the six degrees of freedom for both the rear and front doors relative to the body side opening is realized using the nets in the fixture, as shown in the Figure 2.5.

For the process under study, as shown in Figure 2.5, it is seen that one net is used for F/A constraint, two nets for H/L, and three nets for I/O, which follows the 3-2-1 rule of fixturing. The F/A net controls the C-post gap between the car body and the rear door. The H/L nets align the door character line to the body side character line and maintain the gap between the header of door and the roof. The I/O (flushness) is controlled by the hinge which is pre-assembled to the door by the hinge assembler shown in Figure 2.6. Thus, when the door is positioned on the body side opening by the hanging fixture, the bolts on the hinge are tightened to the car body to complete the door hanging process.

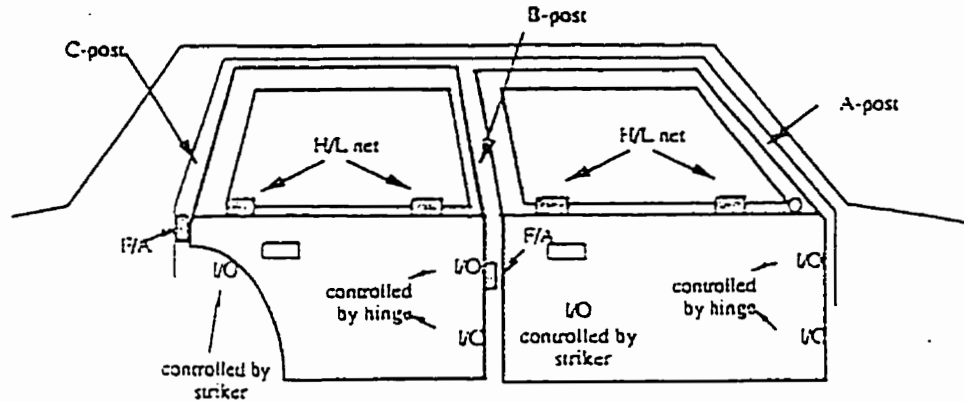


*Figure 2.5 The 6 degree of freedom constrains for positioning a door on body side opening*

As was described in the beginning of the section, the front door is fit to the front hem of the rear door in B-post for gap control. Thus a well-fitted rear door is essential for the consequent front door fitting and fender fitting. The 3-2-1 rule of fixturing for front door is similar to that used in the rear door fit as discussed.

The hinge assembler shown in Figure 2.6 pre-assembles the hinge to the door. As can be seen in the figure, the F/A netting arrangement is different from the one used for door hanging. So there will be nine (9) nets to adjust when adjustment is required. They are 1 F/A and 2 H/L nets for the door hanging fixture and the six nets for the hinge assembler.

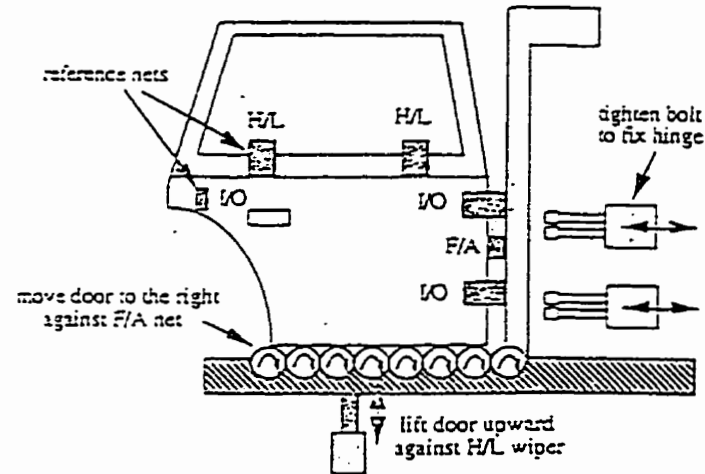


Figure 2.6 Hinge assembler [source: (Wu, 1991)]

### 2.1.3.2 Door Fitting

When a door is hung on the side opening with the hinge, any further fitting action has to be accomplished by distorting the door to obtain the required appearance. Since the hinges have been tightened to the body, it is mostly the flushness, especially in areas remote to the hinge location, that is being changed by the manual door twisting. The correction in F/A and H/L direction is not prominent. The twisted doors tend to spring back, which results in dimensional inconsistency. Different personal preference also results in inconsistency in the dimensional quality.

### ***Problems with Current Door Hanging and Fitting Process***

Through the previous investigation of the current practice of door hanging and fitting process, the problems are summarized as follows:

1. The spring-back after bending the doors may introduce inconsistency and thus, may not always be effective. This inconsistency in the current practice of door fitting needs to be alleviated with a systematic hanging fixture adjustment approach.
2. The capability of correcting the gap deviations through door fitting is not well understood. Consequently, the variational fault sources cannot be effectively located for corrections.
3. A systematic procedure is not available for door hanging fixture adjustment. The current practice of door hanging fixture adjustment is done by investigating the measurement data, followed by a heuristic decision. The investigating and decision-making procedure is time-consuming if not ineffective.

#### **2.1.4 Discussion**

In the above subsections, the different manufacturing processes that might affect the quality of the automobile have been explained.

As a result of these manufacturing processes, different sources of dimensional variations and/or deviations can be identified. Dimensional variation is defined as the unintended part-to-part differences in the output of a production process, whilst dimensional deviation is defined as the unintended differences between the actual dimensions produced and the dimensions called for by the design.

For the door fitting problem, the key characteristics that contribute to the quality of the automobile can be summarized as follows:

1. The body opening dimensions,



2. The door dimensions,
3. The relative position and orientation of the door with respect to the body opening.

The dimensional variation of the size of the opening and/or the door can result in difficulties in the fitting process, and/or uneven gap and flushness. The width and straightness variation of the opening can represent the dimensional quality of the opening. Studies indicated that the variation of measurements made for points on the opening edge can be as high as 3 mm in the I/O direction and about 1 mm in the F/A and H/L direction (Roan, 1993). Similar values were found for the door (Wu, 1991).

## 2.2 Automobile Body Fit and Dimensional Variation

Shortening launch time, the period from no production to full production, while simultaneously satisfying requirements, became a priority of the most advanced automobile manufacturers.

North American auto-makers and their suppliers are demonstrating world-class quality in styling, power trains, electronics, etc., but not in body fit. The body fit quality or the dimensional integrity of the BIW and of panels(doors, board, and deckled), and the panel fitting processes are the main aspects upon which the automobile quality general, and consequently, customers' satisfaction depend on (Weber and Hu, 1993). The lack of competition in body fit was shown from the following benchmark data of the characteristic dimensional variation(in 6 sigma) for automobile BIW openings:

Japan	2.0 mm
Europe	2.5 mm
Domestic	>3 mm

Variation reduction, expressed in terms like the above mentioned characteristic figures, not only will reduce cost and increase customers satisfaction eventually, but it has become a selling point in its own right. The Japanese automakers were the first to recognize such a fact and use it. Toyota have demonstrated their body fit perfection in their Lexus commercial where ball bearings shown rolling smoothly around the body panels. Nissan claimed that their technology has brought infinity to within 0.008 of an inch of perfection.

In order to catch up with Toyota, Nissan and other world-class automakers, North American competitors, manufacturers and suppliers have started to pursue a technological infrastructure that would allow them to achieve truly competitive body fits-consistently and with little or no time lost during the launch cycle. An excellent example of such an awakening is the formation of the “2 mm program” which will be discussed in more detail in the following section.

### **2.2.1 The 2 mm program**

The 2 mm program is a joint venture between the government, the industry and the academia. The research is jointly funded by General Motors, Chrysler, the Auto Body Consortium(a group of automotive tooling suppliers that works together to develop the most competitive technologies to design, process and produce automobile bodies) and supported with funding from the US Government through its Advanced Technology Program(ATP) which was established in 1988 and is administered by the National Institute of Standards and Technology(NIST).

The main objective of the 2 mm program was to advance automobile body manufacturing technologies and process control methodologies to achieve world-class BIW dimensional quality:

- 2 mm total variation(6 sigma) for BIW openings;

- 1.5 mm total variation(6 sigma) for major panels and subassemblies such as door, side frames, etc.
- 1 mm total variation(6 sigma) for stamped sheet metal parts(e.g., door inner, quarter panels, etc. ).

Another objective was to improve the scientific understanding of the sheet metal assembly processes and to establish a technical infrastructure for the future sheet metal process control and assembly systems.

Several projects were assigned to ensure the successful achievement of the research and development objectives. Four major areas of research were identified:

1. Dimensional Measurements Technology
2. Process Control Methodology
3. Body Assembly Technology
4. Technology Transfer Models

## **2.3 Flexible and Fixtureless Assembly**

Automobile assembly consists of four main processes, which are stamping, body assembly, paint and final assembly. Among these processes, the body assembly process has the lowest level of flexibility.

Classically, positioning jigs that are mechanically rigid and exclusively designed for each type of a vehicle are used. The jigs, or fixtures, used in the main body assembly line are the largest and most complex. In the event of a model changeover, normally 12 months of tool design and fabrication plus large sum of capital investment are required to prepare a Body Main Line. The limitation in the flexibility of such lines is clear because of their rigid mechanical structure.

Eliminating such dedicated and inflexible fixtures is a particularly vital issue that leads to the concept of fixtureless assembly. This is not a technique, and it is not even fully achievable today. It is part of a long-range goal that calls for a new approach to manufacturing and assembly.

### **2.3.1 Flexible Tooling and Assembly Systems**

In recent years, the volume of research work and applications related to the development of flexible assembly systems have increased significantly. Most of the published results, however, are from the electronic and computer industries.

In the aerospace industry, hard automation of the assembly process is possible, but not cost effective due to the small batch sizes. To overcome this limitation the Flexible Assembly System for the assembly of airframe components was developed as a flexible assembly cell that could replace the dedicated tooling and be able to quickly reconfigure itself for new types of subassemblies

In the automotive industry, the leading automakers as well as the tooling and technology providers have produced different solutions and methodologies in the pursuit of flexibility.

The FLEXTOOL™ developed by FANUC Robotics, to equip automotive manufacturers with a flexible manufacturing tool, is an example of such technology (Kosmala, 1994). FLEXTOOL™ is a system of robotic manipulators (acting as re-programmable positioners) designed to locate and fixture automotive components for assembly . The main features of this system are listed in the following:

1. Compact positioning units : These are 4-axis units designed to precisely locate and clamp sheet metal work, with the freedom to move around in the space of the tooling and product.

2. Common datum “patches” : The common datum patch is a small area of sheet metal surface on the workpiece which is common among the parts being run on the Flextool fixture. Datum patches adds to the flexibility and convertibility between models.
3. Shimming by software : While adjusting fixed locators on hard tooling means grinding or shimming the blocks, Flextool relies on graphical software to achieve the same effect. This is achieved by controlling the shim moves on the screen using a control menu which in turn initiates a command to the positioners to move correspondingly . In addition all the previous moves are recorded in a database for retrieval and comparison.
4. Open architecture control : Its main feature is the ability to communicate with other vendors equipment through the ethernet or remote I/O and to modify the programmable locators position using off-line simulation. On the other hand the user is denied access to the trajectory generator or controller for both the robots and the programmable locators.

### **2.3.2 Fixtureless Assembly**

Fixtureless Assembly was defined in (Hoska, 1988) as the ability to process and assemble parts without the use of fixtures or part-orientation devices that are totally dedicated to - while not part of a product. Items targeted for elimination include: any tool, fixture, part-presentation/orientation device, or piece of processing equipment that would need to be changed or discarded if the product changes.

Fixtureless Assembly involves many challenges and research areas that has to be addressed. Some of these challenges are the following:

- The development of an accurate sensor/vision system that keeps track on the position and orientation of the parts to be processed.

- The development of a system coordination and control algorithms.
- The development of an efficient fault-tolerance strategies which enables the system to respond to errors and take correction action in real time.
- The development of proper/robust tooling designs that would facilitate the completion of the task.

One system which implemented this approach and made it almost a reality is Nissan's Intelligent Body Assembly System (IBAS) (Abe *et al.*, 1995). The following briefly describes the basic concepts of IBAS, and some of the fundamental technologies associated with it.

### ***IBAS***

The Nissan (IBAS) system was developed to produce various type of vehicles using the same production line by varying the vehicle CAD model. In addition the system has to able to simulate the whole production process using the vehicle CAD data , thus evaluating the production cycle time and anticipate problems in the production process. The basic components are

1. NC Locator : It is a programmable jig that provides the same function as "conventional jigs" but with higher flexibility because it can adapt to variations in the CAD model.
2. On-line body accuracy measurement system : The major points that are crucial for the accuracy of the welding or assembly of the car body are measured using a laser sensor. The variation between the actual part and its CAD model is monitored and countermeasures are adopted to counteract this variation.

3. Operation monitoring and failure diagnosis system : This system monitors the operating conditions of the NC locator. When a failure occurs in the system it leads the operator to the cause of the failure and the countermeasure for recovery.
4. Off-line programming : This is achieved through designing the system trajectory according to the part CAD model and the required task to be accomplished. Checking for collision and cycle time calculations are then conducted. This process takes place simultaneously with the production process so it saves production time because it does not require the physical locators or devices to be available for programming.

## 2.4 Direct Calibration

In order to accurately measure the position and orientation of an object in a reference ("world") coordinate system by a robot-camera system, various components in the system have to be calibrated. This includes the determination of the pose (that is, the position and orientation) of the robot base with respect to the robot frame, the robot hand with respect to the robot base, the camera with respect to the robot hand, and the object with respect to the camera. These four tasks are respectively known as robot base calibration, robot manipulator calibration (in short, robot calibration), hand/eye calibration and camera calibration. Robot base calibration can sometimes be considered as a sub-task of robot calibration.

There has been an extensive research aimed at solving each of the above tasks. Conventionally, each of these tasks is handled individually. One may start by calibrating the camera to determine the relative pose between the object and the camera, followed by calibrating the hand/camera to determine the pose between the robot hand and the camera, and then use the camera and hand/eye models to calibrate the robot to determine the pose

of the robot hand in the world coordinate system. After all system components are individually calibrated, the pose of an object in the robot world system can be determined.

Such a multistage approach has two main advantages (Mooring, 1991). First, since system calibration is performed by calibrating its components or subsystems separately, each component calibration task is relatively simple. Second, if some of the system components have changed their location or parameters, calibration needs only be repeated for these system components. For example, if the camera changed its focal length, only the camera needs to be recalibrated.

The multi-stage approach, however, has some drawbacks. The first problem is that parameter estimation errors in early stages propagate to the later ones. The second problem is the validity of the hand/eye calibration stage. More specifically, it is commonly assumed in most hand/eye calibration problems solved in the literature that the relative motions of the robot and the sensor are accurately known. While the relative motion of the sensor is measured by an external device, the relative motion of the robot is computed by the use of the robot link parameters, combined with the robot joint position readings. Prior to robot calibration, an assumption of a known robot geometry is only a gross approximation.

A step towards solving some of the problems encountered in the multistage calibration methods is the concept of *autonomous calibration* (Bennet, *et al.*, 1991; Zhuang *et al.*, 1993). Autonomous calibration was defined in Bennet *et al.*, (1991) as an automated process that determines the system model parameters using only the system's internal sensors, and it was used for a robot and a monocular camera rigidly mounted to the robot hand. In Zhuang, *et al.*, (1991) a simultaneous strategy, based on the same concept, was proposed for a system of a robot and two instrumented movable cameras. In both cases, the advantage was stated basically as eliminating the propagation errors which exist in multistage approaches. However, the whole concept still depends on identifying



and developing a model-based algorithm that solves for kinematic parameters of the robot and the camera(s).

In summary, the traditional approaches used in sensor-guided assembly systems rely mainly on model-based algorithms for transformation of sensor data into estimates of part location, which can be critically sensitive to the accuracy with which the model represents the actual parts in production. These conventional calibration methods - which are expensive, time consuming and difficult to perform - ultimately tend to be inaccurate due to poor robustness with respect to the unavoidable variations present in assembly operations on the factory floor.

Another concept which can be used for workcell calibration is the concept of *direct calibration*, which was defined in Murray and Pohlhammer, (1994) as a non-model specific, straightforward method of whole system calibration for sensor-guided flexible assembly systems. The entire assembly system - the robot, the sensors, and the parts to be assembled - is calibrated for the required assembly task in a single procedure to directly determine the relationship between the part feature information in sensor coordinates and the part location (position and orientation) in robot coordinates. Murray and Pohlhammer conducted simulations for a simple 3-DOF problem and examined the ability of direct calibration to provide robust estimates of the location of a planar body.

The preliminary results indicated that the method holds significant promise for enabling flexible assembly to achieve its potential for revolutionizing the assembly of high-volume products.

## 2.5 Optimal Door Fitting

An optimal door fit refers to a position and an orientation in space of a manufactured door within a manufactured car-body opening, at which the maximum gap value between the car-body opening and the door is at its minimum value. A low quality

fit may result in water leakage, wind noise and difficulty in door closing. Moreover it affects the aesthetic value of the car. In fixtureless assembly, the door positioning process is automated where an industrial robot can be used to position the door relative to the body opening, with the end-effector working as the hanging fixture. With the advancement in sensing and machine vision technology, (Rotvold, 1995; Pasek, 1993) it is now possible to develop a flexible assembly system that conducts in-line measurements for both the door and the body opening. The points sampled by the sensing system are in turn processed through an optimization algorithm to minimize the gap between the door and the body opening. Mathematically the problem can be stated as follows:

1. Given a set of  $N$  measured points  $A_i$ ,  $i = 1 \dots N$ , on a manufactured door.
2. Given a set of  $N$  corresponding points  $B_i$ ,  $i = 1 \dots N$ , on a manufactured body-opening.
3. Find the door's position and orientation that will minimize the Gap-deviation  $D$  where

$$D = \left( \frac{1}{N} \sum_i^N \| (evaluated\ gap)_i - (nominal\ gap)_i \|^p \right)^{1/p} \quad (1)$$

This problem was first tackled by Wu *et al.* (1994), where they solved the problem as a least squares minimization ( $p = 2$ ) problem. Although pioneering the solution of the optimal door fit problem, their choice of the power  $p$  in Equation 1 was arbitrary and did not make a study on its best value. Moreover, they used the gradient descent optimization method and did not address the point that this method lingers in local minima. These issues were addressed by subsequent researchers as shown in sections 2.5.1 and 2.5.2. Another approach that was used to position parts in assemblies using linear programming was proposed by Turner (1990). His method is limited to finding any mating position and does not seek a position with minimum gap value between the mating parts. Moreover,

linear programming cannot be used with the door fitting problem as it is a non-linear programming problem.

### 2.5.1 Choice of Fitting Objective Function

The exponent  $p$  in equation (1) dictates the type of the objective function used for minimizing the gap deviation. When  $p = 2$ , the problem becomes a least squares minimization and when  $p = \text{infinity}$ , which is equivalent to the maximum deviation, the problem becomes a Tchebychev approximation (Rice, 1964). Qian et al. (1996) criticized the use of the least squares function and showed that it does not give the optimal solution. They showed a case study where the application of the least squares method to the door fitting problem led to a deviation value 30% higher than the real optimum obtained by minimizing the maximum gap. However, they assumed that there are no measurement errors associated with the measured points on the door and the body-opening.

The choice of the minimization function has been tackled in the area of computational metrology (ElMaraghy *et al.*, 1990; Yu, 1992; Nassef and ElMaraghy, 1996). Hopp (1993) showed that low values of  $p$  increase the bias of the optimization algorithm towards the average deviation value leading to incorrect evaluation of the deviation. On the other hand, high values of  $p$  make the optimization algorithm very sensitive to measurement errors which may also lead to incorrect evaluation. Since the laser measurement technology used in fixtureless assembly have a high threshold of error ( $\pm 50$  microns), the minimization of the maximum gap might not be suitable for the door fitting problem.

Another issue concerning the choice of the objective function is that the measured points do not represent the whole door edge (or body opening edge) but only a sample, and hence are susceptible to sampling error. Dowling et al. (1995) were the first to point

out this problem in the evaluation of straightness and flatness deviations in metrology and recommended the use of the least squares function.

### **2.5.2 Global vs Local Optimization**

Shalash et al. (1996) showed that the minimum gap deviation problem is a multi-modal problem. The results showed that the gradient descent search and direct search methods lingered in local minima, which may lead to the evaluation of door positions yielding gap deviations which are out of tolerance. They proposed the use of genetic algorithms (Goldberg, 1989) as global optimizers. Their door fitting results showed gap-deviation values less than that obtained by direct search.

## **2.6 Issues Related To Research Motivations**

There are several research gaps in the above survey which are addressed in this thesis. These are:

1. The direct calibration approach was applied in a two-dimensional form. How can this approach be extended to the three dimensional form ?
2. Since the door fitting problem is an optimization problem, is it a unimodal or multimodal problem ?
3. What is the most appropriate optimization method to solve the door fitting problem ?
4. There are several forms for the gap-deviation function (equation (1)). Which of these forms is most appropriate for the door fitting problem ?

### 2.6.1 Direct Calibration

The estimation of automotive parts location when handled by robotic manipulators was solved, for the first time, using the direct calibration method by Murray and Pohlhammer (1994). They applied that method to the estimation of windshield locations and their aperture locations as well. Their work was limited to the two dimensional problem without validating this simplification. However this simplification does not fit in the handling of automotive doors due to the high manufacturing errors occurring in the I/O direction. An extension of the direct calibration method to estimate the location of rigid bodies in three dimensional space is needed.

### 2.6.2 Optimal Door-Body Fitting

Wu et al. (1994) were the first to solve the door fitting problem in a mathematical programming form. However, they did not address the type of the objective function they are using. If the objective function (equation 1) is multimodal and if either gradient descent or direct search methods are used, then there is a high probability that the search will linger in a local minimum missing the global one. The minimum gap-deviation value achieved by the above search methods will greatly depend on the initial values of the independent parameters. Missing the global minimum value of the gap-deviation might lead to out of tolerance door fits. The issue of the objective function multimodality need to be addressed.

While Wu et al. (1994) used the widely used least squares function, Qian et al. (1996) recommended the minimization of the maximum gap. However, as pointed out earlier, there is a tradeoff between the sensitivity to measurement errors and the bias to the average deviation value. The best value of the exponent  $p$  in equation 1, which will minimize both criteria should be estimated.

### **3. CHAPTER THREE**

## **DIRECT CALIBRATION OF AN AUTOMOBILE DOOR FITTING**

To date, the primary technological limitation to widespread application of flexible assembly is the lack of an approach for efficient and accurate intercalibration between all components of the assembly cell. Whenever sensors are used in a robotic flexible/intelligent assembly cell to compensate for variations in part locations, part-to-part variations and robot inaccuracies, the relationships between all elements of the complete assembly process (the robot, the sensors and the parts to be assembled) must be accurately known. However, the calibration of sensor-guided robotic assembly systems has been traditionally considered a process related to the individual components of the system, and one that is independent of the parts to be handled and the assembly task at hand (Murray, 1994). In this chapter a new method of whole system calibration for sensor-guided flexible assembly systems in 3-D space is presented and applied to the door fitting problem.

### **3.1 Automating the Door Fitting Process**

The current practice in fitting a car door is usually accomplished through two steps:

1. The door is hung on the side opening with a hanging fixture which constrains the door's six degrees of freedom so that it can be positioned correctly with respect to the body opening

2. When the gap and flush do not meet the dimensional quality requirements, the door is further fit manually by door-fitting operators, and this is usually accomplished by bending and twisting the door.

The hanging fixture is usually designed to be insensitive to variations in the geometry of the door or the body opening. This desired insensitivity (or robustness), however, is not always possible to achieve, due to two main factors: wear and uncertain geometry introduced by variations in the parts.

Furthermore, most of today's automatic assembly systems are implemented using the deterministic task approach. In such systems, parts are pushed together against hard locators, while sensing is used mainly to monitor the presence or absence of parts or to inspect certain quality characteristics. The behavior of such systems is not completely predictable due to the uncertainties from numerous sources such as variations in material and parts, fixturing or positioning errors and auxiliary manufacturing process equipment errors.

The solution proposed in this thesis is based on the elimination of the door positioning errors during the fitting process. The first goal of this research is to draw the guidelines of an automated, sensor-guided system which can perform on-line dimensional error compensation functions without human intervention. The development of such a system will address the various sources of uncertainties involved in the assembly process.

Once the door fitting process is automated, high quality door-body fits can be accomplished by utilizing the dimensional data acquired by the sensing system and further fitting the door relative to the body opening through an optimization algorithm. The subject of optimal door fitting is addressed in Chapter 4, while the rest of this chapter will deal with the integration and calibration of the system.

## 3.2 Proposed Strategy and System layout

### 3.2.1 System Layout and Components

The essential task in the door fitting process is to move the door to a desired position relative to the body opening within a specified tolerance. So far as there is no changes in the car design, the process can be considered as a positioning problem.

To provide a satisfactory performance and get an adequate fit for every door and body opening coming into the process, the automated optimal door-body fitting system is proposed. The general layout of the system is shown in Figure 3.1.

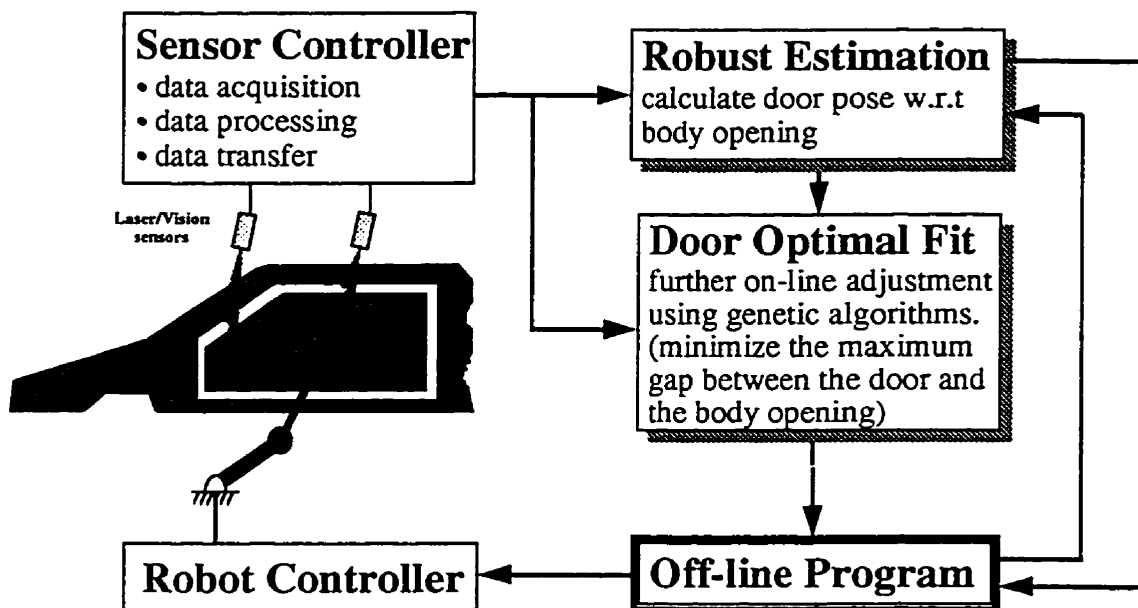


Figure 3.1 System layout

It has to be emphasized that while fully automated assembly requires the integration of the control system and off-line programming, they are not considered here. The work presented in this thesis deals only with system calibration, positioning and fitting of the door into the body opening.



The proposed system can be divided into a few separate functional blocks or subsystems:

- Sensing subsystem. A number of non-contact optical sensors are used to measure the incoming doors and car body opening before the fitting process begins. The sensors provide dimensional information about each door and body opening involved in the process. The set of data, acquired by the sensors, is used to calibrate the whole system in the calibration stage. Once the calibration is done, it will be used to determine the coordinate frame from which other set of data is referenced. The latter is compared to design intent (CAD data) for final adjustments.
- Manipulating and transfer subsystems. The transfer subsystem holds the BIW and bring it to the fitting station. At this stage the body opening is stationary; however, its position would vary from car-to-car relative to the world coordinate frame of reference. The manipulator which locates and grabs the door is an industrial robot programmed to execute a certain path which can be modified using results of the measurements and adjusting algorithms. The robot has to provide the necessary accuracy and load capacity. In addition, the flexibility exhibited in the end-effector (suction cups) must be as low as possible. The feasibility and improvements of such properties is, however, beyond the scope of this work.
- The computational subsystem. It comprises two major algorithms: (1) An estimation algorithm which is responsible for estimating the door position in 3-D space relative to a fixed (nominal) coordinate frame. The algorithm is part of a more general technique which deals with the calibration with the calibration phase as well as the production phase, and (2) a fitting algorithm which is responsible for ensuring an optimal fit of the door by minimizing the gap between the door and the body opening. A number of fitting points along both of them are measured

relative to a pre-determined coordinate frame and gaps are compared to the nominal values. Finally, the errors between the actual and the nominal gaps are optimized using a certain objective function which reflects the quality of the fit.

### **3.2.1.1 Visual On-line Sensing**

As a result of the recent advances in sensing technology many on-line sensors for industrial applications have been developed (Bieman and Pogue, 1986; Rotvold, 1995; Pastorius, 1995). In the automotive assembly application the sensing system should meet the following requirements:

- high measurement rate
- high measurement accuracy and repeatability
- capability of extracting different types of information from the sensed object
- insensitivity to electromagnetic noise and mechanical vibration.

Optical Coordinate Measuring Machines (OCMMs) satisfy most of those requirements, and their suitability to automotive monitoring and assembly applications was verified. In the following, light is shed on OCMMs and on how they can be utilized on the factory floor.

OCMMs were first introduced in 1988 from machine vision gauging. Their sensors are optical devices which are based on the principle of laser triangulation (Figure 3.2). Each sensor employs a combination of laser source to create a structured light pattern and a CCD camera (with an array of photosensitive detector) which captures the image of the laser light reflected from the part. Both the laser and the camera are usually enclosed in a common housing for accurate alignment of their optical axis. The laser is equipped with optics to project a pattern of structured light. The character of this pattern (line, plane or multiple planes) depends on the type of the sensor and the feature measured. During the

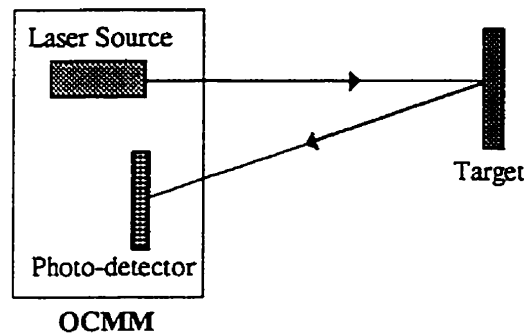


*Figure 3.2 Sensing using Laser Triangulation*

manufacturing process, each sensor is calibrated to determine its internal geometry and optical characteristics and establish the sensor coordinate frame. Under operation, the position of a feature or checkpoint is calculated with respect to the sensor coordinate frame. Then, through a transformation of the coordinate frame, the absolute position of the points can be calculated. The absolute position can then be compared with the design intent to determine the amount of deviation in each direction

Calibration of OCMM (determining the coordinate frame of each sensor) can be done using another measurement system, such as a CMM or a set of theodolites (Dewar, 1988).

In the context of process control, OCMMs can provide the opportunities to quickly and efficiently improve the dimensional quality of the automobile because it can measure the dimensions of each BIW produced, resulting in 100% measurement. The accuracy and repeatability of the OCMM measurements are good for automobile BIW assembly processes - an accuracy of 0.1 mm and repeatability of  $\pm 0.02$  mm were reported in (Pastorius, 1995). In addition, an OCMM is better suited than a CMM and hard gauges since it provides the largest sample size which is available from the assembly process.

Typically, a number of sensors are located around the part at some pre-selected locations. They are usually mounted on simple brackets, and different types (surface, edge,

and/or hole) can be mixed in a single station. All sensors can be connected to one system controller. The controller is a multifunctional unit combining functions of A/D converter, sensor multiplexer, image processing, data extraction and interfacing.

### 3.2.1.2 Visual Fixturing vs. Hard fixturing

The main purpose of the fixture is to guarantee known positions for the part. Locating a rigid part on the fixture is carried out, most of the time, according to the 3-2-1 principle to fulfill the six degrees of freedom constraints. The “3-2-1” principle is a locating method to uniquely locate a rigid body with minimal geometry features (ANSI Y13.5M, 1982). In general, three nets (or locators) are used to define a datum plane in the I/O direction, Two nets are used to define the U/D direction, and one net is used to define the F/A direction (Figure 3.3). For flexible parts, three nets are not sufficient to define the I/O primary plane. Instead,  $N$  (where  $N \geq 3$ ) nets are required. This is called the “N-2-1” principle (Cai *et al*, 1994).

Using hard fixturing for assembly incorporates many problems; besides being very expensive and very inflexible, when the complexity of the part is built up through the manufacturing and subassembly processes, tolerance stack up will be experienced, and this, in turn, will cause part variations from the fixture nets. Tooling holes clearances as well as nets wear add more variation to the process and makes them unreliable references.

As opposed to hard fixturing a visual fixturing technique is proposed. Visual fixturing uses sensors, in an OCMM station, to create reference points for the measured part. Based on the information from the sensors, and by using some algorithms, the difference between the part's actual and desired locations can be found.

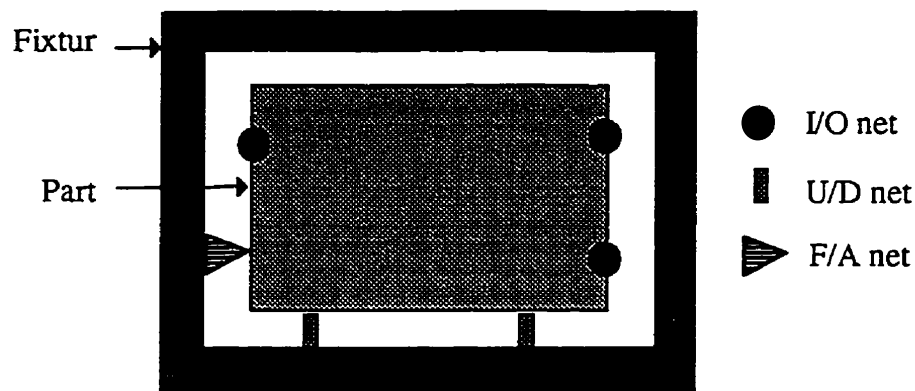


*Figure 3.3 Part Fixturing according to the 3-2-1 principle*

Nominally, a certain part is defined in terms of the coordinates of a set of points. On the other hand, corresponding CAD models of the part can be defined in terms of various features, such as points, lines, and/or planes. While, in principle, the measurement of three non-collinear points gives sufficient information to identify spatial location and orientation for rigid bodies, this was found invalid for industrial parts of complex geometry, and whose features are manufactured with certain accuracy (Pasek, 1993). For that reason, measurements beyond what is necessary and sufficient to create a reference for the part location are required.

### 3.2.2 Assembly Sequence

1. Loading : The automobile body arrives at the fitting station. An industrial robot moves to the door rack and picks up the door (it is assumed that the location of the end effector with respect to the world frame is fixed, so that the robot picks up the door from the same location (in world space) in each case).
2. Move to the measurement position : The robot moves the door in front of the body opening. At this programmed location, laser sensors pointing at the door edge (or some other features) calculates the XYZ coordinates of points along the edge.
3. Estimation of the door location : The sensor readings are mapped (using direct calibration) into an estimation of the door location with respect to the world

coordinate. This location will serve as a “body coordinate system” from which readings to be taken from the body opening will be referenced.

4. Optimal door fitting : The same set of laser sensors (or another one, depending on the cell setup) is used to calculate the XYZ coordinates of points along the body opening edge (which correspond to those along the door), and using an optimization algorithm an optimal fit can be determined, and an incremental adjustment (calculated with respect to the body coordinate system) can be found.
5. Path modification : Once the amount of correction is found, it is sent to the robot controller, and a new position can be calculated. The robot moves the door to its final and “best” location.

### 3.3 Direct Calibration

Direct calibration, as defined in (Murray and Pohlhammer, 1994), is a non-model specific, straightforward method of whole system calibration for sensor-guided flexible assembly systems. The entire assembly system - the robot, the sensors and the parts to be assembled - is calibrated for the required assembly task in a single procedure to directly determine the relationship between the part feature information in sensor coordinates and the part location (position and orientation) in robot coordinates

The concept of direct calibration is quite straightforward and can be implemented by the following three-step procedure. The first two steps are associated with the calibration process, whereas the third step is associated with on-line operation.

1. Acquisition of calibration data : The assembly robot moves the part to be assembled by known amounts under the view of the sensors to generate calibration data.

2. Determination of Process Mapping : The best-fit mapping between sensor data and part location in robot coordinates is determined from the calibration data.
3. Production Usage : During operation, the process mapping is used to yield estimates of part locations with respect to their nominal positions at calibration.

Although the concept is simple, effective implementation reduces to a set of highly coupled trade-offs between mapping performance, mapping method, robustness, sensor configuration, calibration set size, and calibration time. Because the performance of direct calibration is largely determined by how well the general process mapping from sensor data to part location in robot coordinates can be learned from the limited calibration data set, a critical issue is the method used for mapping the process. Two formulations for determining the process mapping are considered in this work, and a discussion of their relative merits is presented in the following section.

## 3.4 Working Example

### 3.4.1 Problem Statement

In order to study the performance of the direct calibration method, the door geometry was simplified (Figure 3.4). The door is allowed to translate and rotate in all six degrees of freedom -  $x$ ,  $y$ ,  $z$ ,  $\alpha$ ,  $\beta$  and  $\gamma$ .

An arbitrary arrangement of the sensors was selected as shown in Figure 3.5. The sensor readings were simulated to give the coordinate deviations for the check points under considerations. For a perfect door located in its nominal location all readings will be zero. Analytically, the sensor readings can be determined by calculating the intersection point between the door edge and the plane crossing that edge (which simulates the laser plane emitted from each sensor).

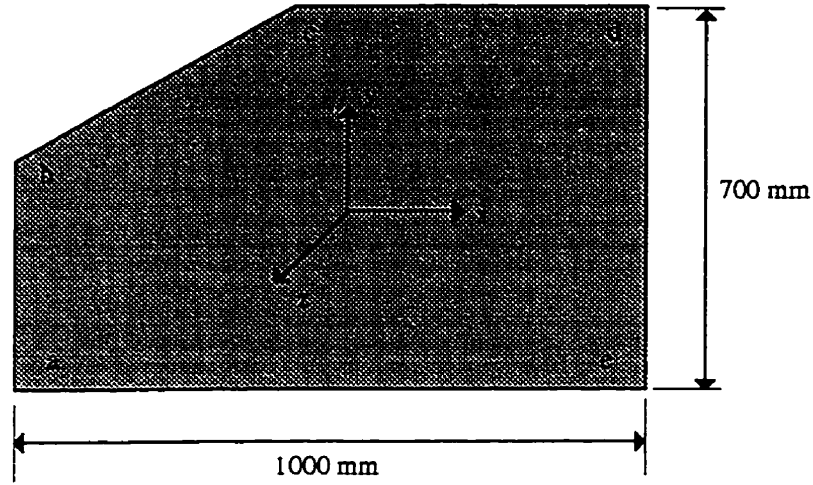


Figure 3.4 Schematic of the planar door

For example  $s_1$ , which reads the  $x$  coordinate of the location shown in Figure 3.5, is found as follows:

- The laser plane is simulated by the plane  $y = -175$
- The edge  $\overline{ab}$  is represented by the line equation:

$$\frac{x - x_a}{x_b - x_a} = \frac{y - y_a}{y_b - y_a} = \frac{z - z_a}{z_b - z_a} \quad (3.1)$$

- Now, the sensor reading can be calculated as :

$$s_1 = x_{\text{actual}} - x_{\text{nominal}} \quad (3.2)$$

where

$$x_{\text{nominal}} = -500 ,$$

and from Equation (3.1)

$$x_{\text{actual}} = \frac{(-175 - y_a)(x_b - x_a)}{(y_b - y_a)} + x_a$$



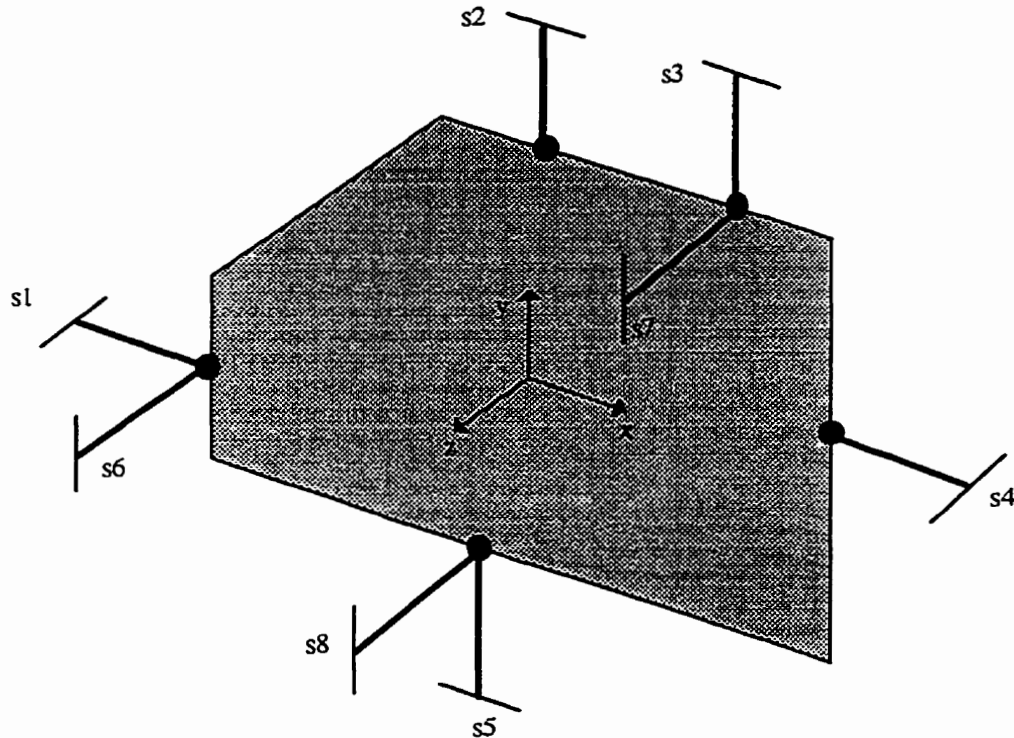


*Figure 3.5 Schematic diagram of sensor's arrangement (door at nominal location)*

Sensor noise can be modeled as a random variable having a zero-mean Gaussian distribution with a standard deviation of 0.05 mm (which represents the kind of noise encountered in most sensors used for such an application). Furthermore, door dimensional variations can be represented by adding certain deviations to the nominal dimensions.

### **3.4.2 Acquisition of Calibration Data**

In the actual assembly/fitting cell, the calibration data would be gathered with the door in the grasp of the robot. The door would be given perturbations in location about the desired nominal location, with data being taken from all sensors at each location.

In this example, the calibration procedure was simulated by analytically generating a set of calibration data for the nominal door. The calibration set consisted of 729 perturbations formed by taking all combinations of a small number of uniform subdivisions

of the pertinent ranges for  $x$ ,  $y$ ,  $z$ ,  $\alpha$ ,  $\beta$ , and  $\gamma$ . Three points at 4 mm intervals were used for  $x$ ,  $y$ , and  $z$ ; and three points, as well, at  $1.5^\circ$  intervals were used for  $\alpha$ ,  $\beta$ , and  $\gamma$ . This gives  $N = (3)^6 = 729$  calibration points that evenly span the part location space. The set of calibration vector is:

$$L_{cal} = \begin{bmatrix} L_1 \\ \vdots \\ L_N \end{bmatrix}_{cal} \quad S_{cal} = \begin{bmatrix} S_1 \\ \vdots \\ S_N \end{bmatrix}_{cal} \quad (3.3)$$

where,

$$L_p = [x_p \ y_p \ z_p \ \alpha_p \ \beta_p \ \gamma_p] \quad (3.4)$$

$$S_p = [s_{1p} \ s_{2p} \ s_{3p} \ s_{4p} \ s_{5p} \ s_{6p} \ s_{7p} \ s_{8p}] \quad (3.5)$$

### 3.4.3 Determination of Process Mapping

Analogous to the forward and inverse kinematics of serial-link manipulators, the process mapping represented by the calibration set of Equation (3.3) can be formulated in either of two directions, which correspond to a *forward* mapping and an *inverse* mapping (Murray, 1994).

#### 3.4.3.1 Inverse Mapping

The inverse process mapping  $f^{-1}$  is approximated by using linear and quadratic combinations of the sensor outputs to yield  $\hat{L}$ , which is an estimate of the location vector:

$$L \cong \hat{L} \equiv \bar{S} \cdot C_{inv} \quad (3.6)$$

where,

$$\bar{S} = [1 \ s_1 \ s_2 \ \dots \ s_8 \ s_1^2 \ s_1 s_2 \ s_1 s_3 \ \dots \ s_1 s_8 \ s_2^2 \ \dots \ s_8^2] \quad (3.7)$$

and  $C_{inv}$  is a constant weighting matrix.

In the terminology of linear regression (Appendix B), this is a second order polynomial multiple regression model with interaction terms between all input variables

(Neter, 1989). The  $N$  calibration patterns correspond to an overdetermined system of linear equations,

$$L_{\text{cal}} = \begin{bmatrix} \bar{S}_1 \\ \vdots \\ \bar{S}_N \end{bmatrix} \cdot N = \bar{S}_{\text{cal}} \cdot C_{\text{inv}} \quad (3.8)$$

which is to be solved for  $C_{\text{inv}}$  as:

$$C_{\text{inv}} = \bar{S}_{\text{cal}}^{-1} \cdot L_{\text{cal}} \quad (3.9)$$

where  $A^{-1}$  is the pseudo-inverse of  $A$  (Appendix B).

### 3.4.3.2 Forward Mapping

In an approach similar to that taken for the inverse mapping, the forward process mapping  $f$  is approximated with a regression model, which yields an estimated sensor vector  $\hat{S}$ ,

$$S \equiv \hat{S} \equiv \bar{L} \cdot C_{\text{for}} \quad (3.10)$$

where

$$\bar{L} = [1 \ x \ y \ z \ \alpha \ \beta \ \gamma \ x^2 \ xy \ xz \ x\alpha \ x\beta \ x\gamma \ y^2 \ yz \ \dots \ \gamma^2] \quad (3.11)$$

and  $C_{\text{for}}$  is a constant weighting matrix.

As before, the  $N$  calibration patterns correspond to an overdetermined system of linear equations,

$$S_{\text{cal}} = \begin{bmatrix} \bar{L}_1 \\ \vdots \\ \bar{L}_N \end{bmatrix} \cdot C_{\text{for}} = \bar{L}_{\text{cal}} \cdot C_{\text{for}} \quad (3.12)$$

which is to be solved for

$$C_{\text{for}} = L_{\text{cal}}^{-1} \cdot S_{\text{cal}} \quad (3.13)$$

### 3.4.4 Production Usage

In production, the door location must be determined from the sensor data for the current door. For the inverse mapping, this is trivial and can be calculated directly from Equation 4. However, to use the forward mapping in production, an iterative procedure is required to calculate the part location for the current part.

#### 3.4.4.1 Iterative Inversion of Forward Mapping

Starting with  $\hat{L}_0$ , as initial guess for location of the current part, the forward mapping is evaluated to obtain  $\hat{S}$ , an estimate of the sensor vector. This estimate is compared with the actual sensor vector,  $S$ . If the sensor vectors do not agree to within some acceptable limit, the location estimate is unacceptable and must be adjusted accordingly. This process is repeated iteratively until the difference between the estimated and the actual sensor vectors is acceptably small, indicating that the location estimate is correct. This iterative inversion procedure minimizes the cost function

$$F_{\Pi} = \frac{1}{2} \sum_{j=1}^8 (\hat{s}_j - s_j)^2 \quad (3.14)$$

The minimization of  $F_{\Pi}$  has been found to be well behaved, and a simplex search algorithm was found to be effective.

### 3.4.5 Simulation Results

The problem was simulated using MATLAB® (MathWorks, 1992) by implementing the concepts and techniques discussed in the previous sections. A calibration data set was generated taking into consideration door variations. The variations were assigned randomly to the door dimensions by adding random perturbations to the spatial coordinates XYZ of the corner points defining the door geometry. As in sensor noise, the variation was assumed to have a Normal distribution with zero mean and standard

deviations equal to  $1/3$  for the X and the Y coordinates; and  $2/3$  for the Z coordinates (the I/O direction).

In order to investigate the effect of sensor noise and door variation on the estimation of the door location, four cases were evaluated:

- a) a nominal door without sensor noise,
- b) a nominal door with sensor noise,
- c) a deformed door without sensor noise, and
- d) a deformed door with sensor noise

For each case, 100 runs were conducted so that in each run a location is generated randomly (based on a uniform distribution which covers a specific space). This will result in 100 actual locations which will be compared to the corresponding estimated ones using the “iterative inversion of forward mapping” technique as was described in section 3.4.4.1.

Figures 3.6, 3.7, 3.8 and 3.9 show the residual errors plotted against the number of runs for the above mentioned cases respectively. shows the performance statistics for all four cases, and Figures 3.6 shows the residual errors plotted against the number of runs for the fourth case (deformed door with sensor noise). For the nominal door, the performance is very good. However, the performance degrades significantly for the deformed door, even without sensor noise. The addition of sensor noise has little effect since the deformed door is already degraded. It is also obvious from both Table 3-1 and Figures 3.8 and 3.9 that for the deformed door (with and without noise) there is a shift (or bias) in the location estimate.

*Table 3-1 Residual errors statistics for the four cases using the iterative forward mapping method*

		x [mm]	y [mm]	z [mm]	$\alpha$ [deg]	$\beta$ [deg]	$\gamma$ [deg]
Nominal part without noise	mean	0.001	0.000	-0.000	0.000	-0.000	-0.000
	sigma	0.007	0.011	0.008	0.003	0.001	0.002
	min	-0.023	-0.025	-0.021	-0.006	-0.004	-0.005
	max	0.017	0.038	0.021	0.008	0.002	0.005
Nominal door with noise	mean	0.014	0.005	0.003	0.005	-0.001	-0.002
	sigma	0.062	0.081	0.043	0.012	0.006	0.019
	min	-0.152	-0.223	-0.106	-0.033	-0.015	-0.044
	max	0.123	0.184	0.100	0.045	0.015	0.042
Deviated door without noise	mean	0.507	0.496	1.018	0.001	-0.003	-0.000
	sigma	0.132	0.219	0.326	0.067	0.039	0.042
	min	0.218	0.003	0.367	-0.158	-0.085	-0.087
	max	0.812	0.946	1.621	0.181	0.087	0.102
Deviated door with noise	mean	0.494	0.491	1.021	0.001	-0.003	-0.001
	sigma	0.142	0.233	0.333	0.068	0.040	0.047
	min	0.222	-0.119	0.331	-0.151	-0.086	-0.120
	max	0.862	1.003	1.664	0.175	0.083	0.112

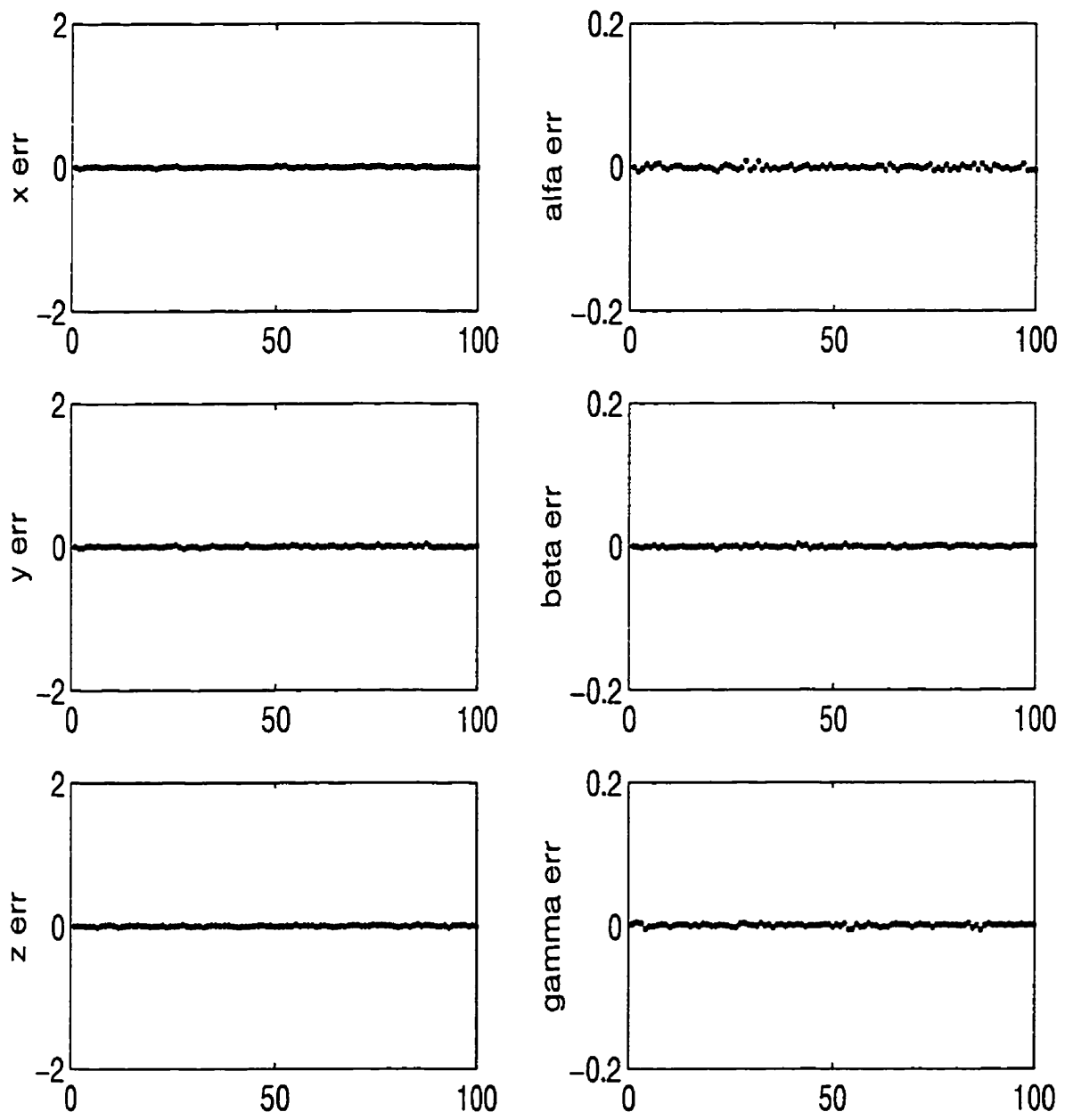


*Figure 3.6 Residual errors using the forward mapping method (nominal door without noise)*

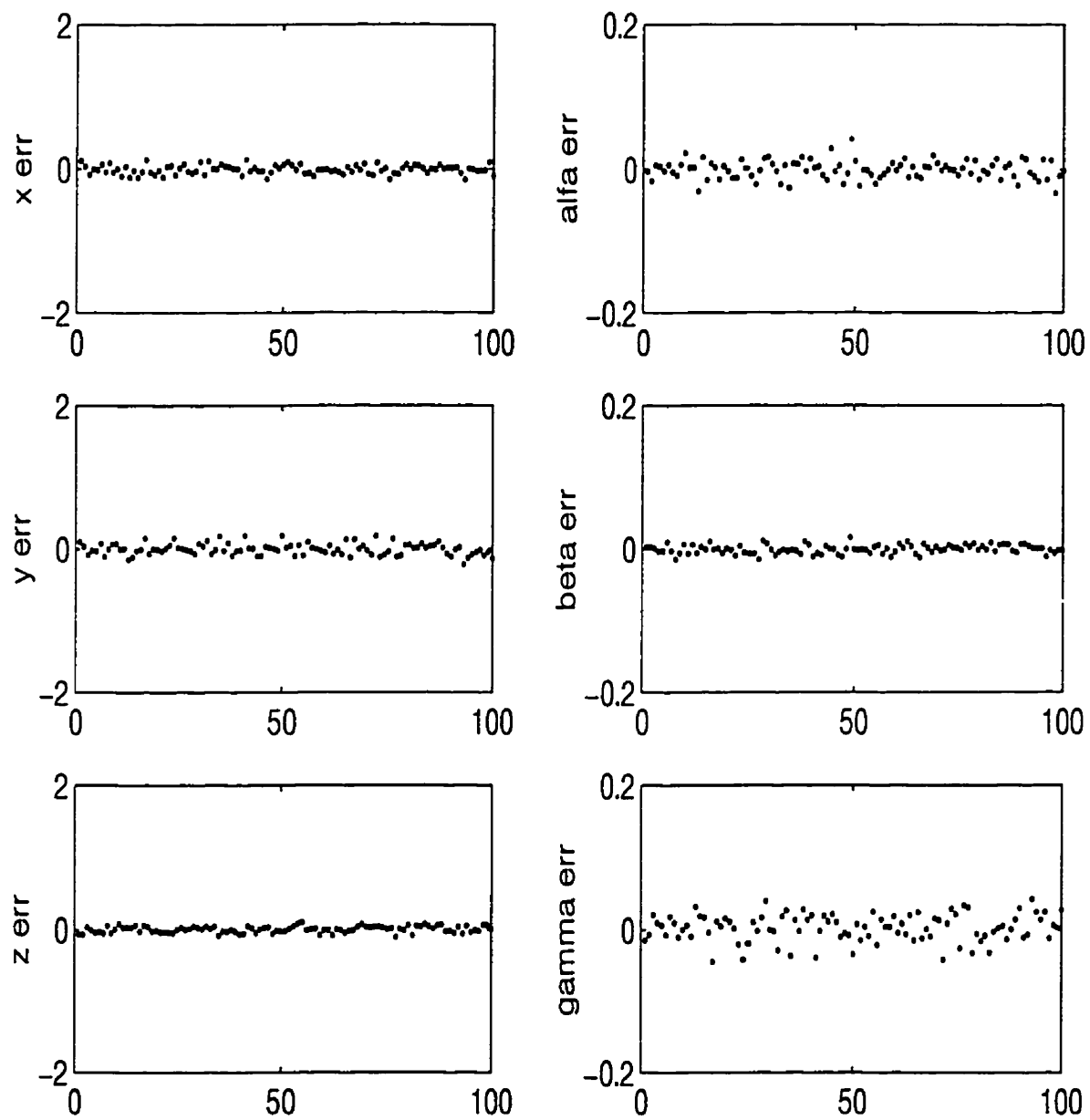
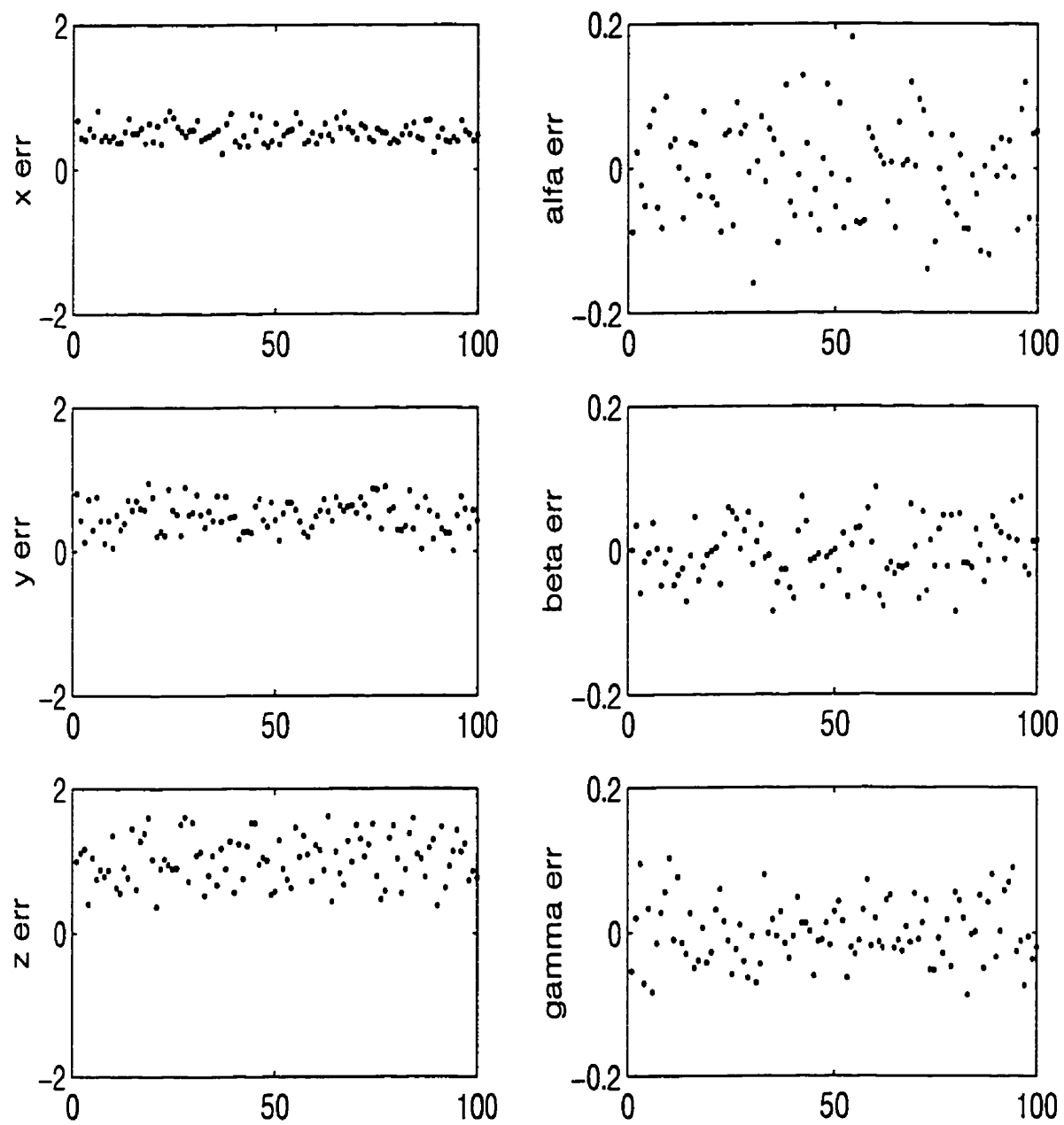


Figure 3.7 Residual errors using forward mapping (nominal doors with noise)





*Figure 3.8 Residual errors using forward mapping (deformed doors without noise)*

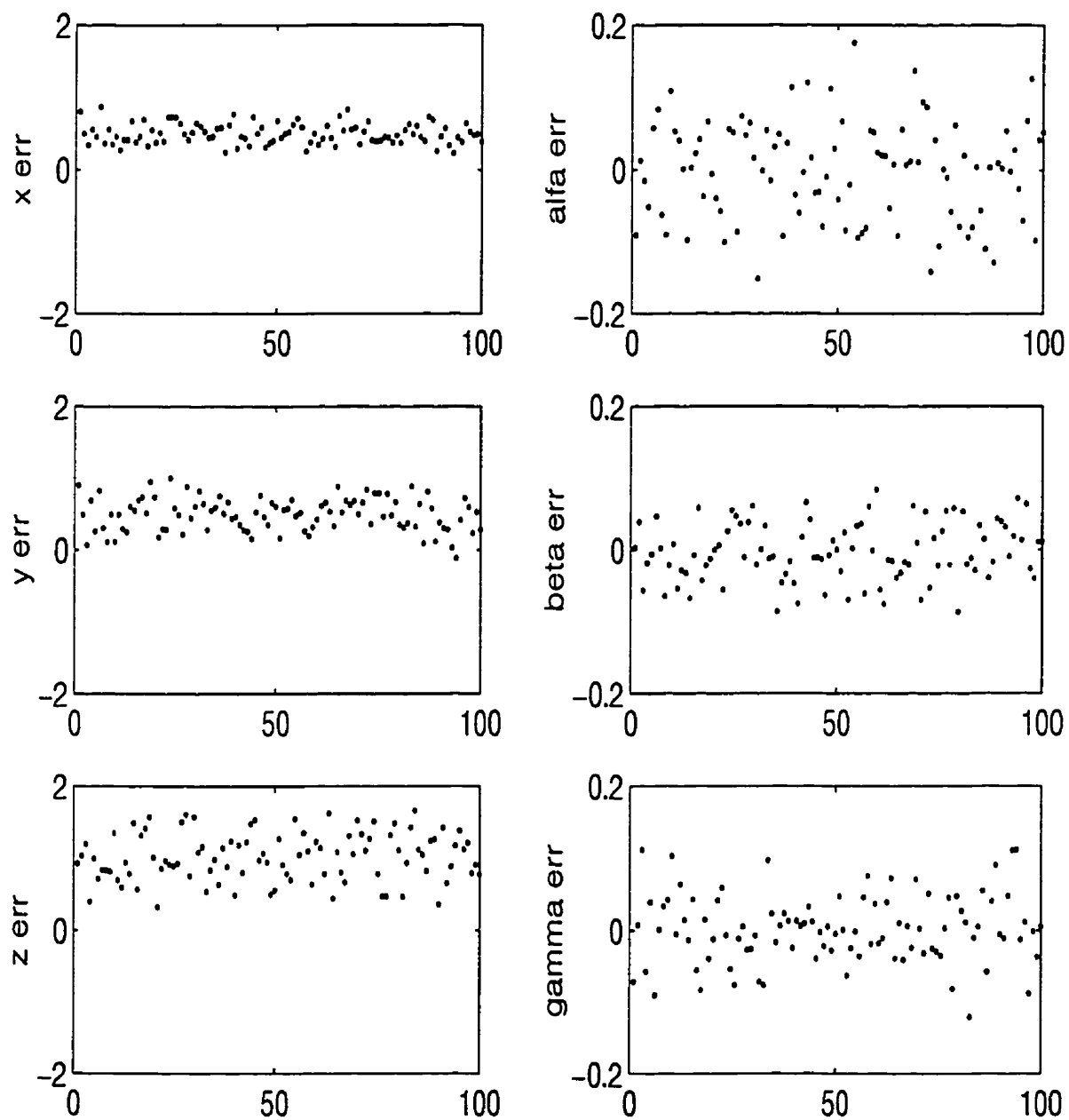
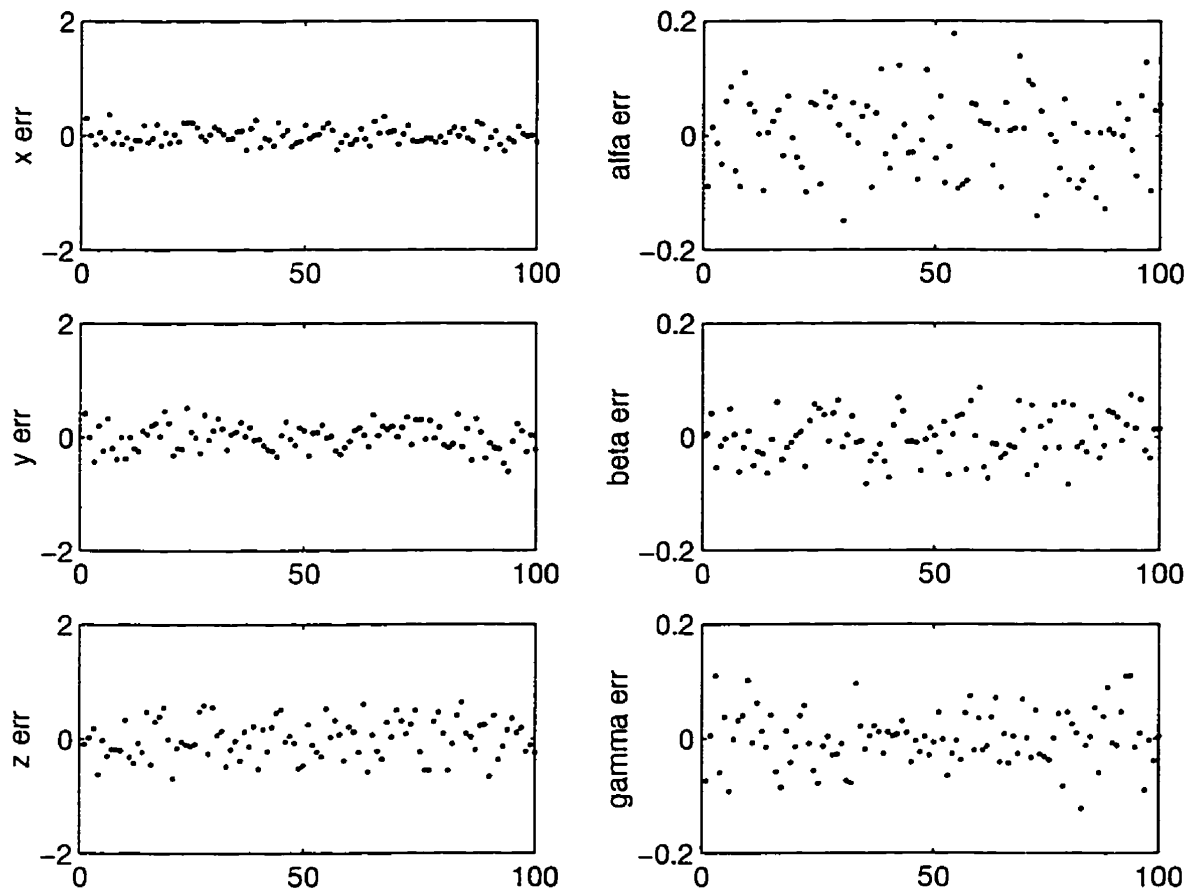


Figure 3.9 Residual error using the forward mapping methods (deformed doors with noise)

The position estimates can be further improved by subtracting the mean error of the estimation model from the values obtained using the iterative forward mapping. By doing so, the position errors will be centered around the zero (the target value) (Figure 3.10) This way the estimation bias is removed from the estimated locations. Other methods that can be explored in future research for removing the estimation bias include the Jackknife method (Shao and Tsui, 1996). This way the estimation bias is removed from the estimated locations. Other methods that can be explored in future search for removing the estimation bias include the Jackknife method (Shao and Tsui, 1996) Although the absolute maximum was reduced almost by 50%, the errors are not small enough due to the relatively high standard deviations associated with the presence of the manufacturing deviation (Table 3-2)

*Table 3-2 Residual errors statistics for the case (c) after subtracting the mean error from the estimates*

		x [mm]	y [mm]	z [mm]	$\alpha$ [deg]	$\beta$ [deg]	$\gamma$ [deg]
<i>Deviated doors with noise</i>	mean	0.000	0.000	-0.000	0.000	-0.000	-0.000
	sigma	0.142	0.233	0.333	0.068	0.040	0.047
	min	-0.271	-0.610	-0.689	-0.149	-0.083	-0.122
	max	0.368	0.512	0.643	0.177	0.086	0.110



*Figure 3.10 Residual errors for the "deviated doors with noise" case after subtracting the mean error*

## **4. CHAPTER FOUR**

# **OPTIMAL DOOR FITTING**

Among automobile body fit and quality concerns, the door fitting problem has been ranked within the top items due to the high warranty cost. An inadequate door fit causes water leakage, wind noise and difficulties in closing. In addition, it affects the car appearance and makes unfavorable impression on the customers about the car quality. Sources that cause such bad fit are mainly the dimensional variation of the door and the body opening as well as the variations of the hanging (fitting) process; for an automated process, such as the one proposed in this work, this will include positioning of the body, repeatability of the robot and measurements errors.

In this chapter, the door fitting problem is defined and formulated. The mathematical formulation is tested for multimodality and an optimization algorithm using genetic algorithms is suggested accordingly. The algorithm is enhanced by combining a genetic algorithms with a direct search method, and comparison of the results are conducted. Finally, the choice of the objective function is discussed and recommendations are made.

### **4.1 Problem Statement**

A door is said to be fitable when all its dimensional measurements are within tolerance after applying a homogeneous transformation to it (Figure 4.1). Hence, a fitable door can be positioned onto the body opening and bolted to it through the hinge subassembly. It is assumed in this thesis that the door is fitable. In addition, it is assumed that the hinge subassembly has no effect on the fitting process; in other words, the door is

free to move in all degrees of freedom without any constraints. The objective in this work, is to find the best (or optimal) fit for such a case.

A best fit can be achieved if a certain function was formulated and its minimal or maximal was determined. This function should represent measurements of the door and

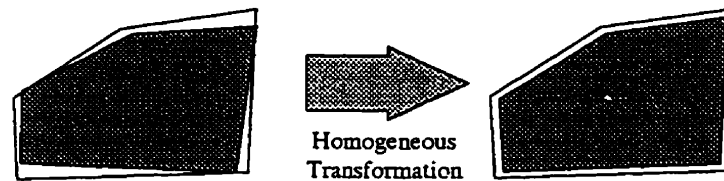


*Figure 4.1 A schematic diagram showing the concept of a fitable door*

the body opening after applying a homogeneous transformation to the door.

#### 4.1.1 Definition of Quality Indexes

Two Key Characteristics that reflect the quality of the door fit are the “gap” and “flushness” of the door with respect to the body opening. The gap is the clearance between the door and the body opening in the x-y plane, and the flush is the clearance in the z-direction (Figure 4.2)

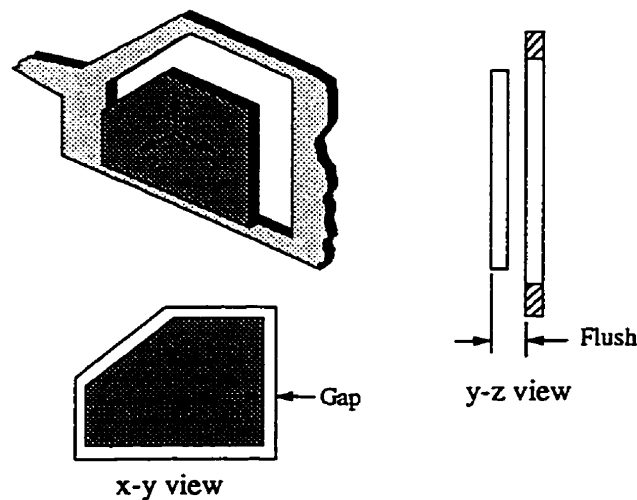


*Figure 4.2 Gap and flush between door and body*

As a measure of the quality of the gap (and flushness)<sup>1</sup>, three indexes are used. These are: (1) maximum gap deviation (MAXD) from design values, (2) average gap width deviation (GWD) and (3) gap parallelism (GP), i.e., gap width variation from top to bottom of the door. In order to calculate these indexes, a number of check points along the door edge, and corresponding points along the body opening edge, have to be selected and the absolute distance between every two corresponding points has to be calculated. Let  $n$  represent the number of check pairs chosen, and the gaps (distances) denoted by  $x_i$  ( $i = 1, 2, \dots, n$ ), then the three door-fit quality indexes can be defined as follows:

$$\text{MAXD} = \max \{ x_i - \textit{nominal gap} \} \quad (4.1)$$

$$\text{GWD} = \frac{\sum_{i=1}^n |x_i - \textit{nominal gap}|}{n} \quad (4.2)$$

$$\text{GP} = \frac{\sqrt{\sum_{i=1}^n (x_i - \textit{nominal gap})^2}}{n} \quad (4.3)$$

These indexes will measure the variation for each individual case (within-car variation as opposed to car-to-car variation). Theoretically, the target values for the three indexes are all zero. However, usually tolerances are specified, and can be selected to reflect a certain quality level.

The objective in this context is to find the best position and orientation of the door that would minimize the gap and flush between the door and the body opening as measured by MAXD, GWD, and GP.

---

<sup>1</sup> From now on, the word "gap" will be used to represent the Euclidean distance between two corresponding points on the door and the body opening

## 4.2 Formulation of the Optimal Fitting Problem

The optimal door fitting problem is formulated as a general unconstrained<sup>2</sup> optimization problem to orient the door in three-dimensional space using a homogeneous transformation, such that the objective function is minimized. The calculated transformation variables can then be used to determine the amount of adjustment required for the robot's end-effector (tool) position to achieve the best fit - through another fixed transformation between the door and the end-effector.

### 4.2.1 Homogeneous transformation

To orient the door in three dimensional space, a homogeneous transformation matrix needs to be obtained. A set of spatial position measurements can be represented with respect to the body frame of reference, which is obtained through the procedure discussed in Chapter 3. The relationship between these two representations can be expressed using the homogeneous transformation matrix  $T$  (Craig, 1989):

$$T = \begin{bmatrix} R_{3 \times 3} & P_{3 \times 1} \\ 0_{1 \times 3} & 1 \end{bmatrix} \quad (4.4)$$

where,

$R$  = Coordinate Rotational matrix

$P$  = Coordinate Transitional vector  $[x \ y \ z]^T$

The convention used to determine  $R$  is the Z-Y-X fixed angles convention,

$R_{ZYX}(\alpha, \beta, \gamma)$  defined by:

$$R_{zyx}(\alpha, \beta, \gamma) = \begin{bmatrix} c\beta c\gamma & -c\beta s\gamma & s\beta \\ s\alpha s\beta c\gamma + c\alpha s\gamma & -s\alpha s\beta s\gamma + c\alpha s\gamma & -s\alpha c\beta \\ -c\alpha s\beta c\gamma + s\alpha s\gamma & c\alpha s\beta s\gamma + s\alpha c\gamma & c\alpha c\beta \end{bmatrix} \quad (4.5)$$

where  $c\alpha = \cos(\alpha)$  and  $s\alpha = \sin(\alpha)$ .

---

<sup>2</sup> Assuming that the hinge subassembly does not impose any constraints on either the rotational or the translational degrees of freedom of the door. The only constraint that would be considered in this work is the minimum gap allowed between the door and the body opening.



For the above convention, rotations are performed in the following order: about the Z fixed axis by  $\gamma$ , about the fixed Y axis by  $\beta$  and finally about the fixed X axis by  $\alpha$ .

Now if a set of measurement data, representing the spatial coordinates of check points along the door, is presented by  $A$ ; and upon translating and/or rotating the door by certain amounts, then the new spatial coordinates of the check points  $A^*$  can be calculated by pre-multiplying  $A$  with the homogeneous transformation matrix  $T$ :

$$A^* = T A$$

where  $A$  and  $A^*$  are  $4 \times n$  matrixes. The first three rows represent the x, y and z coordinates respectively, whilst the forth raw is all ones, and the number of columns  $n$  equals the number of check points along the door.

#### 4.2.2 Objective Function

With the absence of any constraints on positioning the door, and with the objective stated as finding the optimal position of the door in the three dimensional space, the problem can be formulated as a general optimization problem with objective function  $J$ :

$$\min_{x,y,z,\alpha,\beta,\gamma} J(X_i) \quad (4.6)$$

$$J(X_i) = \left[ \sum_{j=1}^n (V_j)^p \right]^{1/p} \quad (4.7)$$

$$V_j = AG_j - NG_j \quad (4.8)$$

$$AG_j = \| B_j - T(X_i) * A \| \quad (4.9)$$

subjected to

$$AG_j(X_i) \leq v$$

where,

$$J(X_i) = \text{objective function to be minimized, function of } X_i$$

- $X_i$  = homogeneous transformation variables (the independent variables), i.e.,  $x, y, z, \alpha, \beta$  and  $\gamma$   
 $V_j$  = The  $j$ th variation of the distance between the  $j$ th measured body opening point and the  $j$ th measured door point  
 $AG_j$  =  $j$ th actual gap  
 $NG_j$  =  $j$ th nominal gap  
 $B_j$  =  $j$ th measured body opening point  
 $A_j$  =  $j$ th measured door point  
 $T(X_i)$  = homogeneous transformation matrix  
 $\nu$  = tolerance on the minimum gap allowed

The objective function to be minimized in the current study as described in Equation (4.7) describes the variation (or error), of the distances (gaps) between the body opening dimensions and corresponding door dimensions, from the desired (nominal) values.

The exponent  $p$  in Equation (4.7) can have any value between one and infinity. When  $p$  is equal to one, the problem becomes minimization of the absolute variation (determining the least variation):

$$\min \left[ \sum_{j=1}^n \|V_j\| \right] \quad (4.10)$$

When  $p$  is equal to two, the problem is a least squares one, where the objective is to minimize the sum of the squared variations:

$$\min \sqrt{\sum_{j=1}^n (V_j)^2} \quad (4.11)$$

And finally when  $p$  is equal to infinity, the problem will be to minimize the maximum variations:

$$\min \left[ \max(|V_1|, |V_2|, \dots, |V_n|) \right] \quad (4.12)$$

The selection of the objective function is a trade off between more than one criteria. This issue will be discussed in more details in section 4.5.

### 4.2.3 Multimodality of the Objective Function

Depending on the formulation of the objective function (Equations (4.10-4.12)), each formulation is expected to have certain characteristics. It is also expected that the door position (or the independent variables) will be different for each formulation. For example, the door position obtained using Equation (4.11) will not coincide with that obtained using Equation (4.12).

The multimodality issue must have a great influence on the optimization performance. An objective function is called multimodal if there were more than one minimum in its working domain, and the problem in this case, is how to reach the global minimum. In the contrary, a unimodal function has only one minimum, which can be found easily using either a gradient descent or a direct search method.

#### 4.2.3.1 Function Visualization

3-D plots for the least squares function (Equation (4.11)) as well as the maximum function (Equation (4.12)) gave a first indication that the objective function is not unimodal. Since there are six independent variables in the objective function, the 3-D plots were drawn against two variables only, while the other four were held constant. Figure 4.3 shows the least squares function as a function of the two variables  $x$  and  $z$ . For this case the function was found to be unimodal; however, for other variables (specially the rotational ones) there was an indication of multimodality in the function's response as depicted by the contours in Figure 4.4. A formal method can be used to test for multimodality taken into account all the variables is, however, desirable. One such method is *genetic algorithms* with *sharing function* which are briefly discussed in the following section.

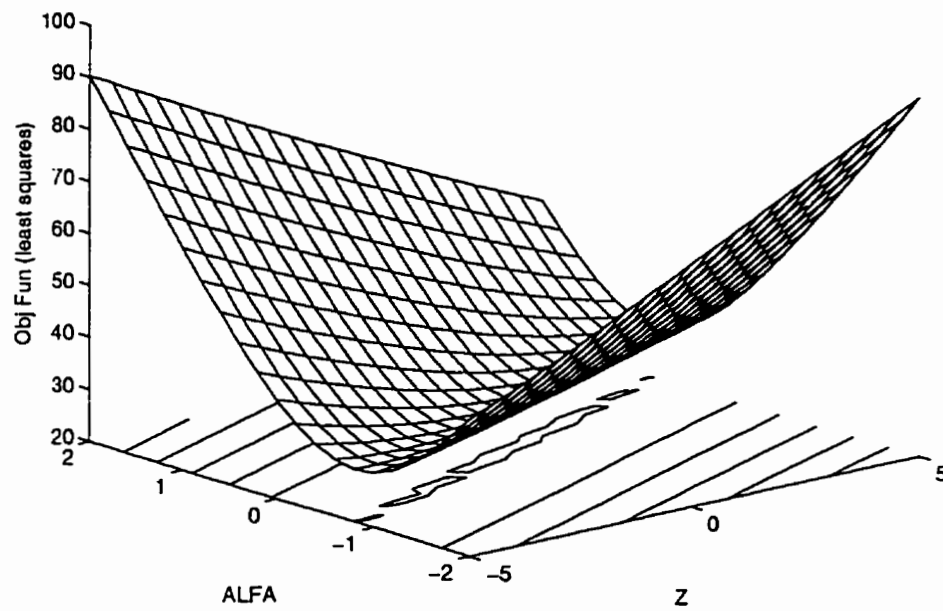


Figure 4.4 The least squares function (function of  $z$  and  $\alpha$ )

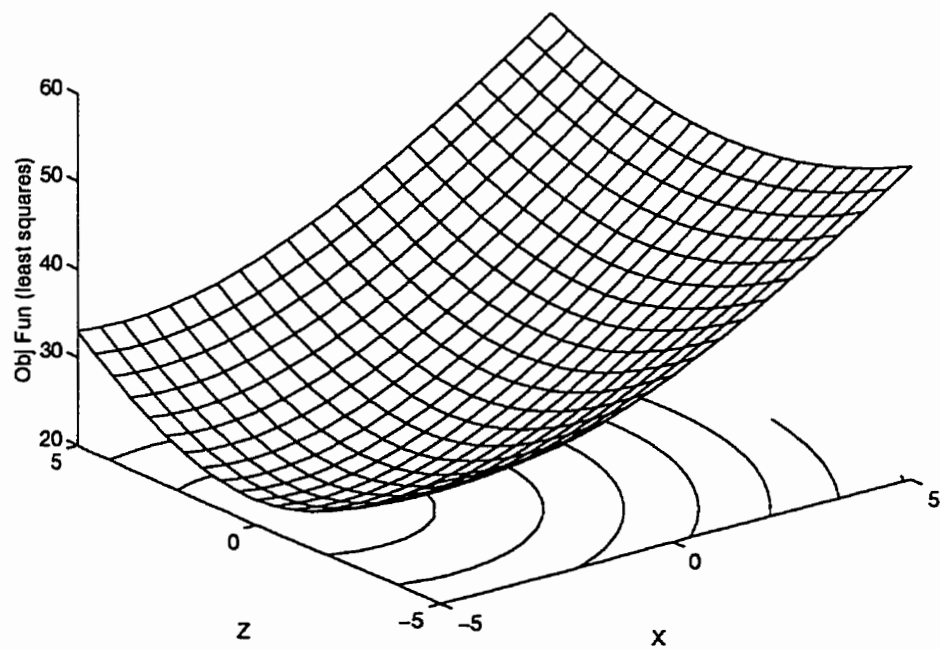


Figure 4.3 The least squares objective function (function of  $x$  and  $z$ )

#### 4.2.3.2 Overview of Genetic Algorithms

Genetic algorithms employ a form of simulated evolution to solve difficult optimization problems which cannot be solved using more conventional methods. Thus, they are often applied to problems that are nonlinear with multiple local optima. Other benefits of genetic algorithms are stated as follows:

- The resulting search is global
- No gradient information is needed
- Potential for massive parallelism
- Task independent optimizers
- They can be hybridized with conventional optimization methods

Genetic algorithms (Appendix A) work with a population of strings that encode the problem's independent variables. For example, to optimize the function  $f(x,y,z)$  the variables  $x$ ,  $y$  and  $z$  are coded as a string which serves as an artificial chromosome. Assuming that the range of variable values which contains the optimal values is known *a priori*. Hence, if the variable  $x$ , for example, has the range  $[a,b]$ , then this range can be coded into a constant length binary string form, such that:

$$\begin{aligned} 0,0,0,0 \dots, 0 &\equiv a \\ 1,1,1,1 \dots, 1 &\equiv b \end{aligned}$$

and consequently, any string having a combination of 0 and 1 values will represent a specific value in the range of  $x$ .

The population of strings (Figure 4.5), which is randomly generated at the beginning, represents a set of chromosomes which is to be evaluated. An evaluation function determines the relative performance of chromosomes in each set.

Genetic operators (reproduction, cross-over and mutation) are then applied with certain probabilities on the chromosomes' population yielding a new population which samples new points in the search space. Chromosomes are probabilistically given the chance to reproduce at a rate that reflects their "fitness" relative to the remainder of the population (best chromosomes receive better chance to reproduce than those of low performance). The transition from one population to another is known as a generation. Generations are produced iteratively until convergence. The manner in which genetic algorithms generate chromosome populations of higher average fitness than the initial one is described by the schema theory (Goldberg, 1989). Schemata are models of similarity in the chromosomes. A schemata

"1 \* \* \* ... \* " (where \* stands for 0 or 1) represents all chromosomes having the first digit equal to one. It has been shown that genetic algorithms tend to let instances of high average fitness schemata proliferate in the population with a near exponential rate. The accumulation of instances of high average fitness schemata leads the chromosomes to converge to the global maximum fitness value

0	0	1	1	• • •	0	chromosome 1
1	0	1	1	• • •	0	chromosome 2
0	1	1	0	• • •	1	chromosome 3
<div style="text-align: center;">• • • •</div>						
0	1	0	1		1	chromosome N

*Figure 4.5 Population of chromosomes*

### 4.2.3.3 Finding Multimodality using Sharing

The visual inspection of an objective function can be used for functions with one or two independent variables. A larger number of independent variables will convert the problem into a hyperspace problem. However one of the methods that can be used to inspect the modality of an objective function is the use of genetic algorithms with sharing.

Take the example of the objective function of a single independent variable shown in Figure 4.6, an initial random population of the independent variable would be

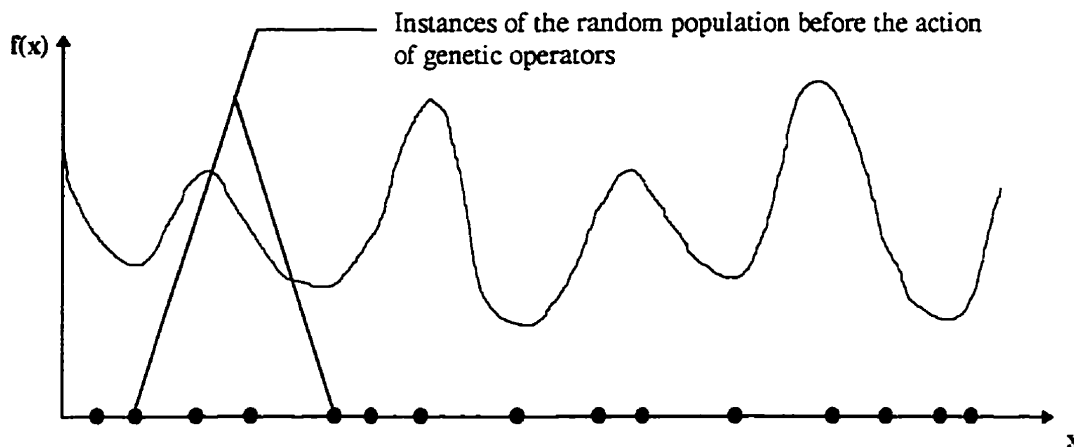


*Figure 4.6 An initial random population of the variable  $x$*

distributed along the variable's domain as shown in Figure 4.6 by the black dots.

After the iterative application of the genetic operators, the instances of the random variable accumulate in the vicinity of the global optimum value of the objective function as shown in Figure 4.7 (a).

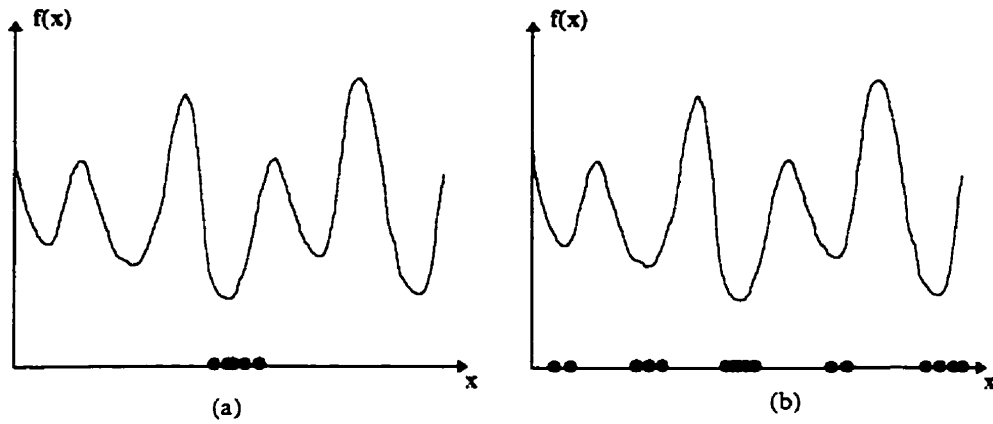


Figure 4.7 Distribution of a variable's instances after applying genetic operators; (a) without using the sharing scheme, (b) using the sharing scheme

Goldberg (1989) described a scheme that uses a *sharing function* to distribute the instances of the random variables among the various minima of the objective function. In this scheme, the fitness function (Section A.2) of each instance of the random variable is converted into another function known as the *shared fitness function* given by the following equation:

$$fs(x_i) = \frac{f(x_i)}{\sum_{j=1}^n s(d(x_i, x_j))} \quad (4.13)$$

where,

- $f$  = The fitness function
- $fs$  = The shared fitness function
- $x$  = An instance of the independent variables in the population
- $d$  = The distance function between two instances of the independent variables. Either of the Euclidean or Hamming distances can be used.
- $s$  = The sharing function which ranges between 0 and 1 and is inversely proportional to the distance  $d$ .



The shared fitness function adds more weight to the instances of the random variable which have a larger Euclidean (or Hamming) distance from the rest of the instances of the random variable in the population. The use of this function results in the creation of a number of sub-populations which accumulate at the various peaks of the objective function by the end of the application of the genetic algorithms (Figure 4.7 (b)). The size of these sub-populations is proportional to the fitness of the corresponding minimum.

The sharing scheme can be used to check for the multimodality of an objective function. If genetic algorithms, with a sharing scheme, are used to minimize a unimodal objective function the population accumulates near the unique optimum value of the function, otherwise if the function is multimodal sub-populations accumulate at the various local minima. (Figure 4.8). A histogram of the distribution of the independent variables after the application of the genetic algorithms with sharing would show a single accumulation of the instances of the independent variables if the function was unimodal (Figure 4.9)

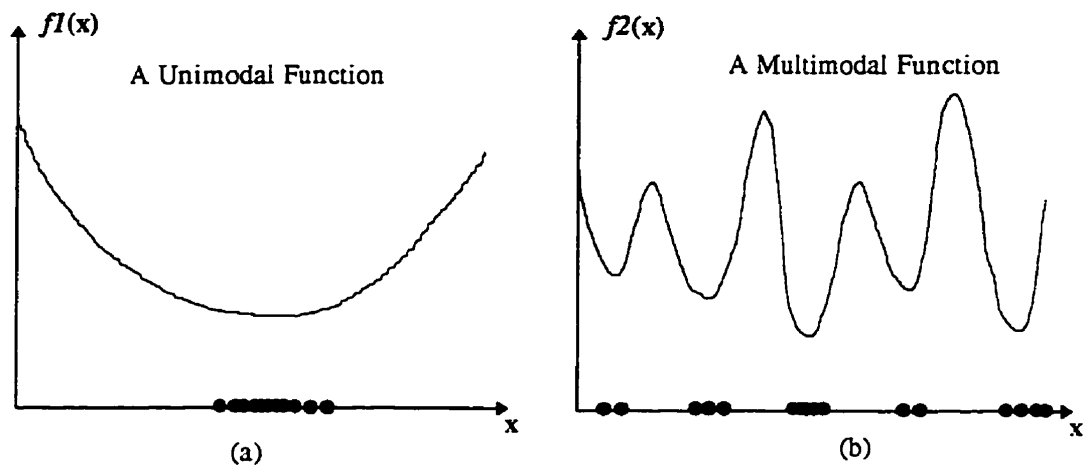


*Figure 4.8 Using the sharing scheme with: (a) a unimodal and (b) a multimodal function*

The above described methodology was used to test the optimal door fitting problem for multimodality. The same example used in the previous sections is used with the following genetic algorithm parameters:

1. Population size = 100
2. Uniform cross over probability = 0.8
3. Tournament selection
4. Triangular sharing function (Goldberg and Richardson, 1987) ( Figure 4.10).

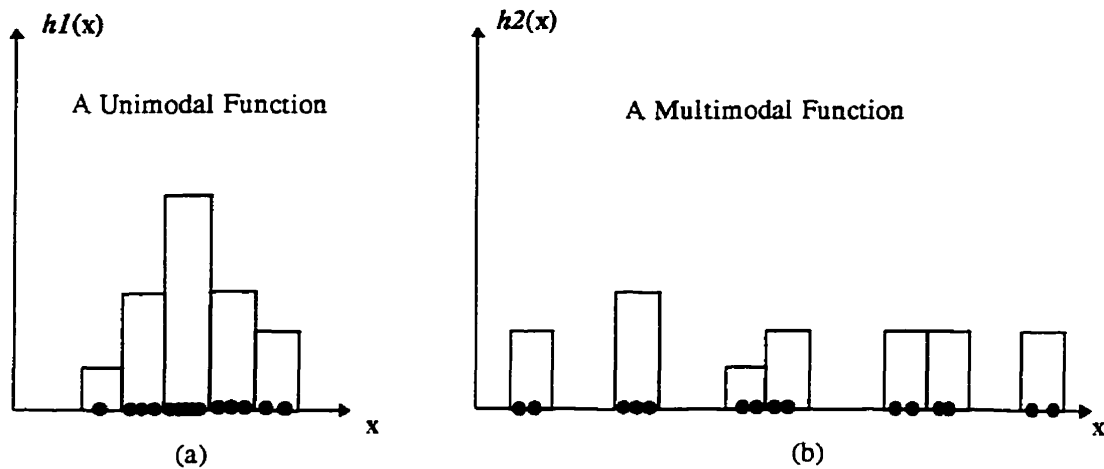


Figure 4.9 Histograms of variable  $x$  for (a) a unimodal and (b) a multimodal function

The histograms of the six independent variables in the final population are shown in Figure 4.11.

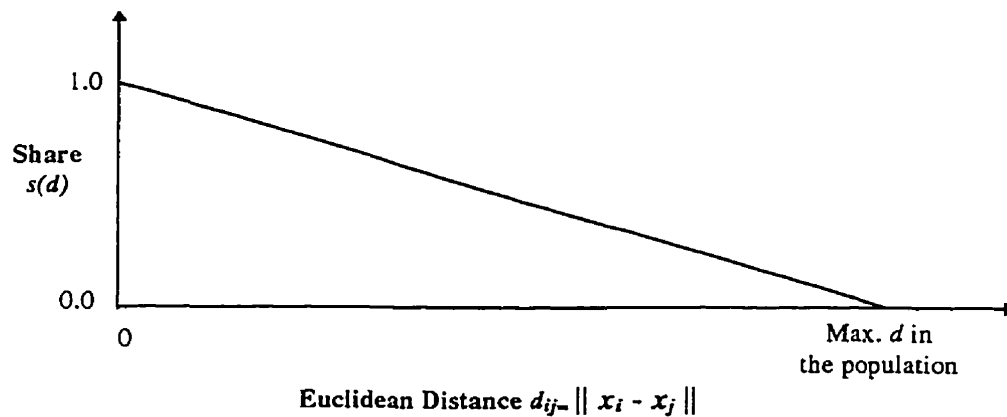


Figure 4.10 Triangular sharing function

The above shown histograms show that sub-populations of the independent variables developed. This shows that the optimal door fitting problem is a multimodal one, and that the issue of global vs. local optimality should be taken into account

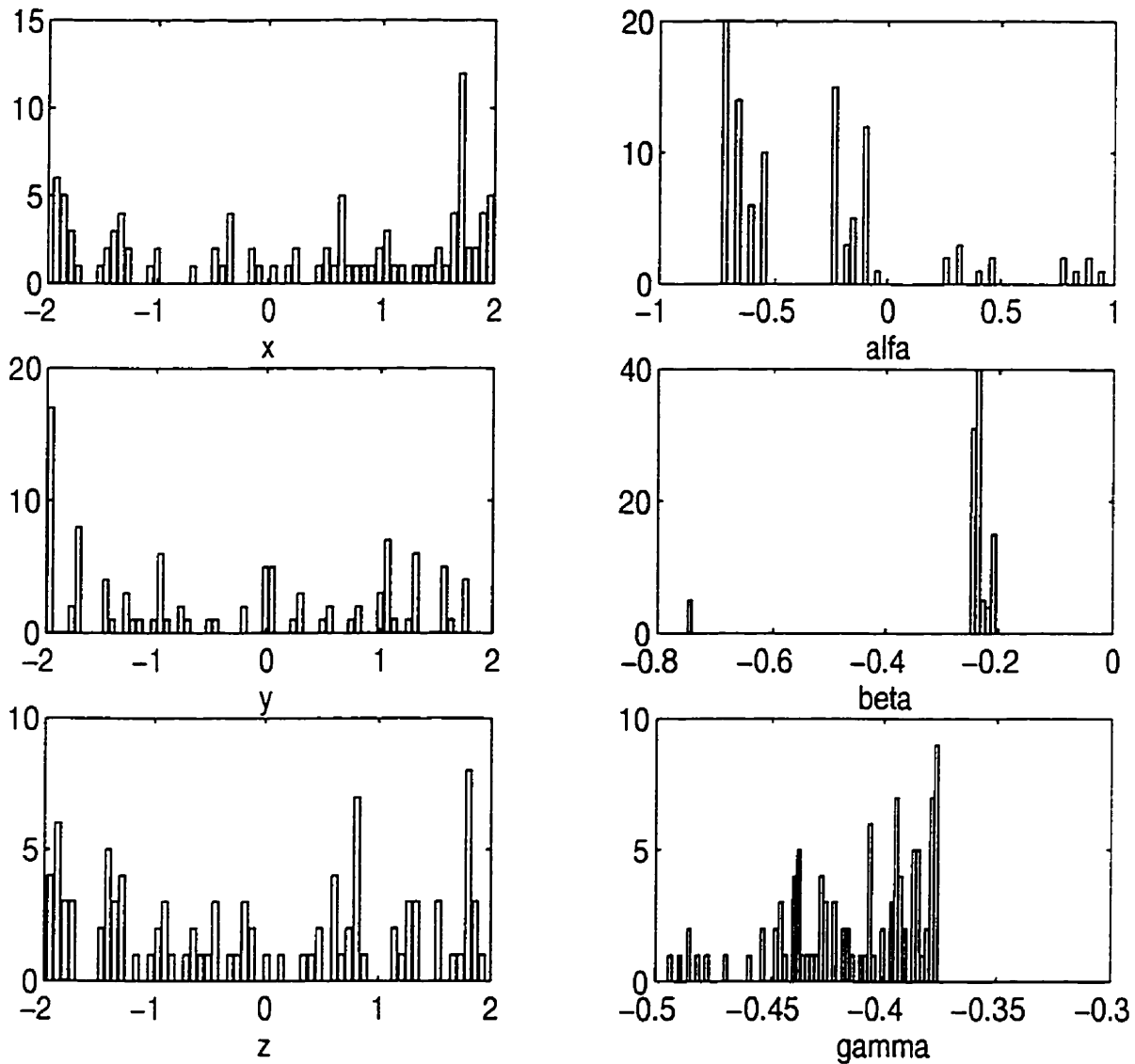


Figure 4.11 Histograms of the independent variables in the door fitting objective function by using the sharing scheme

### 4.3 Solving the Door Fitting Problem using Genetic Algorithms

As a result of the findings in the previous section, it was necessary to use an optimization method which is able to find the global optimum. The simplex search method was found to be capable of reaching the global optimum for only two or three variables (Murthy and Abdin, 1980); for more than three variable, which is the case in this study, it will act like other conventional methods where it is more likely to reach a local minimum

instead. Genetic algorithms, on the other hand, are guaranteed to arrive at a near-global optimal solution, and thus will be used to solve the door fitting problem.

#### 4.3.1 Computer Simulation

In this section, the performance of optimal fitting is evaluated by fitting a simple door to the side opening. The door dimensions and geometry will be the same as those used for direct calibration (Chapter 3). The nominal gap selected for this study was 4 mm. Figure 4.12 shows this configuration for a perfect door, body opening and gap.

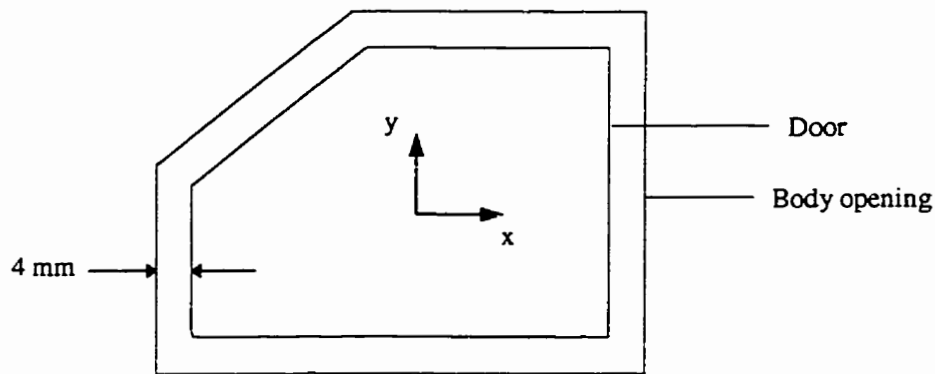


*Figure 4.12 Nominal door, body opening and gap*

The directions of deviation for the fitting points to the nominal gap on GWD, GP and MAXD are first discussed. The effectiveness of the door fitting for different door positions and manufacturing variations on the three fitting dimensional quality requirements, GWD, GP and MAXD are then presented.

The manufacturing variations on the door and the body opening are assumed to be on the same order of magnitude, and both contribute to the variations of the door gaps. The variations are simulated by superimposing Gaussian noises on the nominal values of  $x$ ,  $y$  and  $z$  dimensions.

the gap width deviation, gap parallelism and maximum deviations are calculated before and after fitting.

#### 4.3.1.1 Effects of Relative Deviations and Fitting-point locations on the Quality Indexes

As was formulated in section 4.1.1, the gap width deviation and gap parallelism are evaluated by the first moment and square root of the second moment of the deviation gaps at all fitting locations relative to their nominal directions. The maximum deviation would be the maximum gap amongst all fitting locations relative to their nominal values which is 4 mm in this case. The GWD, GP and MAXD will depend, however, on the direction of the door position deviation relative to the gaps and the spatial location of the fitting points.

Figure 4.13 shows two deviated door points with the same magnitude of deviation,  $d$ , but in different directions. Point  $A'$  is parallel to the nominal door gap. In the case of point  $A'$ , the GWD is  $AG' - NG = d$ , GP is  $d^2$  and MAXD is the same as GWD (although it is meaningless for only one point). For the point  $A''$ , the GWD and MAXD, is  $(AG'' - NG)$  which is smaller than  $d$ , and GP is  $(AG'' - NG)^2$ . More on this issue will be clarified in the following examples.

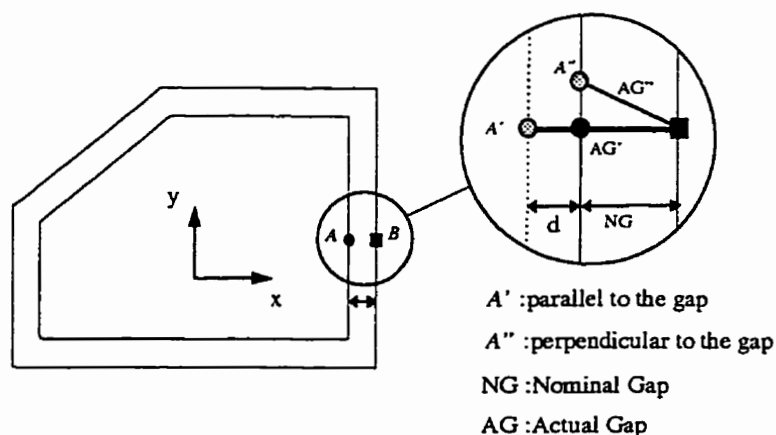
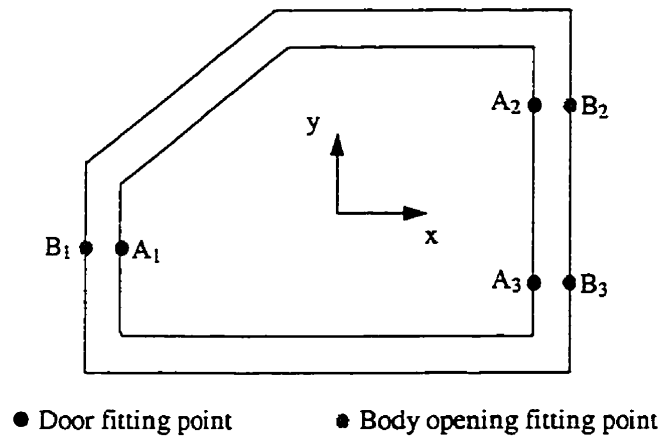


Figure 4.13 Effect of deviating direction

Figure 4.14 shows different fitting point locations subject to the same deviation, say in the x-direction. When the door is shifted to the left, the gaps at point locations 2

and 3 will increase while the gap at point location 1 will decrease. The GWD calculated based on point 2 and point 3 will thus increase and reflect the average width deviation. The GWD calculated based on point 1 and point 2 will, however, be zero and the gap quality problem will need to be reflected through either the gap parallelism or the maximum deviation.



*Figure 4.14 Effect of fitting point locations*

Simulations were conducted for 15 doors with 1 mm position deviation for both parallel and perpendicular cases. Noise, with sigma equal to 0, 0.3, 0.6 and 0.9 , were superimposed on the spatial coordinates of each checking point. Figure 4.15 shows the fitting point locations and the direction of door shift (position deviation) relative to the

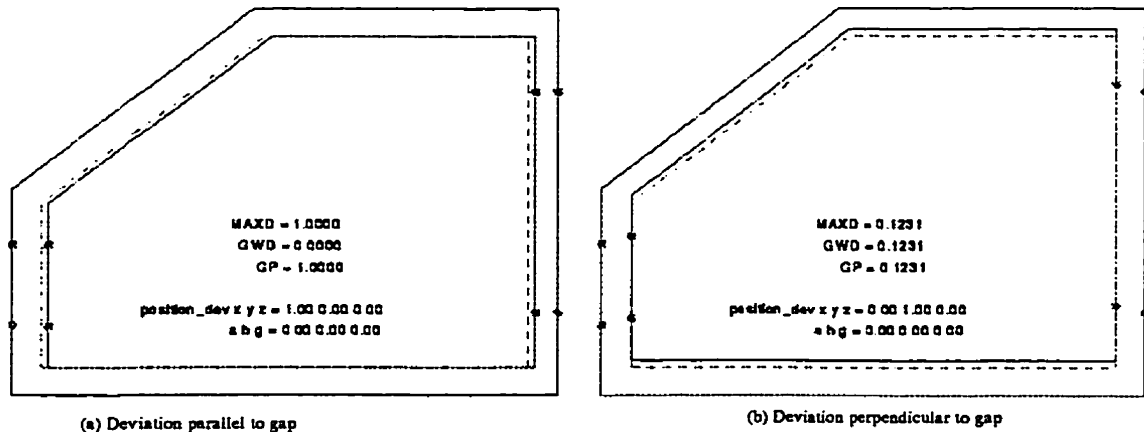


*Figure 4.15 Door and body opening before fit*

gap. Figures 4.16, 4.17 and 4.18 show GWD, GP and MAXD for the fifteen doors upon shifting the door 1 mm in the x-direction (parallel to the nominal gap). the objective function used in this situation is least squares. When there is no manufacturing variation along the door or the body opening edge, the fitting is perfect and quality indexes are equal to zero (the target value). However, upon superimposing the noise which simulates the manufacturing variations, all quality indexes start to deteriorate in proportion with the Standard Deviation (SD) value. For  $SD = 0.9$ , the maximum GWD, GP and MAXD after fit are 1.414, 1.53 and 4.6 respectively. Furthermore, it was shown that GWD after fit is not always better then the corresponding case before fit. Figure 4.19 and Figure 4.20 show the average values of each of GWD, GP and MAXD by (a) shifting the door 1 mm in the x-direction (parallel to the nominal gap) and (b) shifting the door 1 mm in the y-direction (perpendicular to the nominal gap) respectively.

As discussed before, with the absence of manufacturing deviations the GWD before fit for case (a) is zero; the two points on the left hand side have increased the gaps due to the shift in the x-direction while the gaps on the other side have decreased. The amount of GWD for case (b) when there is no noise will depend on the nominal gap value (which is 4 mm in this case); using Figure 4.13 the GWD will be  $(AG'' - NG) = 0.123$  as shown in Figure 4.20.

The gap parallelism before optimal fit for case (a), however, was shown to be much higher than that for case (b) due to the difference of the spatial locations of checking points and the parallel deviated direction in the former case. The trend in MAXD shows the same behavior as in GP. (Notice that the objective function used in those two cases is least squares).

All in all, the three quality indexes, GWD, GP and MAXD work as supplements to each other in reflecting different door gap quality variations and thus need to be combined in considering the door gap quality problems



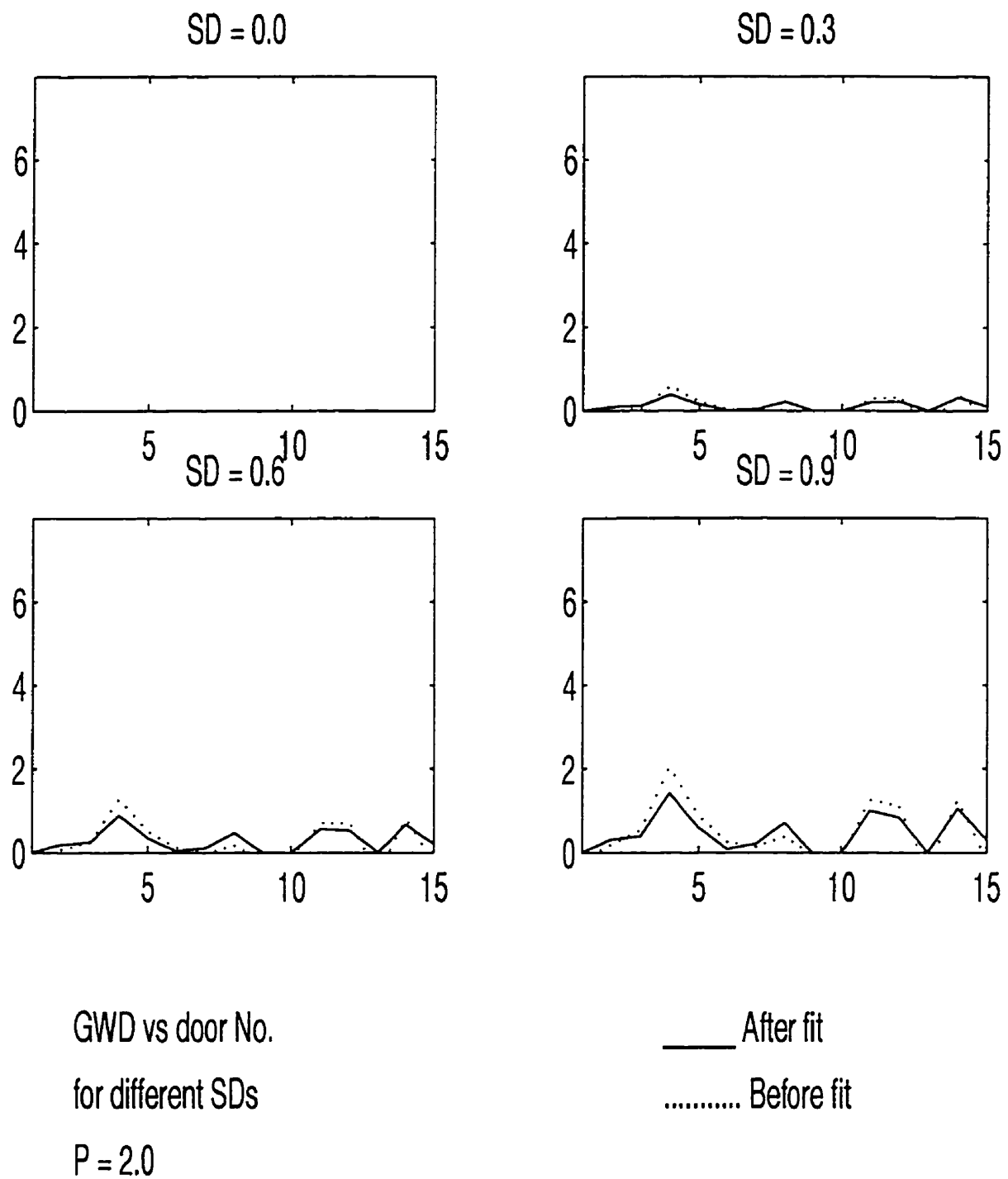


*Figure 4.16 Gap width deviation for the parallel deviation case*

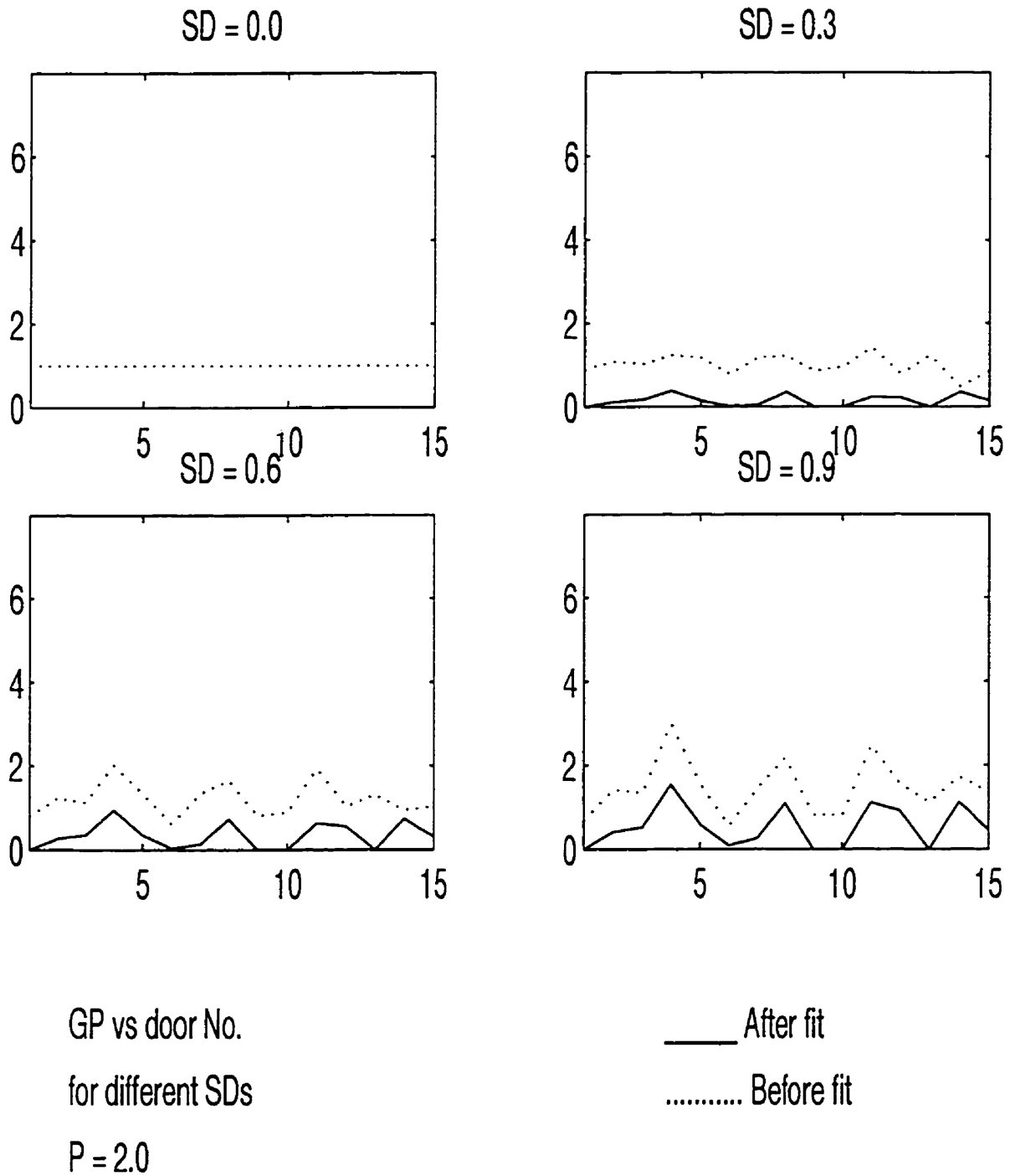


*Figure 4.17 Gap parallelism for the parallel deviation case*

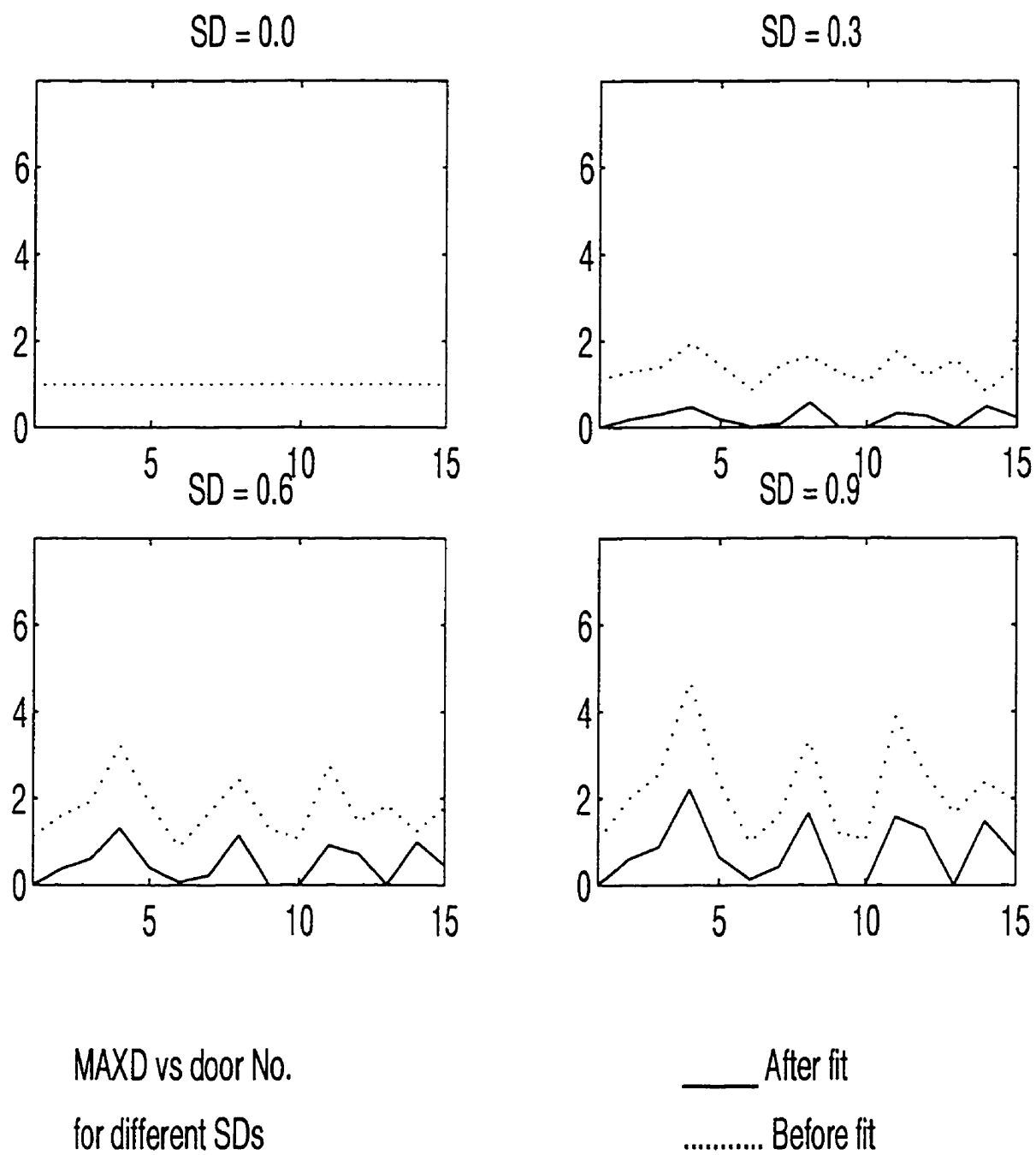


*Figure 4.18 Maximum deviation for the parallel deviation case*

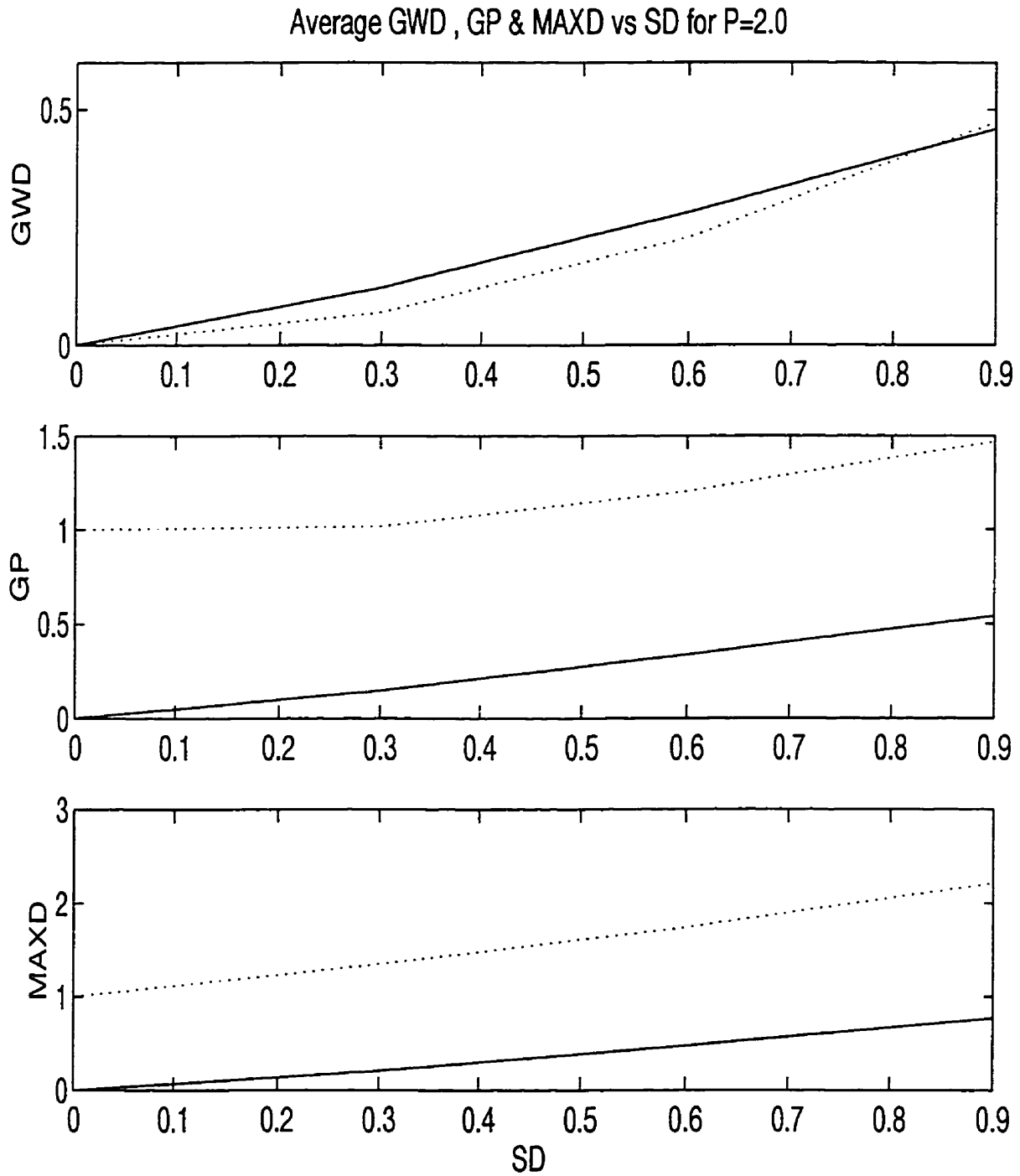


Figure 4.19 Average GWD, GP and MAXD for the parallel deviation case

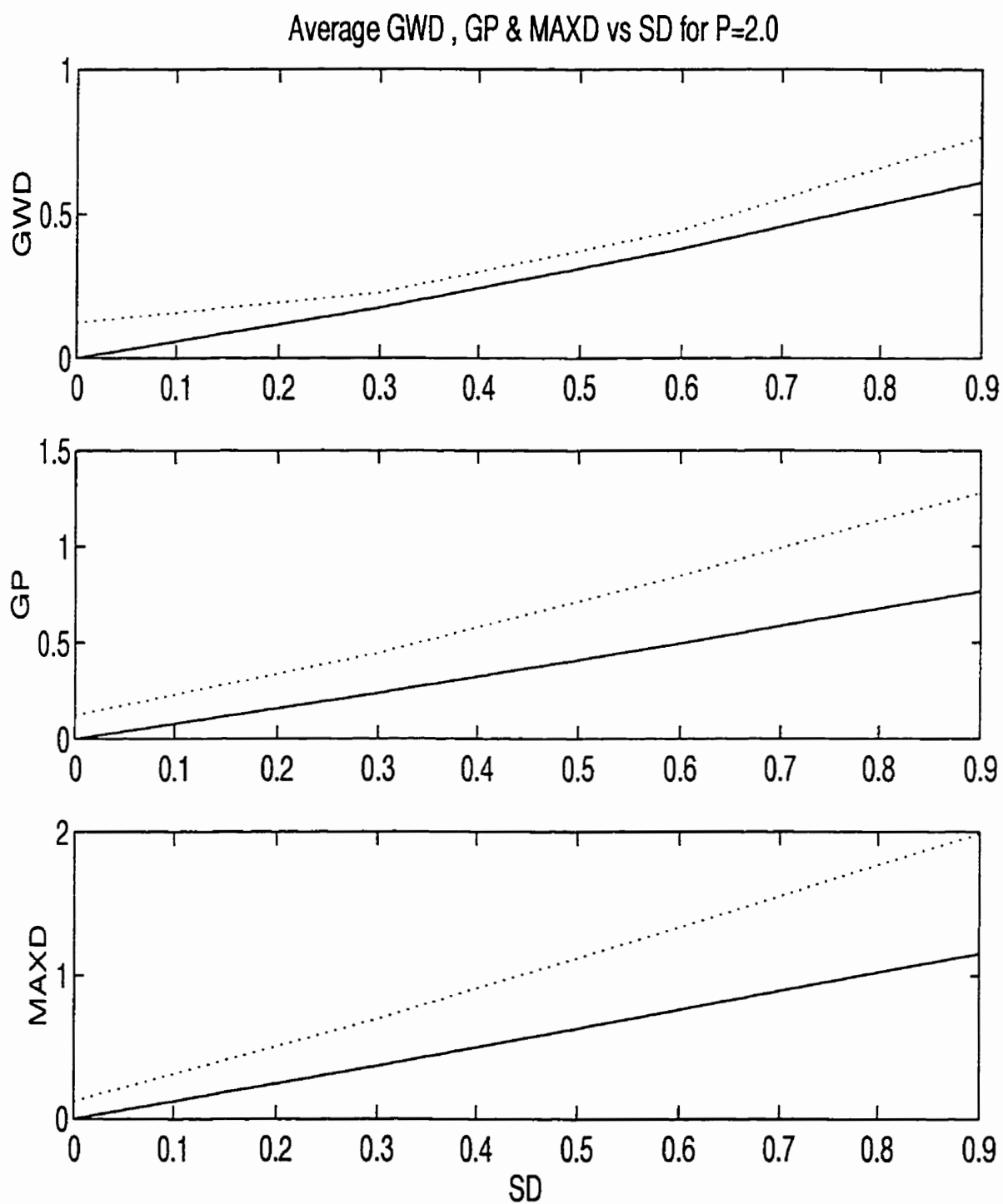


Figure 4.20 Average GWD, GP and MAXD for the perpendicular deviation case

## 4.4 Hybridizing Genetic Algorithms with Direct Search

The performance of genetic algorithms in solving the optimal door fitting problem can be degraded by two main problems. These are: (1) The discretization of the search space and (2) genetic drift.

### 4.4.1 Discretization of the Search Space

Genetic algorithms operate with binary strings. Each string corresponds to a unique set of values of the independent variables. This coding of the independent variables (Appendix A, section A.1) discretizes the search space. If the discretization is coarse, then there is a possibility that the genetic algorithm will arrive at a near optimum value (Figure 4.21).

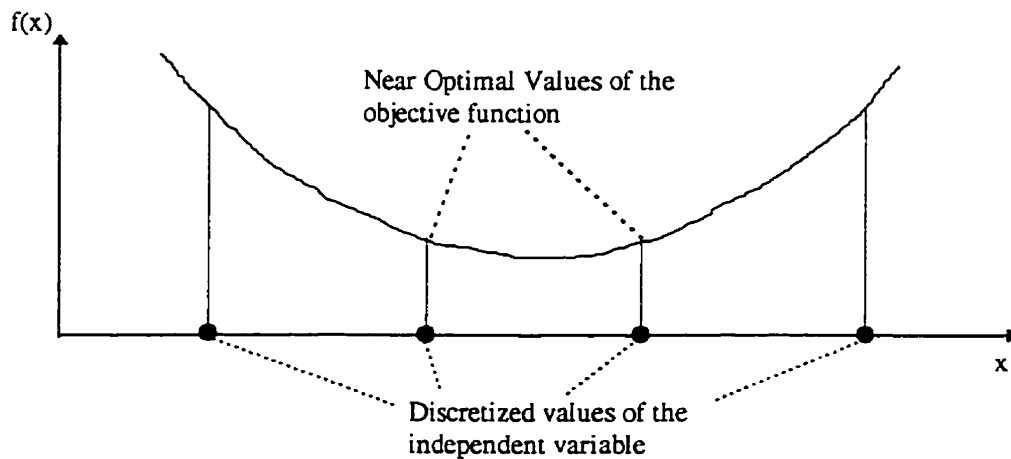


*Figure 4.21 Discretization of the search space in genetic algorithms*

#### 4.4.2 Genetic Drift

The second problem that faces genetic search is known as the genetic drift (Goldberg, 1989; Mahfoud, 1995). Figure 4.22 shows a multimodal objective function where the minima are near to each other in value. When such a function is encountered, the population of the instances of the independent variables will have a tendency to accumulate at the first discovered minimum, which might not be the global one.

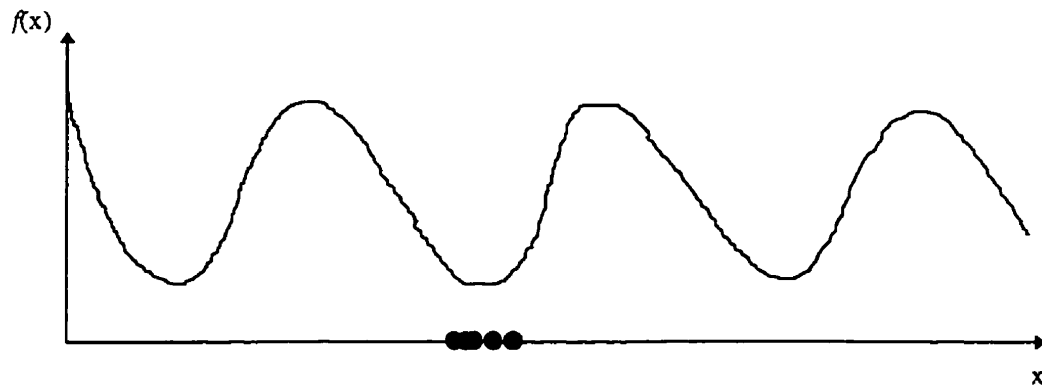


*Figure 4.22 A multimodal function with minima values close to each other*

This problem can be overcome by using a sharing function (section 4.2.3.3) with the search, but since sharing creates sub-populations of the independent variables, these sub-populations might be small in size causing the final population not to have an instance near the global minimum, but rather at a distance from it (Figure 4.23).

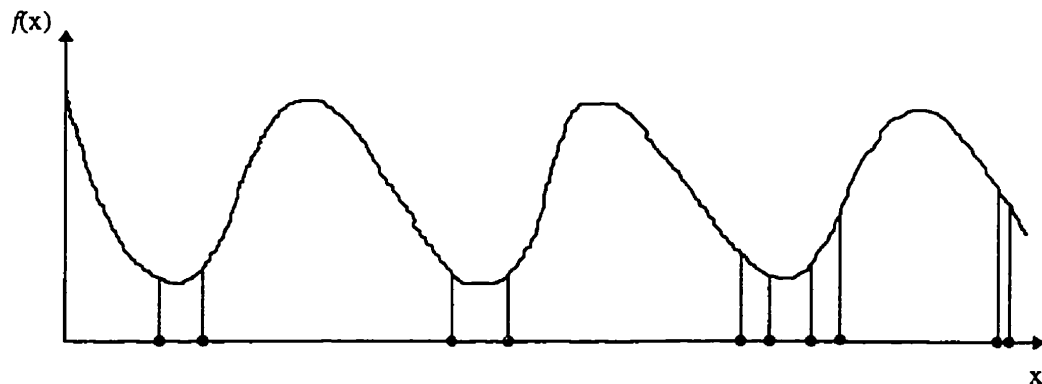


*Figure 4.23 Although using the sharing scheme enables the finding of all minima regions, the convergence to the global minimum would not be accurate enough*

#### 4.4.3 Hybrid Algorithm for solving the door fitting problem

In order to overcome the above mentioned problems, it is suggested that:

1. A sharing function (Equation (4.13)) be used with the search in order to overcome any possibility for genetic drift.
2. The result values of the independent variables, achieved by the genetic algorithms be the starting point for a direct search method such as the Nelder-Meade method as a refinement.

#### 4.4.4 Comparison of the Results

Different Door-Body opening configurations were simulated with a combination of positioning and manufacturing errors. Sigma of manufacturing errors was selected as before. Positioning errors were selected randomly with a uniform distribution from -2 to 2 for x,y and z; and from -0.1 to 0.1 for  $\alpha$ ,  $\beta$  and  $\gamma$ . The fitting algorithm was run using the direct search method, genetic algorithms and the hybrid approach. The direct search was able to reach the global minimum accurately in many runs; however, there were cases where it failed in doing so. On the other hand, using genetic algorithms resulted in fairly good results consistently, and that is why when hybridized with the direct search method the required objective was achieved: to reach the global minimum for all situations. Figure 4.24 shows a case with positioning and manufacturing variations and compares the quality indexes after fit for each method with that before fit. The results are also tabulated in Table 4-1.

*Table 4-1 Quality indexes before and after fitting*

	Before Fit	After Fit		
		Direct search	Genetic algorithms	Hybrid approach
GWD	0.33	0.46	0.17	0.03
GP	1.56	0.82	0.59	0.38
MAXD	2.91	1.11	0.96	0.42



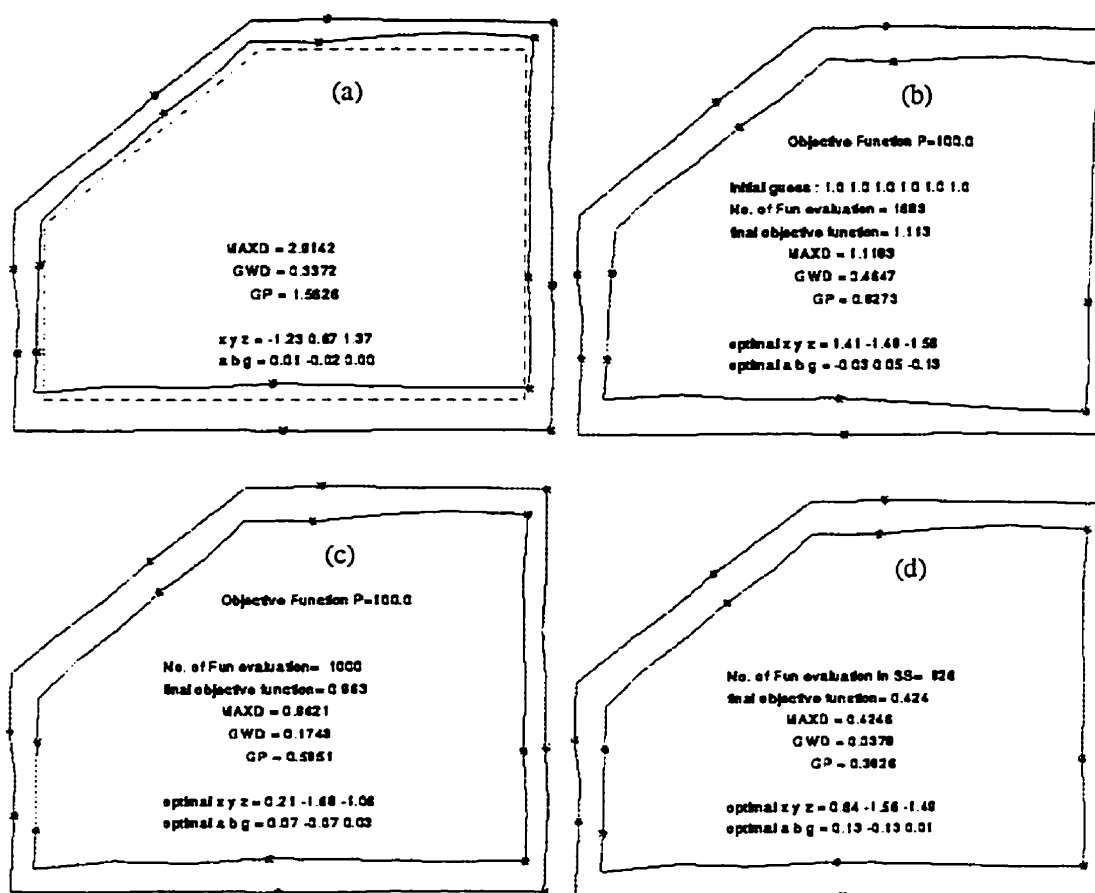


Figure 4.24 Simulation results: (a) Door without fit, (b) simplex search fit, (c) genetic algorithm fit, (d) hybrid approach fit

## 4.5 Choice of the Objective Function

Equation (4.7) showed that there is a family of objective functions that can be used for the door fitting problem depending on the value of the exponent  $p$ , where  $p$  ranges from one to infinity. The fitting objective is a well known subject in computational metrology. Hopp (1993) showed that the choice of the exponent  $p$  depends on two main criteria. These are: (1) susceptibility to bias and (2) susceptibility to measurement errors. Dowling *et al.* (1995) showed that there is a third criterion which is the sampling error. The following sections discuss each of these criteria and gives an insight into its importance regarding the optimal door fitting problem.

### 4.5.1 Susceptibility to Bias

Figure 4.25 shows a schematic diagram for the inputs and output of an optimal door fitting algorithm. The measured points along the door and the body opening along with the exponent  $p$  are inputs to the optimization algorithm, while the output is the optimum door location and orientation giving the minimum gap between the body opening and the door. Hopp (1993) showed that the fitting objective can be expressed as a special

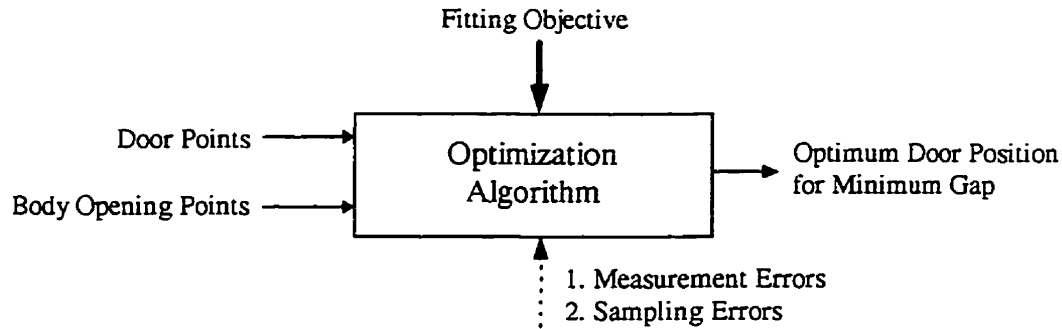


Figure 4.25 Schematic diagram of the fitting algorithm

case of the general criterion called  $L_p$  - norm estimation, where the problem is to find the independent variables (the door location and orientation) that will minimize the  $L_p$  norm:

$$L_p = \left[ \frac{1}{n} \sum_i |r_i|^p \right]^{1/p} \quad (4.14)$$

where:

$L_p$  = Deviation from the nominal gap

$r_i$  = The residual deviation from the nominal gap at point  $i$  on the door and the body opening.

$n$  = Number of points on the door (or the body opening)

$p$  = Exponent defining the fitting criteria which ranges from 1 to infinity.

The above symbols are used for different parameters in the area of computational metrology, and are assigned to their appropriate equivalents in the door fitting problem. Hopp (1993) indicated that as  $p$  approaches infinity the bias of the fit to the average error is minimized (Figure 4.26), provided that there is no measurement or sampling errors (as pointed out by Dowling *et al.* (1995)).

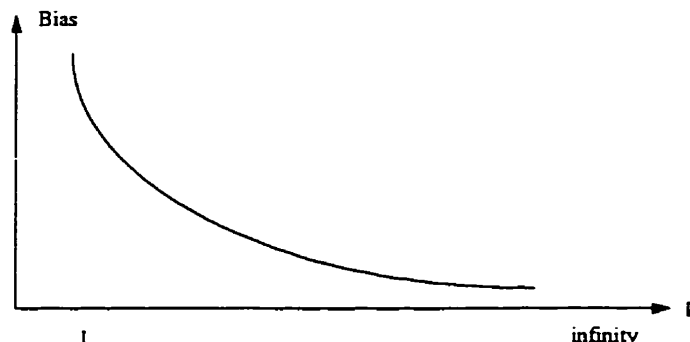
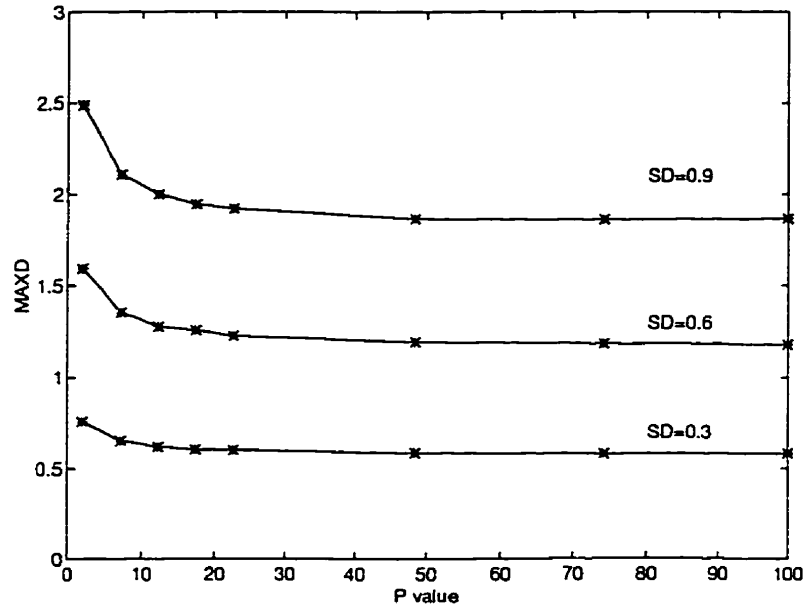


Figure 4.26 The effect of  $p$  on the bias of the fit

This susceptibility to bias was demonstrated by Qian *et al.* (1996), who compared the least squares fitting criteria ( $p=2$ ) with the maximum gap error criteria ( $p=infinity$ ) for the door fitting problem. Their results showed that using the least squares criteria led to door fits with large gaps, whereas the maximum deviation criteria arrived at lower values of the maximum deviation. The trend of the bias for the door fitting example shown in the previous sections is shown in Figure 4.27 which shows the values of the maximum deviation for different values of  $p$ .

#### 4.5.2 Susceptibility to Measurement Errors

Although the maximum deviation criterion has the least bias, it is very susceptible to unaccounted for errors such as the measurement errors and can mislead the optimization algorithm to wrong door locations and orientations. Objective functions using lower  $p$  values filter out these errors. Hence there is a tradeoff between the measurement errors and the bias (Figure 4.28)



*Figure 4.27 MAXD vs p for different SDs*

The degree of the sensitivity depends on the probability distribution of the measurement errors. The laser cameras used in the door fitting problem have an accuracy of  $\pm 0.025$  mm to  $\pm 0.075$  mm and are assumed to follow a normal distribution curve. In order to find the effect of the measurement error on the accuracy of fit for the optimal door fitting problem, the following procedure is proposed.

1. Points on a nominal door are generated and a nominal body opening are generated (for which the nominal door position is the optimal door position).
2. A set of measurement errors, generated from the laser camera probability distribution, are added to the door and body opening points.
3. The maximum deviation of any door point from the optimal location is then recorded.
4. The maximum deviation of any door point from the optimal location is then recorded.

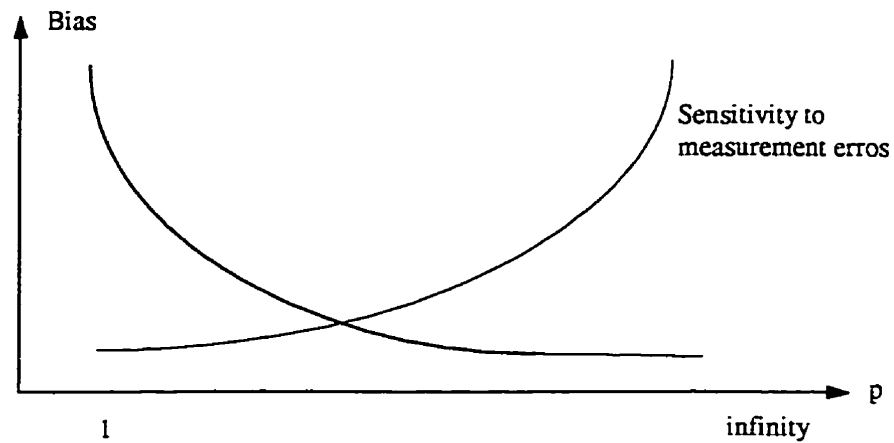


*Figure 4.28  $L_p$  - norm uncertainties*

The above procedure was applied to the door fitting example used in the previous sections and was tried for different values of the exponent  $p$ . The measurement errors were assumed to vary between  $-75$  and  $+75$  microns and follow a normal distribution.

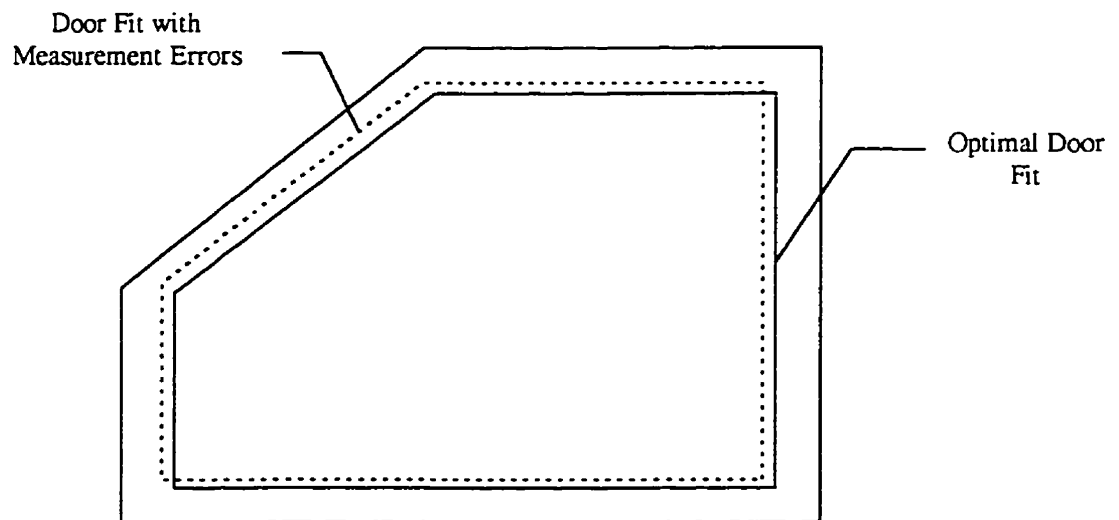


*Figure 4.29 Effect of measurement errors on door fit*

These values are the maximum deviations associated with any of the available commercial laser cameras. The result of the simulation is shown in Figure 4.30.

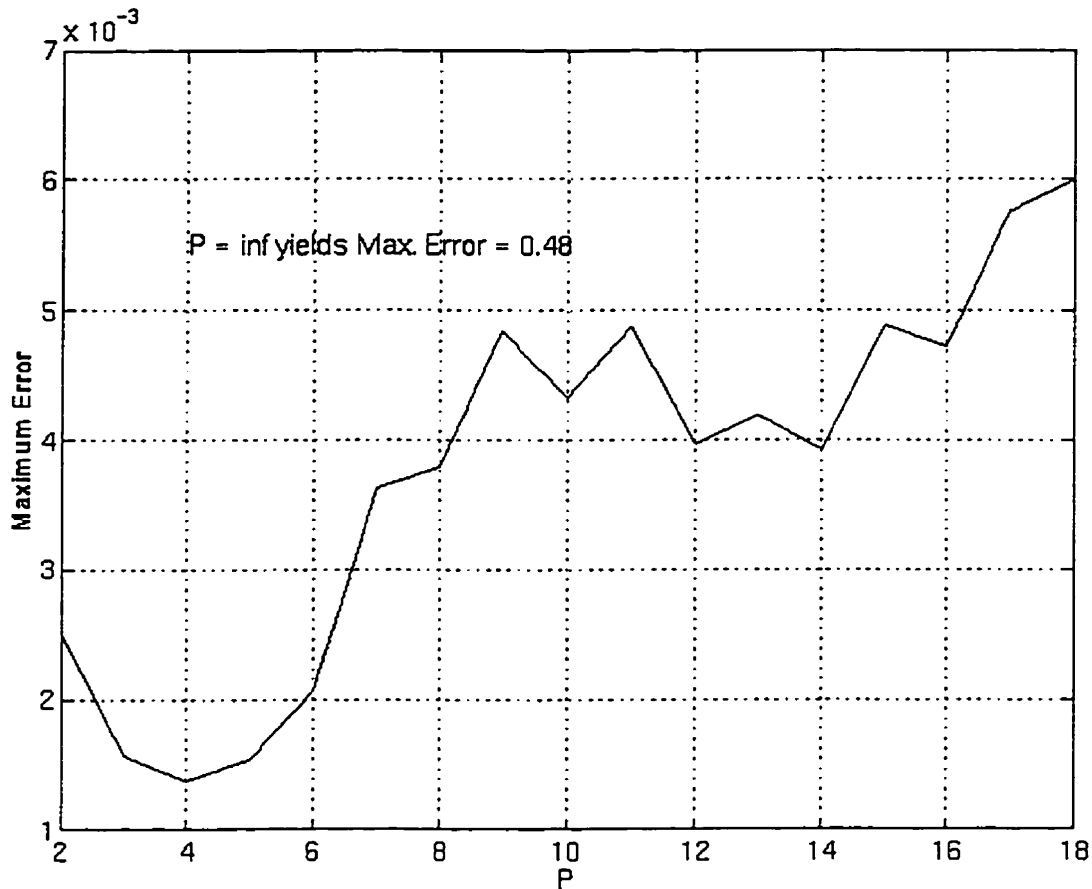


Figure 4.30 The maximum gap error vs.  $p$

Although very low  $p$  values gave the least deviations, the order of magnitude of the deviations is very low and hence it can be assumed that in the case of the optimal door fitting problem, the noise caused by the measurement errors is not significant. This conclusion can be attributed to the fact that the range of measurement errors of laser scanners is small in comparison with the overall dimensions of the door and the body opening. From the above discussion it can still be concluded that the maximum deviation criteria can be used for the optimal door fitting problem.

#### 4.5.3 Susceptibility to Sampling Error

Dowling *et al.* (1995) pointed out another problem that arises in the area of computational metrology. Since the measured points represent a sample of the whole part

geometry, there is a sampling error associated with such a sample unless the number of measured points is large enough to be representative of the whole part (The part in the optimal door fitting case is either the door or the body opening). They demonstrated their claims by the evaluation of the straightness and flatness of a flat surface. However, for the optimal door fitting problem, laser scanners measure a large number of points on the door, or the body opening. Hence it can be assumed that these points give a good representation of the part's geometry.

# **5. CHAPTER FIVE**

## **CONCLUSIONS**

### **5.1 Introduction**

The objective of the research presented in this thesis was to develop an algorithm for the optimal fitting of automobile doors within car body openings, and to develop a methodology for the direct calibration of door handling workcell. To achieve this objective, several sub-problems had to be addressed. These include:

1. The extension of the direct calibration methodology from a two-dimensional formulation to the three-dimensional case.
2. Determining whether the optimal door fitting problem is a multimodal or unimodal problem.
3. Investigating the choice of fitting criteria for the optimal door fitting problem.
4. Developing an optimization algorithm for the optimal door fitting problem.

The methodologies used to address these tasks are summarized in the following section.

### **5.2 Summary and Discussions**

This thesis presented a new method for the optimal fitting of manufactured doors within manufactured car body openings, along with a methodology for the direct calibration of robotic workcells used to handle the automobile door.



For direct calibration of robotic workcells handling automobile doors in a three-dimensional workspace, two mapping methods were investigated. The input to either method was a set of calibration sensor and location data. A relation which estimates the door's location using the sensor readings was sought. In the first mapping method a relation is created between the sensor data and the location data, which directly maps the sensor readings into door location. In the second mapping method a forward relation is created which maps the location data into sensor readings using the calibration data. The estimated sensor readings are then compared with the actual ones in an optimization routine where the independent variables are the door's six degrees of freedom (location and orientation). An initial guess for the location is found using the inverse mapping method. The optimum result would be the estimate of the door's location and orientation that correspond to the actual sensor readings. Both methods were used for the estimation of grasped door location and a comparison between both methods was conducted which showed the superiority of the forward mapping method.

An investigation was conducted to determine whether the optimal door fitting objective function is multimodal or unimodal. Genetic algorithms with a sharing fitness function was used to distribute a population of the independent variables over the different minima. A unimodal function accumulates the whole population at the same minima, while a multimodal function divides the population into sub-populations, each accumulated in the vicinity of a local minima. When these tests were conducted on the optimal door fitting problem sub-populations of the independent variables were observed which leads to the conclusion that the objective function is indeed multimodal.

An investigation of the door fitting criteria was conducted. It was found that minimizing the maximum gap between the door and the body opening leads to better door fits than minimizing the average gap. Moreover, the measurement errors were found to be very minute to affect the performance of the fitting algorithm.

The door fitting problem was solved using a hybrid optimization routine which incorporates genetic algorithms with direct search. The door location in three dimensional space with respect to the body opening reference frame, represented the independent variables of the optimization routine, and the largest gap between the door and the body opening was the objective function. Genetic algorithms were used as a global optimization method and their result was used as the initial point for a direct search method for further refinement of the optimization. Throughout the simulations, it was assumed that the door is free from any hinge constraints.

### 5.3 Contributions

1. An extension of the direct calibration method from two to three-dimensional workspace has been developed. Previous research in direct calibration of the automotive assembly applications was restricted to two\_dimensional space, hence cannot be used for positioning parts in three dimensional space using robotic manipulators. The performance of the developed method was enhanced by subtracting the estimation bias from the estimated locations.
2. For the first time in the published literature, the door fitting objective function was found to be multi\_modal. Previous work in the area used methods which lingered in local minima of the objective function.

3. An investigation was conducted to evaluate the effect of measurement errors on the choice of door fitting criteria. It was concluded that given the current accuracy of commercial laser sensors ( $\pm 0.025$  mm to  $\pm 0.075$  mm) and relatively large door dimensions, the measurement errors are of little effect on the fitting process.
4. An algorithm was developed that enables optimum door fitting in car body openings. The main contribution of the algorithm is its ability to result in uniform gaps between the door and the body opening by utilizing a global optimization technique, namely genetic algorithms.
5. To avoid the search space discretization problems, which might degrade the performance of genetic algorithms, a hybrid approach was adopted. The results of the genetic algorithms were fed as an initial guess to a direct search method to move the "extra mile" to the global minimum value of the gap.

## 5.4 Future Research

1. In the area of direct calibration, an investigation of the minimum number of sensor readings needed for building the mapping relation is required. Moreover, the comparison that have been presented in previous literature between direct calibration and multistage calibration is qualitative in nature and a quantitative comparison between both approaches is needed.
2. An investigation is needed to identify the minimum number of laser sensors needed to inspect the door and body opening, without affecting the quality of the door fit, in order to reduce the cost of the assembly process.

3. A further insight to the door fitting problem can be obtained by considering hinge subassembly in the optimization routine.
4. A statistical analysis of the door fitting process is needed where the manufacturing processes are simulated, the door fitting process is simulated and the percentage of door/chassis assemblies falling outside the design range is calculated. Monte Carlo simulation is recommended for such a study.

# REFERENCES

- [1] Abe, K., Hayashi, A. and Sakaino, M., 1995, "An Update on Nissan Intelligent Body Assembly System," *Proc. of the International Body Engineering Conference*, Detroit, Michigan, pp. 1-7.
- [2] American Society of Mechanical Engineers, 1982, "*Dimensioning and Tolerancing*," ANSI Y13.5M Standard.
- [3] Bard, Y., 1974, *Nonlinear Parameter Estimation*, Academic Press.
- [4] Barth, D., 1994, "Management of Manufacturing System Flexibility - The Example of Body-in-White Manufacturing Systems," *International Body Engineering Conference, Body Assembly and Manufacturing*, pp. 40-48.
- [5] Bennet, D., Geiger, J. and Holerbach, J., 1991, "Autonomous Robot Calibration for Hand Eye Coordination," *Int. Journal of Robotics Research*, Vol. 10, No. 5.
- [6] Bieman, L. H. and Pogue, J. H., 1986, "Visual Fixturing for Sheet Metal Gaging," *Proc. of the MVA/SME Vision '86 Conf.*, pp. 137-148.
- [7] Brooke, L., 1994, "The Flex Factor," *Automotive Engineering*, Nov. 1994, pp. 50-60
- [8] Cai, W., Yuan, J. and Hu, S.J., 1994, "Optimal Fixture Design for Sheet Metal Holding," *Proc. of IBEC 94, Body Assembly and Manufacturing*, pp. 123-128.
- [9] Ceglarek, D. and Shi, J., 1995, "Design Evaluation of Part to Part Joints for Dimensional Integrity of Body In White," *Proc. of the International Body Engineering Conference, Body Design and Engineering*, pp. 11-19.

- [10] Ceglarek, D. and Shi, J., 1995, "Dimensional Variation Reduction for Automotive Body Assembly," *Manufacturing Review, ASME*, Vol. 8, No. 2, pp. 139-153.
- [11] Ceglarek, D., Shi, J. and Wu, S. M., 1993, "Auto-Body Assembly Diagnostic: A Knowledge-Based Approach," *Manufacturing Science and Engineering, ASME*, Vol. 64, pp. 401-411.
- [12] Chen, C., Trivedi, M. and Bidlack, C., 1992, "Simulation and Graphical Interface for Programming and Visualization of Sensor-based Robot Operation," *Proc. of the 1992 IEEE International Conf. on Robotics and Automation*, Nice, France, pp. 1059-1101.
- [13] Craig, J.J., 1989, *Introduction to Robotics: Mechanics and Control*, 2nd Edition, Addison-Wesley.
- [14] Davies, J.L. and Gill, K.F., 1993, "Automated Bumper Assembly using a Vision Guided Robot," *Proc. of the Inst. of Mechanical Engineers*, Vol. 207, pp. 61-72.
- [15] Dewar, R., 1988, "Self-Generated Targets for Spatial Calibration of Structured Light Optical Sectioning Sensors with Respect to an External Coordinate System," *Proc. of SME Vision '88 Conf.*, pp. 13-21.
- [16] Dowling, M.M., Griffin, P.M., Tsui, K-L. and Zhou, C., 1995, "A Comparison of the Orthogonal Least Squares and Minimum Enclosing Zone Methods for Form Error Estimation," *Manufacturing Review, ASME*, Vol. 8, No. 2, pp. 120-138.
- [17] ElMaraghy, W.H. and Prior, T., 1996, "An Industrial Approach to Intelligent Assembly," *Proc. of the 27th Annual ISIR Conf.*, Milan, Italy.
- [18] ElMaraghy, W.H., ElMaraghy, H.A. and Wu, Z., 1990, "Determination of Actual Geometric Deviations Using Coordinate Measuring Machine Data," *Manufacturing Review, ASME*, Vol. 3, No. 1, pp. 32-39.

- [19] Goldberg, D., 1989, *Genetic Algorithms in Search, Optimization and Machine Learning*, Addison-Wesley.
- [20] Goldberg, D. and Richardson, J., 1987, "Genetic Algorithms with Sharing for Multimodal Function Optimization," *Proceedings of the Second International Conference on Genetic Algorithms*, pp. 41-49.
- [21] Goldberg, D. and Kuo, C.H., 1986, "Genetic Algorithms in Pipeline Optimization," *Journal of Computing in Civil Engineering*, Vol. 1, No. 2, pp. 128-141.
- [22] Holland, J., 1975, *Adaptation in Natural and Artificial Systems*, University of Michigan Press.
- [23] Hopp, T., 1993, "Computational Metrology," *Proceedings of the 1993 Int. Forum on Dimensional Tolerancing and Metrology*, Dearborn, Michigan, pp. 207-217.
- [24] Hoska, D., 1988, "FLAM: What it is. How to achieve it," *Manufacturing Engineering*, April 1988, pp. 193-198.
- [25] Hu, S.J., Wu, S.K. and Wu, S.M., 1991, "Multivariate Analysis and Variation Reduction, Case Studies in Automobile Assembly," *Transactions of NAMRI, SME*, pp. 303-308.
- [26] Kalker, C.M. and Offermans, M.F., 1995, "A General Design Program Based on Genetic Algorithms," *Proceedings of the 1995 Design Engineering Technical Conferences, Advances in Design Automation, ASME*, pp. 81-88.
- [27] Kosmala, J. B., 1994, "FLEX-TOOL™ A Tool for Body Shop Flexibility," *Proc. of IBEC 94, Body Assembly and Manufacturing*, pp. 87-94.

- [28] Mahfoud, S., 1995, "A Comparison of Parallel and Sequential Niching Methods," *Proceedings of the Sixth International Conference on Genetic Algorithms*, pp. 136-143.
- [29] MathWorks, 1992, *MATLAB Reference Guide*, The Math Works Inc.
- [30] Mooring, B. W., Roth Z. S. and Driels, M.R., 1991, *Fundamentals of Manipulator Calibration*, John Wiley and Sons.
- [31] Mortenson, M.E., 1985, *Geometric Modeling*, John Wiley and Sons.
- [32] Murray, W.R. and Pohlhammer, C.M., 1994, "Robust Estimation of the Location of A Planar Body: Results from Simulations," *Proc. of the 1994 Int. Mechanical Engineering Congress and Exposition*, Chicago, Illinois, pp. 1103-1109.
- [33] Murthy, T. R. and Abdin, S. Z., 1980, "Minimum Zone Evaluation of Surfaces," *International Journal of Machine Tool Design and Research*, Vol. 20, pp. 123-136.
- [34] Nassef, A.O. and ElMaraghy, H.A., 1996, "Optimization and Interpolation Issues in Evaluating Actual Geometric Deviations from CMM Data," *Proc. of 1996 ASME International Mechanical Engineering Congress and Exposition, Symposium of Recent Development in Tolerancing and Metrology for Control and Improvement of Manufacturing Processes*, MED-Vol. 4., pp. 425-432.
- [35] Pasek, Z.J., 1993, *An Adaptive Assembly System for Automotive Applications*, PhD Thesis, University of Michigan, Ann Arbor.
- [36] Pastorius, W., 1995, "In-Process Monitoring for Assembly Operations," *Proc. of IBEC 95, Body Assembly and Manufacturing*, pp. 1-6.



- [37] Plut, W.J. and Bone, G.M., 1996, "Limited Mobility Grasps for Fixtureless Assembly", *Proceedings of the IEEE International Conference on Robotics and Automation*, Minneapolis, Minnesota, pp. 1465-1470.
- [38] Qian, W., Hsieh, L. and Seliger, G., 1996, "On the Optimization of Automobile Panel Fitting," *Proc. of the 1996 IEEE Int. Conf. on Robotics and Automation*, Minneapolis, Minnesota, pp. 1268-1274.
- [39] Rao, S.S., 1996, *Engineering Optimization: Theory and Practice*, John Wiley and Sons.
- [40] Rice, J. R., 1964, *The Approximation of Functions*, Addison-Wesley.
- [41] Roan, C. and Hu, S. J., 1995, "Monitoring and Classification of Dimensional Faults for Automotive Body Assembly," *The Int. J. of Flexible Manufacturing Systems*, Vol. 7, pp. 103-125.
- [42] Roan, C., 1993, *Identification, Monitoring, and Diagnosis for Dimensional Control of Automobile Body Assembly*, PhD Thesis, University of Michigan, Ann Arbor.
- [43] Roston, G. P. and Sturges, R. H., 1995, "A Genetic Design Methodology for Structure Configuration," *Proceedings of the 1995 Design Engineering Technical Conferences, Advances in Design Automation*, ASME, pp. 73-80.
- [44] Rotvold, O., 1995, "An Enabling Metrology Concept for Body in White Process Control," *Proc. of IBEC 95, Body Design and Engineering*, pp. 20-27.
- [45] Seber, G.A.F., 1977, *Linear Regression Analysis*, John Wiley and Sons.
- [46] Shalash, E.S., Nassef, A.O. and ElMaraghy, W.H., 1996, "A Hybrid Optimization Approach for the Door Fitting Problem," *Proceedings of the Pacific Conference on Manufacturing 96*, Seoul, Korea, pp. 262-267.

- [47] Shao, J. and Tsui, K.L., 1996, "Form Tolerance Estimation using Jackknife Methods," Proc. of 1996 ASME International Mechanical Engineering Congress and Exposition, Symposium of Recent Development in Tolerancing and Metrology for Control and Improvement of Manufacturing Processes, MED-Vol. 4., pp. 433-446.
- [48] Slocum, A., 1992, *Precision Machine Design*, Prentice-Hall, Englewood Cliffs, New Jersey.
- [49] Turner, J.U., 1990, "Relative Positioning of Parts in Assemblies using Mathematical Programming," *Computer Aided Design*, Vol. 22, No. 7, pp. 394-400.
- [50] Weber, T.W. and Hu, S.J., 1993, "The Development of Advanced Technologies and Systems for Controlling Dimensional Variations in Automobile Body Manufacturing: The 2mm Program," *Proc. of the Body Engineering Conference, Automotive Body Design and Engineering*, pp. 80-86.
- [51] Whitely, D., 1993, "Tutorial 2: Advanced Genetic Algorithm Topics," *ICGA-93, 5th International Conference on Genetic Algorithms*, Conference Tutorial.
- [52] Wu, S.-K., 1991, *A Methodology for Optimal Door Fit in Automobile Body Manufacturing*, PhD Thesis, University of Michigan, Ann Arbor.
- [53] Wu, S.-K., Hu, J. and Wu, S.M., 1994, "Optimal Door Fitting with Systematic Fixture Adjustment," *Int. Journal of Flexible Manufacturing Systems*, Vol. 6, pp. 99-121.
- [54] Wu, S.-K., Hu, J. and Wu, S.M., 1994, "A Fault Identification and Classification Scheme for an Automobile Door Assembly Process," *Int. Journal of Flexible Manufacturing Systems*, Vol. 6, pp. 261-285.

- [55] Yu, W. 1992, "Minimum Zone Evaluation of Form Tolerances," *Manufacturing Review, ASME*, Vol. 5, No. 3, pp. 214-220.
- [56] Zhuang, H. and Roth, Z., 1992, "Robot Calibration using the CBC Error Model," *Journal of Robotics and Comp. Int. Manufacturing*, Vol. 9, No. 3. pp. 227-237.
- [57] Zhuang, H., Wang, L. and Roth, Z., 1993, "Simultaneous Calibration of a Robot and a Hand-Mounted Camera," *Proc. of IEEE International Conference on Robotics and Automation*, Atlanta, GA, Vol. 2, pp. 149-154.

# APPENDIX A

## FUNCTION OPTIMIZATION WITH GENETIC ALGORITHMS

Genetic algorithms have been used with wide acceptance as a method of global optimization. The algorithms work on a population of values for the independent variables with functions that emulate the biological genetic operators (Holland, 1975). Researchers (Goldberg, 1989) in the area of genetic algorithms tested them on several functions and were shown to outperform other methods in optimizing combinatorial and multimodal functions. The method has been applied in several engineering areas as function optimizers (Goldberg and Kuo, 1986; Roston and Sturges, 1995; and Kalker and Offermans, 1995).

### A.1 Coding

Consider a function  $f(x)$  of the variable  $x$ . If genetic algorithms are to be used to find the value of  $x^*$  such that :

$$f(x^*) \leq f(x), \quad \forall x \quad \text{minimization} \quad (\text{A.1})$$

$$f(x^*) \geq f(x), \quad \forall x \quad \text{maximization} \quad (\text{A.2})$$

the first step is to code the variable  $x$  into a binary string, that can be used by the genetic operators. This operation is known in the genetic algorithms literature as the coding of the independent variable. Coding discretizes the possible values of the independent variables. Assume that  $x$  ranges from zero to 31, and that each consecutive possible values of  $x$  differ by one, i.e.

$$x \in [0, 1, 2, \dots, 30, 31] \quad (\text{A.3})$$

A binary string representing  $x$  would have five locations, where each location  $i$  can assume a value of zero or one and where the value of each location  $i \in \{0,1,2,3,4\}$  is multiplied by  $2^i$

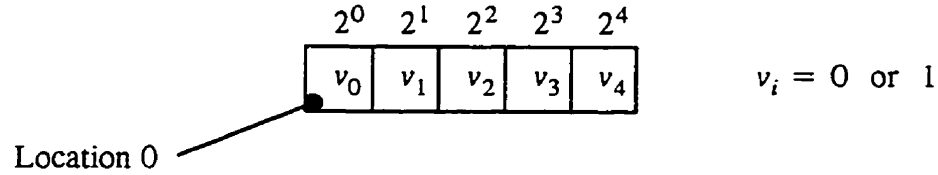


*Figure A.1 Genetic Chromosome*

It is obvious that if all locations are equal to one the value of the string becomes 31 and if all location are equal to zero the value of the string becomes zero.

#### **A.1 .1 Coding of Continuous Variable**

Assume that a variable  $x$  is to be coded where:

$$x \in \mathbb{R}, \quad \mathbb{R} = \text{real values line} . \quad (\text{A.4})$$

and that  $x$  ranges from a value  $a$  to a value  $b$

$$a \leq x \leq b \quad (\text{A.5})$$

Assume that  $x$  is to be discretized to a set of  $n$  possible values  $x_i$  such that:

$$x_i \in \{x_1, x_2, \dots, x_n\} \quad (\text{A.6})$$

$$x_1 = a \quad (\text{A.7})$$

$$x_n = b \quad (\text{A.8})$$

$$x_{i+1} - x_i = \text{DIFF} \quad (\text{A.9})$$

where DIFF is a predetermined difference between  $x_{i+1}$  and  $x_i$ . The variable  $x$  is to be represented by a binary string having  $n+1$  locations, where each location  $i$  has a value:

$$\text{Val}(i) = r2^i \quad i \in \{0, 1, 2, \dots, n\} \quad (\text{A.10})$$

and where the whole string assumes the value

$$\text{Val}(\text{string}) = a + \sum_{i=0}^n \text{Val}(i) \quad (\text{A.11})$$

The values of  $r$  and  $n$  are determined as follows:

$$\text{DIFF} = r2^1 - r2^0 \quad (\text{A.12})$$

$$\text{DIFF} = r \quad (\text{A.13})$$

If the value of all locations is equal to one, the value of the string becomes a geometric series:

$$\begin{aligned} \text{Val}(\text{string}) &= a + \sum_{i=0}^n r2^i \quad (\text{A.14}) \\ &= a + r(2^{n+1} - 1) \end{aligned}$$

but,

$$\text{Val}(\text{string}) = b \quad (\text{A.15})$$

Let

$$v = b - a \quad (\text{A.16})$$

then

$$n = \log_2 \left[ \frac{v}{r} + 1 \right] \quad (\text{A.17})$$

Since  $n \in \mathbb{R}$ , and  $n$  should be integer, the value:

$$N = \text{integer}(n) \quad (\text{A.18})$$

is used and a new value for  $r$  is computed

$$r = \left\lfloor \frac{v}{2^{N+1} - 1} \right\rfloor \quad (\text{A.19})$$

### A.1 .2 Coding of an Integer Variable

If the possible value of the variable  $x$  belongs to the integer line:

$$x \in \{0, 1, 2, 3, \dots, m\} \quad (\text{A.20})$$

then  $x$  is already discretized with a minimum value of zero, a maximum value of  $m$  and a difference between every consecutive values equal to one (i.e. DIFF=1). The coding method described in the previous section can be used. This may lead to strings of small length which can lead to an early loss of strings with high fitness once the genetic operators are in action. This problem can be solved by using a smaller value of DIFF and the following function for string evaluation

$$\text{Val}(\text{string}) = a + \text{integer} \left[ \sum_{i=0}^m r 2^i \right] \quad (\text{A.21})$$

## A.2 Fitness Function

Genetic algorithms are supposed to maximize a function known as the fitness function. Thus any objective function to be optimized by genetic algorithms should be converted into a fitness function form. If the optimization problem at hand is a maximization problem, then the fitness function  $F$  equal to the objective function  $f$ . If the problem at hand is a minimization problem, the value of the fitness function is equal to some large value  $V$  minus the value of the objective function.

$$F = V - f \quad (\text{A.22})$$

### A.2 .1 Fitness Function Scaling

In order to avoid the early loss of high strings, fitness function scaling is a common practice (Goldberg, 1989). Several methods are proposed for scaling the fitness function. The objective of the scaling is to make the chromosomes with maximum fitness have a re-scaled fitness value twice as large as the re-scaled average fitness. Linear scaling is the most widely used method Figure A.2 .

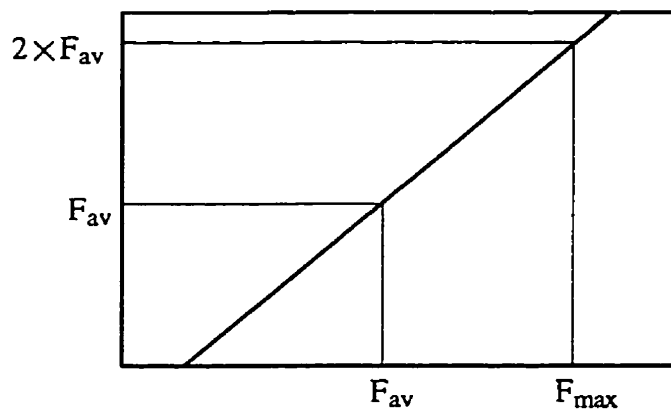


Figure A.2 Fitness Function Scaling

Linear scaling has one disadvantage. It may lead to negative re-scaled values. This problem can be solved by re-scaling the less than average chromosomes such that the minimum fitness chromosome is re-scaled to zero fitness.

### A.3 General Procedure of Genetic Algorithms

After a problem is coded into a binary string, a population of random valued strings is formulated and is used for making new generations of strings iteratively. The strings are known in the genetic algorithms literature as “*chromosomes*”, and the location of each binary digit in the chromosomes is known as a *gene*. Assume that genetic algorithms are used to optimize a function of one variable  $f(x)$ . The general genetic algorithms optimization procedure is:



**Procedure: GEN-ALG**

- A. Code the range of possible values of the variable  $x$  into a binary string as shown in section A.1
- B. Construct the fitness function for the objective function as shown in section A.2 .
1. Generate a population of  $N$  chromosomes. Each chromosome has a randomly chosen binary digit in each of its genes as shown in Figure A.3 . Each chromosome represents a random instance of the independent variable  $x$ .

chromosome 1	0	1	0	1	1
chromosome 2	1	1	0	0	1
chromosome $N$	1	1	0	0	0

*Figure A.3 A Genetic Population*

2. Generate a new population of chromosomes using the reproduction operator.
3. Apply the cross-over operator on the new generation.
4. Apply the mutation operator on the new generation.
5. If the generation number is less than the maximum number of generations go to step 2, otherwise stop.

6. Find the chromosome with the largest fitness value in the final generation. Decode the chromosome and deliver its equivalent value of the independent to the optimum value of the objective function.

In the case of a multidimensional optimization, each independent variable is enclosed into a sub-chromosome and put together in a row to form a larger chromosome as shown in Figure A.4 .

$2^0$	$2^1$	$2^2$	$2^3$	$2^4$	$2^0$	$2^1$	$2^2$	$2^3$	$2^4$	$2^0$	$2^1$	$2^2$	$2^3$	$2^4$
0	1	0	1	1	1	1	1	1	1	0	1	0	0	1

*Figure A.4 A chromosome for 3 variables*

In such a case the reproduction operator is applied to the larger chromosome, while the mutation and cross-over operators are applied to each sub-chromosome.

## A.4 Genetic Operators

The previous section referred to three genetic operators used iteratively to maximize a fitness function. These operators are reproduction, mutation and cross over. The operators emulate the action of equivalent genetic operations in biology.

### A.4 .1 Reproduction

Given a population of  $N$  chromosomes, the fitness function  $f_i$  is evaluated for each chromosome. Each chromosome is then assigned a value:

$$v_i = \frac{f_i}{\sum_{i=1}^N f_i} \quad (\text{A.23})$$

forming a discrete probability distribution over the population. The purpose of the reproduction operator is to replace the old population with a new population of chromosomes selected from the old population such that:

$$\overline{f_{\text{new}}} > \overline{f_{\text{old}}} \quad (\text{A.24})$$

where  $\overline{f}$  is the average fitness value of the population. The reproduction operator is a method of chromosome selection based on its fitness value. The main method used for selection is the roulette wheel selection (Goldberg, 1989). The selection process proceeds as follows:

1. The interval  $[0,1]$  is divided into subintervals  $I_i$  whose length is equal to the value  $v_i$  of its corresponding equal chromosome.

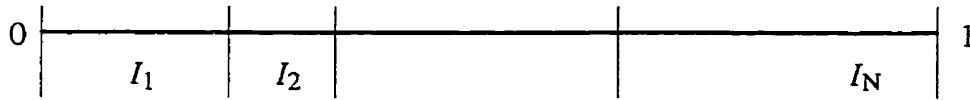


*Figure A.5 Roulette Wheel Selection*

2. A random number  $U \in [0,1]$  is generated and the value of  $U$  is checked for the subinterval within which it lies. The chromosome corresponding to the subinterval is delivered as the selected chromosome.

The selection process is repeated  $N$  times for the whole population.

#### **A.4 .2 Cross Over**

After the old population is replaced by a new one, an even number of chromosomes are selected from the new population to undergo cross-over. The number of chromosomes

selected for cross-over is determined by the cross-over probability  $P_c$ . Every successive pair of chromosomes in the population is picked up and a random number  $U \in [0,1]$  is generated. If  $U$  is less than  $P_c$ , the pair of chromosomes undergo cross-over. The cross-over operator acts as follows:

1. A location  $l$  in the pair of chromosomes is picked at random

$$l \in \{1, 2, 3, \dots, L\} \quad (\text{A.25})$$

where  $L$  is the number of genes in the chromosomes.

2. All binary bits in the genes right of the position  $l$  are swapped between the pair of chromosomes under cross-over (Figure A.6 ).

Cross Over Location

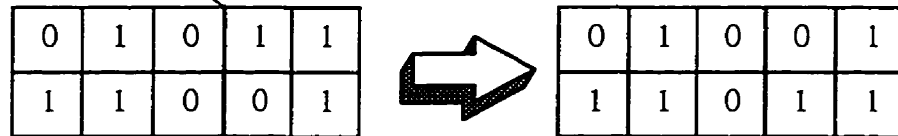


*Figure A.6 Cross Over*

#### **A.4 .3 Mutation**

A number of chromosomes is picked from the new population to undergo mutation based on a mutation probability  $P_m$ . For every chromosome in the population a random number  $U \in [0,1]$  is generated. If  $U$  is less than  $P_m$ , the chromosome undergoes mutation. The mutation operator is applied as follows:

1. A random position  $l$  is picked where:

$$l \in \{1, 2, 3, \dots, L\} \quad (\text{A.26})$$

2. The binary value at the gene positioned at  $l$  is flipped.

## A.5 Schema Theorem

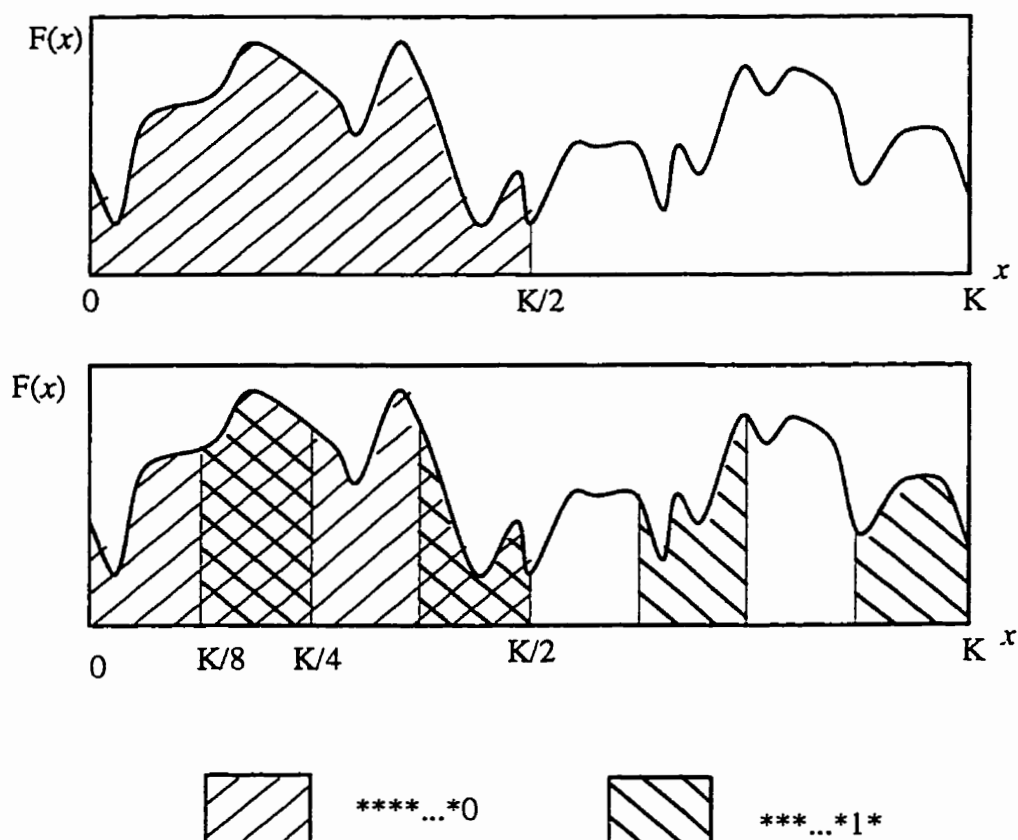


Figure A.7 A Function with Schemata

How genetic algorithms arrive at the global optimum of the functions they optimize is understood in view of what is known as a chromosome whose genes can have one of the following three values: “0”, “1”, or “\*”, where “\*” is a wild-card value that can have “0” or “1” in its place. Figure A.7 shows a function  $F(x)$  of one variable  $x$  which ranges from zero to an arbitrary value  $K$ . The schema  $0***...*$  represent all values of  $x$  less than  $K/2$  and more than zero, while the schema  $*1**...*$  represents all values of  $x$  between  $iK/8$  and  $(i+1)K/8$ ,

$i \in \{1,3,5,7\}$ . Figure A.7 shows that the schema  $0***...*$  has an average fitness value larger than the average fitness value of the schema  $*1**...*$ . In a population of chromosomes, each chromosome has  $l$  genes, each is a member of  $2^l$  schemata. Let  $M(H,t)$  be the number of chromosomes representing a schema  $H$  at time  $t+1$  under the effect of reproduction is equal to:

$$M(H, t + 1) = M(H, t) \frac{f(H)}{\bar{f}} \quad (\text{A.27})$$

where  $f(H)$  is the average fitness of the chromosomes representing  $H$  and  $\bar{f}$  is the average population fitness. Equation (A.27) shows that a schema with a high average fitness would have more representatives in a population than a schemata with a lower average fitness. If reproduction is solely used, only replications of the original population will be selected. Cross-over is responsible for introducing new chromosomes representing new schemata in the search. The number of chromosomes representing a schema  $H$  at time  $t+1$  is thus equal to

$$M(H, t + 1) = M(H, t) \frac{f(H)}{\bar{f}} p_s \quad (\text{A.28})$$

where  $p_s$  is the probability that  $H$  survives to time  $t+1$ . Holland (1975) shows that  $p_s$  is given by the relation

$$p_s \geq 1 - p_c \frac{\delta(H)}{l-1} \quad (\text{A.29})$$

where  $p_c$  is the cross-over probability and  $\delta(H)$  is the defining length of the schema  $H$  given by the number of genes between the every consecutive non \*-valued genes. Holland (1975)

showed that using a combination of reproduction and cross-over, schemata with above average fitness and small defining length will be tried at an exponential rate.

## **A.6 Advanced Operators**

Variations of the standard genetic algorithms operators have been investigated in previous research (Whitley, 1993). Two of these variations are discussed in the following sections.

### **A.6 .1 Tournament Selection**

Some researchers proposed alternative schemes for the selection of chromosomes from population, other than the roulette wheel selection. One of these schemes that proved to be less biased is the tournament selection. Tournament selection work as follows (Goldberg, 1989): Draw two chromosomes from the old generation using tournament selection, then accept the one with the higher fitness as the winner and insert it in the new population. The process is continued until the population is full.

### **A.6 .2 Uniform Cross-Over**

Uniform cross-over is a generalized version of the one point cross-over discussed in the previous sections. Uniform cross-over works as follows: for each gene in the two chromosomes undergoing cross-over, randomly decide if the values of the genes are to be swapped or not. Uniform cross-over is unbiased operator. At the same time uniform cross-over is more disruptive in processing schemata than one point cross-over. Researchers in the area of genetic algorithms (Whitley, 1993) suggested that uniform cross-over is best used with small population sizes.

# APPENDIX B

## MULTIPLE LINEAR REGRESSION

### B.1 Linear Regression Models

Let  $y$  be a random (measured) variable depending on the parameters  $x_1, x_2, \dots, x_p$ . For example  $y$  can be a physical quantity measured at different temperatures, pressures, etc. The measured variable  $y$  is function of the parameters  $x_1, \dots, x_p$  and can be expressed as

$$y = f(x_1, x_2, \dots, x_p) + \varepsilon \quad (\text{B.1})$$

where  $\varepsilon$  is the measurement error. If no a priori model is available then  $f(\cdot)$  can be approximated by a linear regression model, that is

$$\hat{y} = f(x) = \beta_0 + \sum_{i=1}^n \beta_i h_i(x) \quad (\text{B.2})$$

where  $x = (x_1 \ x_2 \ \dots \ x_p)^T$ ,  $\hat{y}$  is the estimate of  $y$ ,  $h_i$  are functions of  $x$  and  $\beta_i$  are unknown parameters that have to be determined so as to minimize some objective function (usually the error  $y - \hat{y}$ ). The problem at hand could be written in matrix form as

$$\begin{bmatrix} y_1 \\ y_2 \\ \vdots \\ y_m \end{bmatrix} = \begin{bmatrix} h_{11} & h_{12} & \dots & h_{1n} \\ h_{21} & h_{22} & \dots & h_{2n} \\ \vdots & \vdots & \ddots & \vdots \\ h_{m1} & h_{m2} & \dots & h_{mn} \end{bmatrix} \begin{bmatrix} \beta_0 \\ \beta_1 \\ \vdots \\ \beta_p \end{bmatrix} + \begin{bmatrix} \varepsilon_1 \\ \varepsilon_2 \\ \vdots \\ \varepsilon_m \end{bmatrix} \quad (\text{B.3})$$

where  $m$  is the number of available data. Equation (B.3) can be written in a more compact form as

$$y = H\beta + \varepsilon \quad (\text{B.4})$$



Matrix  $H$  is referred to as the *regression matrix* or the *design matrix*. Similarly, the estimated vector  $\hat{y}$  is

$$\hat{y} = H\beta \quad (\text{B.5})$$

As an example, let  $h_i(x) = x_i$ . Then Eq. (B.3) becomes

$$\begin{bmatrix} y_1 \\ y_2 \\ \vdots \\ y_m \end{bmatrix} = \begin{bmatrix} 1 & x_{12} & \dots & x_{1n} \\ 1 & x_{22} & \dots & x_{2n} \\ \vdots & \vdots & \ddots & \vdots \\ 1 & x_{m2} & \dots & x_{mn} \end{bmatrix} \begin{bmatrix} \beta_0 \\ \beta_1 \\ \vdots \\ \beta_p \end{bmatrix} + \begin{bmatrix} \varepsilon_1 \\ \varepsilon_2 \\ \vdots \\ \varepsilon_m \end{bmatrix} \quad (\text{B.6})$$

It is not unusual, however, to find the functions  $h_i$  in the form of polynomials and trigonometric functions, especially in curve fitting problems (Seber, 1977).

## B.2 Parameter Estimation

The oldest and most widely used estimation technique is the least squares estimation. In this method the parameters  $\beta_i$  are determined to minimize the function

$$\phi(\beta) = (y - H\beta)^T V^{-1} (y - H\beta) \quad (\text{B.7})$$

where  $V$  is the covariance matrix of the measured variable  $y$ . In the following we assume, for simplicity, that  $V = I$  (the identity matrix). The vector  $b$  must, then, satisfy

$$\frac{\partial \phi}{\partial \theta} = -2H^T(y - H\beta) = 0 \quad (\text{B.8})$$

which yields

$$H^T y = H^T H \beta \quad (\text{B.9})$$

If the experiment is well designed the, matrix  $H$  is of full rank. In this case Eq. (B.9) can be solved for  $\beta$  as

$$\beta = [H^T H]^{-1} H^T y \quad (\text{B.10})$$

where  $A^+$  is the pseudoinverse of the matrix  $A_{mn}$  defined as

$$A^+ = \begin{cases} A^T [AA^T]^{-1} & m \leq n \\ A^{-1} & m = n \\ [A^T A]^{-1} A^T & m \geq n \end{cases} \quad (\text{B.11})$$

Using Eq. (B.10) is not recommended, however. Indeed the method is not computationally stable since it involves direct matrix inversions. Instead, the following more stable and robust methods should be used. It is to be noted that these method also provide a least squares solution. Their main advantage is that they do not involve direct matrix inversion in either their decomposition process or in the solution of the problem at hand.

### B.2 .1 QR decomposition

In QR decomposition, a matrix  $A_{mn}$  is written in the form

$$A = Q \begin{bmatrix} R \\ 0 \end{bmatrix} \quad (\text{B.12})$$

where  $Q$  is an  $m \times m$  orthogonal matrix ( $Q^{-1} = Q^T$ ) and  $R$  is an  $r \times n$  upper triangular matrix, where  $r$  is the rank of matrix  $A$ . Using this decomposition Eq. (B.9) can be written as

$$A\beta = Q \begin{bmatrix} R \\ 0 \end{bmatrix} \beta = \tilde{y} \quad (\text{B.13})$$

with  $A = H^T H$  and  $\tilde{y} = H^T y$ . Eq. (B.13) can the be reduced to

$$\begin{bmatrix} R \\ 0 \end{bmatrix} \beta = Q^T \tilde{y} \quad (\text{B.14})$$

Now one can solve for the vector  $\beta$  using backward substitution since the matrix  $R$  is upper triangular. The robustness and stability of the QR decomposition comes at price, however. The computation time is almost double that of pseudoinverse solution for large matrices.

## B.2 .2 SVD decomposition

In SVD decomposition, a matrix  $A_{mn}$  is written in the form

$$A = USV^T \quad (\text{B.15})$$

where  $U$  and  $V$  are  $m \times m$  and  $n \times n$  orthogonal matrices, respectively and  $S$  is an  $m \times n$  diagonal matrix the entry of which are the singular values of the matrix  $A$ . Hence, a linear system of the form

$$Ax = y \quad (\text{B.16})$$

can be solved for  $x$  as

$$x = V S^{-1} U^T y \quad (\text{B.17})$$

Note that  $S^{-1}$  is simply  $\text{diag}\left(\frac{1}{s_{11}}, \frac{1}{s_{22}}, \dots, \frac{1}{s_{mn}}, 0, \dots, 0\right)$ . If matrix  $A$  is singular or near-singular then one or more of the entries of  $S$  are zero (up to the machine precision). In this case one can still find an optimal solution solution in the sense of least squares. This is achieved by setting  $(S^{-1})_{ii}$  to zero if the entry  $s_{ii}$  is zero or near zero.

## APPENDIX C

# GEOMETRIC TRANSFORMATIONS AND RELATIONSHIPS

### C.1 Translation

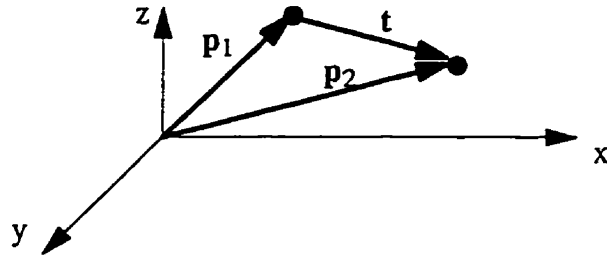


*Figure C.1 Point Translation*

### C.2 Transformation Matrix

The position vector  $\mathbf{p}$  can be represented in the 3-dimensional space by the vector:

$$\mathbf{p} = [x \ y \ z \ 1] \quad (\text{C.1})$$

Using the above form, the transformation to another position vector  $\mathbf{q}$  can be established

using the  $4 \times 4$  transformation matrix  $T$ .

$$q = pT \quad (C.2)$$

$$T = \begin{bmatrix} T_{rot_{1,1}} & T_{rot_{2,1}} & T_{rot_{3,1}} & 0 \\ T_{rot_{1,2}} & T_{rot_{2,2}} & T_{rot_{3,2}} & 0 \\ T_{rot_{1,3}} & T_{rot_{2,3}} & T_{rot_{3,3}} & 0 \\ t_x & t_y & t_z & 1 \end{bmatrix} \quad (C.3)$$

### C.3 Transformation Matrix Construction

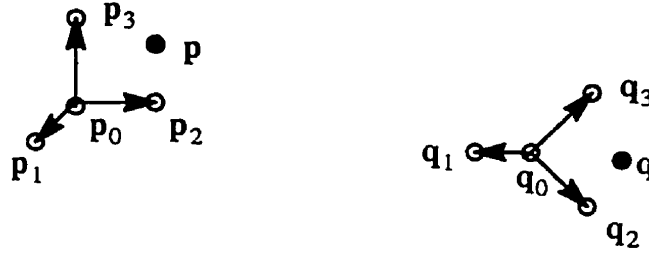


Figure C.2 Three Point Transformation

Figure C.2 shows a reference frame represented by two unit vectors  $\overline{p_0p_1}$ ,  $\overline{p_0p_2}$  &  $\overline{p_0p_3}$ . The frame is to be transformed into the new reference coordinates  $\overline{q_0q_1}$ ,  $\overline{q_0q_2}$  &  $\overline{q_0q_3}$ . The transformation matrix elements can be derived using procedure P1 (Mortenson, 1985). Although the points shown in Figure C.2 make a right hand orthogonal frame of axes, the procedure is described in general for the transformation of any set of 3 points

#### Procedure P1:

1. Let

$$V_1 = p_2 - p_1 \quad (C.4)$$

$$W_1 = q_2 - q_1 \quad (C.5)$$

$$\mathbf{V}_3 = \mathbf{V}_1 \times (\mathbf{p}_3 - \mathbf{p}_1) \quad (\text{C.6})$$

$$\mathbf{W}_3 = \mathbf{W}_1(\mathbf{q}_3 - \mathbf{q}_1) \quad (\text{C.7})$$

$$\mathbf{V}_2 = \mathbf{V}_3 \times \mathbf{V}_1 \quad (\text{C.8})$$

$$\mathbf{W}_2 = \mathbf{W}_3 \times \mathbf{W}_1 \quad (\text{C.9})$$

The vectors  $\mathbf{V}_1$ ,  $\mathbf{V}_2$  and  $\mathbf{V}_3$  form a right-hand orthogonal frame. The same argument applies for the set of vectors  $\mathbf{W}_1$ ,  $\mathbf{W}_2$  and  $\mathbf{W}_3$ .

2. Evaluate the unit vectors:

$$\mathbf{v}_1 = \frac{\mathbf{V}_1}{|\mathbf{V}_1|} \quad (\text{C.10})$$

$$\mathbf{v}_2 = \frac{\mathbf{V}_2}{|\mathbf{V}_2|} \quad (\text{C.11})$$

$$\mathbf{v}_3 = \frac{\mathbf{V}_3}{|\mathbf{V}_3|} \quad (\text{C.12})$$

$$\mathbf{w}_1 = \frac{\mathbf{W}_1}{|\mathbf{W}_1|} \quad (\text{C.13})$$

$$\mathbf{w}_2 = \frac{\mathbf{W}_2}{|\mathbf{W}_2|} \quad (\text{C.14})$$

$$\mathbf{w}_3 = \frac{\mathbf{W}_3}{|\mathbf{W}_3|} \quad (\text{C.15})$$

3. Let,

$$[\mathbf{v}] = [\mathbf{v}_1 \ \mathbf{v}_2 \ \mathbf{v}_3] \quad (\text{C.16})$$

$$[\mathbf{w}] = [\mathbf{w}_1 \ \mathbf{w}_2 \ \mathbf{w}_3] \quad (\text{C.17})$$

4. The rotation matrix  $\mathbf{T}_{\text{rot}}$  is equal to:

$$\mathbf{T}_{\text{rot}} = [\mathbf{v}]^{-1}[\mathbf{w}] \quad (\text{C.18})$$

5. The translation vector  $\mathbf{t}$  is equal to:

$$\mathbf{t} = \mathbf{q}_1 - \mathbf{p}_1[\mathbf{v}]^{-1}[\mathbf{w}] \quad (\text{C.19})$$

The translation vector as well as the rotation matrix can be substituted into equation (C.3) to obtain the transformation matrix  $\mathbf{T}$ . The derived transformation places point  $\mathbf{p}_1$  at the coordinates of  $\mathbf{q}_1$ , coincides the direction of the vector  $\overline{\mathbf{p}_1 \mathbf{p}_2}$  with the direction of the vector  $\overline{\mathbf{q}_1 \mathbf{q}_2}$  and coincides the plane formed by the points  $\mathbf{p}_1$ ,  $\mathbf{p}_2$  &  $\mathbf{p}_3$  with the plane formed by the points  $\mathbf{q}_1$ ,  $\mathbf{q}_2$  &  $\mathbf{q}_3$ . Thus a point  $\mathbf{p}$  in the  $\mathbf{v}$  system is transformed into the point  $\mathbf{q}$  in the  $\mathbf{w}$  system.

## C.4 Normal Distance Between a Point and a Line

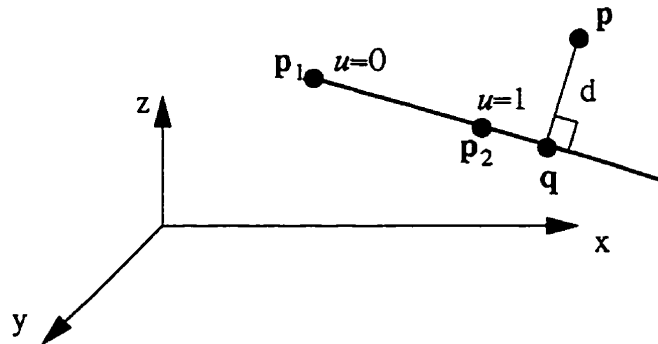


*Figure C.3 Normal Distance between a Point and a Line*

The minimum distance between a point and a line in space is equal to the perpendicular distance between the point and the line. Figure C.3 shows a line represented

by two points  $\mathbf{p}_1$  and  $\mathbf{p}_2$ . The line parametric equation is given by:

$$\mathbf{p}(u) = \mathbf{p}_1 + u(\mathbf{p}_2 - \mathbf{p}_1) = \begin{bmatrix} x_1 \\ y_1 \\ z_1 \end{bmatrix} + u \left( \begin{bmatrix} x_2 \\ y_2 \\ z_2 \end{bmatrix} - \begin{bmatrix} x_1 \\ y_1 \\ z_1 \end{bmatrix} \right) \quad (\text{C.20})$$

The distance between  $\mathbf{p}$  and the line is given by:

$$d = |\mathbf{p} - \mathbf{q}| = \left| \begin{bmatrix} x - x_q \\ y - y_q \\ z - z_q \end{bmatrix} \right| \quad (\text{C.21})$$

At the point  $\mathbf{q}$  the dot product of the vectors  $\overline{\mathbf{p}_1 \mathbf{p}_2}$  and  $\overline{\mathbf{p} \mathbf{q}}$  is equal to zero.

$$(x_2 - x_1)(x - x_q) + (y_2 - y_1)(y - y_q) + (z_2 - z_1)(z - z_q) = 0 \quad (\text{C.22})$$

Since,

$$\mathbf{q} = \mathbf{p}_1 + u_q(\mathbf{p}_2 - \mathbf{p}_1) \quad (\text{C.23})$$

where  $u_q$  is the value of the parameter  $u$  at the point  $\mathbf{q}$ , equation (C.23) can be substituted into equation (C.22) yielding:

$$u_q = \frac{(x_2 - x_1)(x - x_1) + (y_2 - y_1)(y - y_1) + (z_2 - z_1)(z - z_1)}{(x_2 - x_1)^2 + (y_2 - y_1)^2 + (z_2 - z_1)^2} \quad (\text{C.24})$$

Having obtained the value of  $u_q$ ,  $\mathbf{q}$  can be calculated from equation (C.23) and consequently the minimum distance  $d$  can be calculated from equation (C.21).

## C.5 Normal Distance Between a Point and a Plane

Figure C.4 shows a point  $\mathbf{p}$  projected on a plane represented by three points  $\mathbf{p}_1$ ,  $\mathbf{p}_2$  and  $\mathbf{p}_3$ . Using the procedure described in section C.4 a point  $\mathbf{p}_0$  is found on the vector  $\overline{\mathbf{p}_2 \mathbf{p}_3}$ , such that the vectors  $\overline{\mathbf{p}_2 \mathbf{p}_3}$  and  $\overline{\mathbf{p}_1 \mathbf{p}_0}$  are perpendicular.



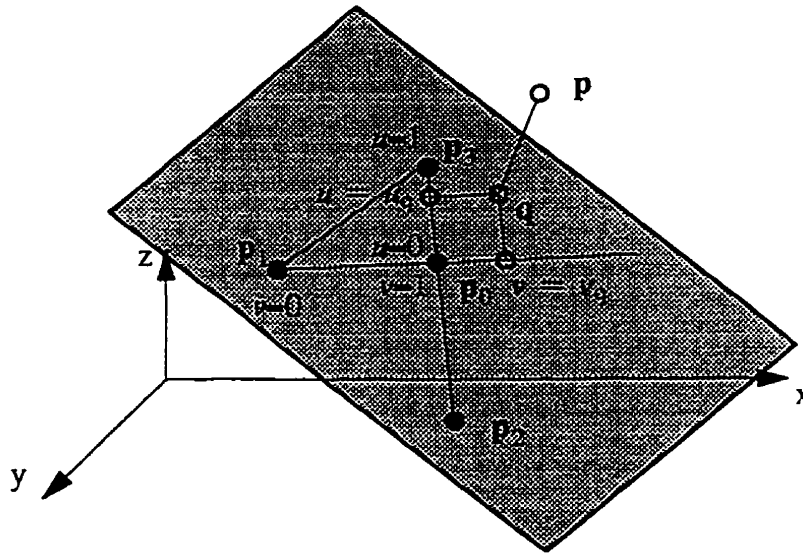


Figure C.4 Minimum distance between a point and a plane

The points  $\mathbf{p}_1$ ,  $\mathbf{p}_0$  and  $\mathbf{p}_3$  are used to construct the following parametric equation of the plane:

$$\mathbf{p}(u, v) = \mathbf{p}_1 + u(\mathbf{p}_0 - \mathbf{p}_1) + v(\mathbf{p}_3 - \mathbf{p}_0) \quad (\text{C.25})$$

Point  $\mathbf{q}$  can be found by projecting  $\mathbf{p}$  on the vector  $\overline{\mathbf{p}_2 \mathbf{p}_3}$  to obtain  $u_q$  and on the vector  $\overline{\mathbf{p}_1 \mathbf{p}_0}$  to obtain the  $v_q$  and substituting into equation (C.25). The minimum distance between  $\mathbf{p}$  and the plane is equal to the magnitude of the vector  $\overline{\mathbf{p} \mathbf{q}}$ .

## VITA AUCTORIS

NAME: Essam Shalash

PLACE OF BIRTH: Dubai, United Arab Emirates

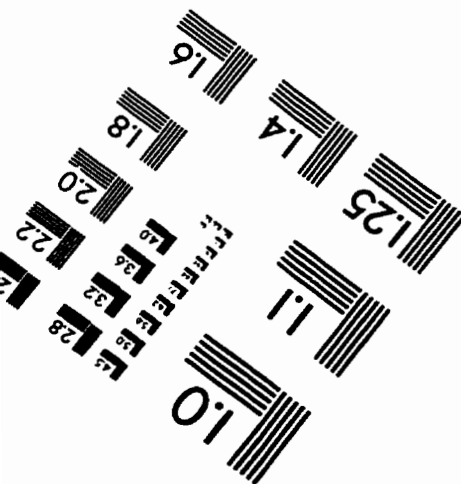
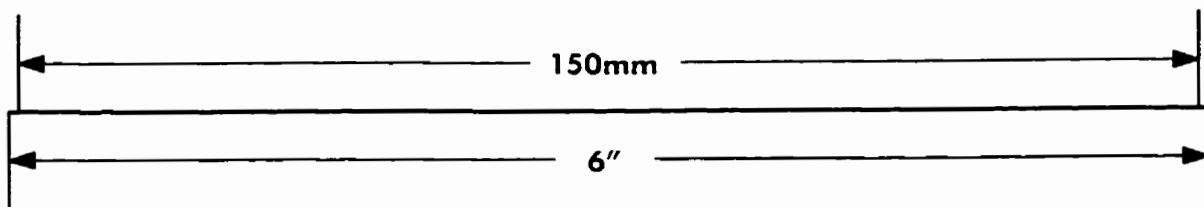
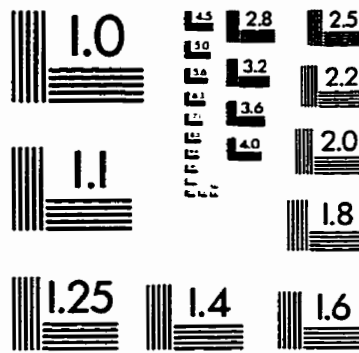
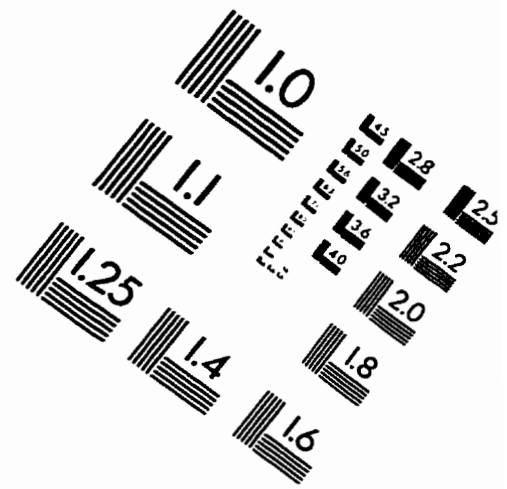
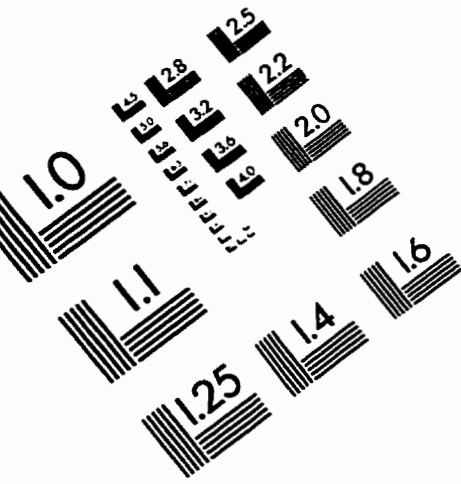
YEAR OF BIRTH: 1969

EDUCATION: Al-Imam Malik High School, Dubai, U.A.E.  
1983 – 1987

University of United Arab Emirates, Al-Ain, U.A.E.  
1987 – 1993, B.Sc.

University of Windsor, Windsor, Ontario, Canada  
1994 – 1996, M.A.Sc.

# IMAGE EVALUATION TEST TARGET (QA-3)



APPLIED IMAGE, Inc  
1653 East Main Street  
Rochester, NY 14609 USA  
Phone: 716/482-0300  
Fax: 716/288-5989

© 1993, Applied Image, Inc., All Rights Reserved

